

Seismic Re-Engineering of the Valdez Marine Terminal (VMT)
Contract No. 556.07.0007

Rock Slope Stability of the VMT

Prepared for

**The Prince William Sound
Regional Citizen's Advisory Council (RCAC)**

Prepared by

Terry R. West, Ph.D., P.E., C.P.G.

and

Kyu Ho Cho, Ph.D., P.E.

September 2007

The opinions expressed in this PWSRCAC commissioned
report are not necessarily those of PWSRCAC.

TABLE OF CONTENTS

	Page
EXECUTIVE SUMMARY (to include abstract by Dr. James Beget)	i
1. INTRODUCTION	1
2. BACKGROUND	1
3. SCOPE OF WORK	4
4. SITE GEOLOGY	8
5. SEISMIC SETTING	9
6. FIELD INVESTIGATIONS	10
6-1. First Visit - July 2006	10
6-2. Second Visit - August 2006	12
7. DATA ANALYSIS	13
7-1. Rock Slope Stability Analysis	13
7-1-1. Types of Rock Slope Failure	14
7-1-2. Kinematic Analysis.....	14
7-1-3. Kinetic Analysis.....	21
7-1-4. Probability of Failure.....	26
7-2. Rock Slopes in VMT	28
7-2-1. Limitation of Analysis	28
7-2-2. BWT Slope	31
7-2-3. PVR Slope	47
7-2-4. West Manifold Slope	64
7-2-5. West Tank Farm Slope	72
7-2-6. East Tank Farm Slope.....	83
7-2-7. Other Slopes.....	91
7-3. Analysis of Aerial Photographs above VMT	91
8. CONCLUSIONS.....	102
9. RECOMMENDATIONS	105
REFERENCES CITED.....	106

EXECUTIVE SUMMARY

The primary purpose of this project was to evaluate the stability of rock slopes of the VMT during potential earthquake conditions. Field reconnaissance and a detailed fracture survey of the rock slopes were conducted by Dr. Terry R. West and his associates in July and August 2006.

During the fracture survey more than 300 discontinuity values were measured in the field. The discontinuity data were measured on those relatively critical slopes including the Ballast Water Treatment Plant (“BWT Slope”), the Power House and Vapor Recovery Plant (“PVR Slope”), the West Manifold Building (“WM Slope”), the West Tank Farm Slope (“WTF Slope”), and the East Tank Farm Slope (“ETF Slope”). Discontinuity data were also obtained from the less critical slopes including the Power House Road Slope, the Tea Shelter Slope, and the rock quarries located on the southern portion of the VMT site.

Using these fracture data and existing rock cut information available at the time of this investigation, an analysis of rock slope stability was conducted using kinematic and factor of safety (deterministic) methods. Because of the uncertainty of the information, the probability of failure method was also employed to evaluate the stability of the VMT slopes in this study. Assumptions concerning rock mass strengths were made based on the literature and experience of the authors.

Based on the kinematic and kinetic analyses, it is anticipated that the external loading conditions equal to $0.7H_w/H_{\text{slope}}$ or equal to pore pressure of $0.6H_w/H_{\text{slope}}$ with 0.1g of horizontal acceleration will cause the BWT Slope to become unstable. For the PVR Slope, the external loading conditions equal to $0.85H_w/H_{\text{slope}}$ or equal to pore pressure of $0.8H_w/H_{\text{slope}}$ with 0.1g of horizontal acceleration or $0.55H_w/H_{\text{slope}}$ with 0.2g of horizontal acceleration may cause the PVR Slope to become unstable. For the West Manifold Slope, the external loading conditions equal to $0.35H_w/H_{\text{slope}}$, and the external loading conditions equal to pore pressure of $0.15H_w/H_{\text{slope}}$ with 0.1g of horizontal acceleration may cause the West Manifold Slope to become unstable. For the East Tank Farm Slope, the external loading conditions equal to $0.7H_w/H_{\text{slope}}$ or the external loading conditions equal to pore pressure of $0.45H_w/H_{\text{slope}}$ with 0.1g of horizontal acceleration may cause the East Tank Farm Slope to become unstable. For the West Tank Farm Slope, the external loading conditions equal to $0.65H_w/H_{\text{slope}}$ or the external loading conditions equal to pore pressure of $0.5H_w/H_{\text{slope}}$ with 0.1g of horizontal acceleration may cause the East Tank Farm Slope to become unstable. Details concerning drainage holes at VMT were not provided for this study. These data are required along with rock bolt distributions in order to perform a more precise evaluation of slope stability for the site.

To reduce the risk of the existing slopes at this time, the ditches above the rock slopes should have steep enough grades to avoid water-ponding to prevent infiltration of ponded water which can increase pore pressures. Also, it is recommended that any cracks at the top of the slope be sealed with grout or asphalt. It is also recommended that the piezometers which are clogged in the VMT slopes be regularly cleaned and measured frequently to monitor pore pressures. It is also recommended that more rock bolts be installed in the areas where the existing rock bolts are loosened and where rock bolts have not been installed following a further study to establish these details. Finally, a contingency plan should be developed to address an increase in pore pressure due to increased precipitation, as higher pore pressures could lead to slope instability.

1. INTRODUCTION

The Valdez Marine Terminal was constructed between 1974 and 1977 at the southern end of the 800 mile long Trans-Alaska Pipeline. An extensive amount of rock excavation was necessary to build the platform on which the facility was constructed. Nearly thirty years have passed since that time and it is a well-established fact that rock slopes weather, relax and deteriorate with time due to exposure to climatic conditions. Because of the vast amount of crude oil stored in tanks on the site, failure of the rock slopes could cause a major oil spill and possibly a major fire on the VMT site. With this concern in mind the Prince William Sound, Regional Citizen's Advisory Council (RCAC) authorized a study of the stability of the rock slopes under various conditions, including seismic loading. Valdez lies within the major subduction zone along the southern coast of Alaska and is located only 38 miles from the epicenter of the Great Alaska earthquake of 1964. Dr. Terry R. West, geological and engineering consultant, was employed to evaluate the slope stability aspects of the VMT, including the effects of seismic shaking. This report is based on field studies conducted in July and August, 2006 and subsequent analysis of the discontinuity data.

2. BACKGROUND

Construction of the Valdez Terminal for Alyeska Pipeline Service Company (Alyeska) was accomplished between 1974 and 1977. The site, consisting of about 1000 acres, involved major construction, including among other engineering works, several extensive, high rock-cut excavations. An estimated 7 million cubic yards of material were removed at the site (Cohen, The Great Alaska Pipeline, p. 108). Difficulties were

encountered when constructing the rock cuts and the foundations for the large oil and ballast water treatment tanks. These were related to problematic, geological and groundwater conditions involving weak rocks, unfavorable orientation of rock discontinuities and high groundwater levels. Weak, foliated rocks, including phyllites, were subject to slope failure. Groundwater levels remained above excavated surfaces (high piezometric levels) for extended periods of time (Bukovansky, 1990).

During an early phase of construction, a rock block slide caused a slope failure on a portion of the PVR slope (Powerhouse and Vapor Recovery). This occurred along the existing foliation which dips at an angle of about 60° from the slope. The original cut slope before failure, based on available photos, appears to have been a near vertical face (Tart, 2002, p. 10). Actually it had a 1/4 to 1 inclination yielding a 76° dip into the cut (Tart, personal communication, 2006). The failed slope is shown on p. 9 of the report (Tart, 2002). Consisting of phyllite, it is no surprise that the slope failed even without any contribution from pore water pressure. The ϕ angle for the phyllite was likely 30° or less, so the dip of the foliation greatly exceeded this ϕ angle and failure was eminent. ($FS = \tan\phi / \tan\theta$, where $\theta = \text{dip angle} = 60^\circ$, $\phi = 30^\circ$, so $FS = 0.33$) Because of this failure occurrence, rock slopes were cut back to the angle of the foliation or about 60° and slope drainage, rock bolts and rock buttresses were added to increase the factor of safety. This new slope angle prevented the foliation from daylighting or intercepting the cut slope. Other information suggests that the slope angle in the failed area was reduced to 45° , also preventing the foliation planes from daylighting on the slope (Bukovansky, 1990).

According to this consulting report (Bukovansky, 1990) stringent earthquake design criteria required the application of mitigating measures to alleviate the high

groundwater levels (high pore pressures). Extensive dewatering measures were implemented (horizontal drains installed) to eliminate or reduce uplift forces on the slopes and below the terminal tanks. Extensive piezometric level monitoring systems were installed during construction in the important cuts and below most terminal tanks to enable long term water level monitoring.

Regarding the earthquake design criteria for the area of Valdez, an M_s of 8.5, surface wave magnitude, was supposedly implemented for the area, which translates into a 0.60g ground acceleration or a ground velocity of 29 inches/second (Design Manual for Pipeline, TAPs 1973, Revised 1974, Table 4.2-1). This value of 0.60g is considered later on in this report, during the evaluation process.

Numerous piezometers were installed in the major rock cuts on the site as shown in Figure 5, page 6 of the 2002 Status Report (Tart, 2002). The PVR slope is the primary area of study in that evaluation. Piezometer No.40 is shown as an example. The Flag level depicts the piezometric surface in the rock slope following placement of a horizontal drain system and subsequent drainage after construction. Page 24 indicates for Piezometer No.40 that the groundwater elevation has been essentially the same, an elevation of 450 feet, for the period 1993 to 2002. The following line of reasoning seems to have prevailed. If the slope was stable in 1976 with the rock bolts in place, the slope should continue to be stable as long as the pore pressure or piezometric level does not increase. It is not clear what amount of seismic loading was assumed in this calculation. Certainly, no seismic effect was involved during the initial failure of the PVR slope during construction.

In the past there has been some concern expressed about rising piezometric levels. The 1990 report by Bukovansky shows on Figure 1 that the annual precipitation at Valdez increased from 55 to 82 inches per year from 1973 to 1989. It is outside the scope of the current study to examine the precipitation record from 1989 to the present, but it is clearly a concern as to how the piezometric levels can be kept at the Flag level and below, if total precipitation continues to increase. Bukovansky expressed concern in his report (1990) about the capability of lowering the groundwater level any further if it begins to rise with increased precipitation. Dr. Singh has also indicated a concern for increased levels of the piezometers (Singh and Associates, 1998).

A concern for rock slope stability was recognized by the current authors when a combination of increased pore pressure and earthquake effects occur which decreases the sliding resistance of the rock mass. This aspect forms the essence of the analysis that is presented in Section 7.

3. SCOPE OF WORK

This study, Seismic Evaluation of Valdez Marine Terminal, was authorized by RCAC (Prince William Sound, Regional Citizen's Advisory Council) to determine the level of safety of the terminal facility under earthquake loading conditions. The Great Alaska Earthquake of 1964 predates construction of the VMT by about ten years. This earthquake, centered between Anchorage and Valdez, registered an M_s (surface wave magnitude) = 8.5, M_w (moment magnitude) = 9.2 magnitude on the Richter scale and caused major damage to the town of Valdez. Although the repeat interval for this major

earthquake is considered by some to be 2500 years, the seismic design for the terminal is based on a repeat event of this magnitude.

The following items were designated in the proposal of work for RCAC by Dr. T.R. West. The overall objective of this work is to evaluate the stability of the rock slopes at and above the Valdez Marine Terminal (VMT) and to determine the probability of failure under various conditions including earthquake shaking. To accomplish this, the following activities were proposed:

- a) Obtain detailed geologic data on the rock mass in question including, but not necessarily limited to, rock type, structure, nature and spacing of fractures, shear strength of fractures and of intact rock strength. Council staff will assist Consultant in obtaining these data from Alyeska Pipeline Service Company and the Joint Pipeline Office.
- b) Review slope stability design and determine current slope stability conditions excluding earthquake loading. Consider both dry and pore pressure conditions.
- c) Determine slope stability based on a deterministic analysis, include earthquake shaking effects.
- d) Determine variability of slope stability factors and perform a probabilistic evaluation of slope stability. Include both kinematic and kinetic aspects of discontinuities. Calculate combined probability of failure and block size occurrences; both sliding and wedge failure considered.
- e) Perform the Colorado Rockfall Simulation Program (CRSP). Evaluate slope failure including runout zone details, ditch width and depth for existing rock slope.

- f) Evaluate earthquake potential; consider both horizontal and vertical acceleration.
- g) Evaluate stability relative to increased pore pressure conditions.
- h) Combined effects of earthquake shaking, plus kinematic and kinetic aspects of slope stability. Calculate probability of failure under combination of conditions.
- i) Review the adequacy of current support system for VMT rock slopes relative to probability of failure criteria.
- j) Determine if additional support is needed for the slope, or if a modification of the slope configuration is required.
- k) Examine maintenance practices and slope deterioration from weathering effects or from relaxation of stresses.
- l) Review construction techniques used to obtain the cut slope geometry, blasting details, pre-splitting, scaling and rock bolting.
- m) Review design and stability of Mechanically Stabilized Earth (MSE) walls on the site.
- n) After detailed analysis, examine existing slopes in regard to results obtained from the evaluation. Check condition of rock bolts, also the bolt spacing and other slope protection considerations. It is anticipated that two trips to the site between June and August, 2006 will be required by the consultant. Three person weeks total are estimated for field activities.
- o) Provide periodic reports to the Council as requested during the evaluation process. Prepare final report for this phase of the work when study is complete.
- p) Consider other issues as Council directs, such as tsunami and undersea landslides related to earthquake shaking.

- q) Coordinate activities and findings with Dr. James R. Beget who is engaged in a complementary geomorphology study of Port Valdez and help assure a seamless interface between the two efforts.
- r) Prepare final report. The final report will be submitted in draft form to the Council by December 31, 2006. The final report revised as necessary will be submitted to the Council by February 16, 2007.

Two visits to the site were accomplished in the summer 2006. The first visit, in July, was made by Terry R. West, Ph.D., P.E., geological and engineering consultant, the principal investigator on this project. The purpose of the visit was to meet with site personnel for Alyeska and to perform a reconnaissance evaluation of the site. Dr. Thomas Kuckertz, project manager for RCAC, was also present. During part of the visit Dr. James Beget, geological consultant, accompanied Dr. West. Mr. Rupert (Bucky) Tart, of Golder Associates Consultants was also present during a portion of the site visit. An adjacent area to the east of the site was also examined, the dam site for the Solomon Gulch Hydroelectric plant. During the following week Dr. West met with Alyeska personnel and the Joint Pipeline Office in Anchorage.

The second visit to VMT occurred in August, 2006. During the visit a three-man team conducted five days of field work, led by Dr. West, aided by Dr. Kyu Ho Cho and another field assistant. A detailed fracture study of the rock slopes in question was conducted in which more than 300 discontinuity values were measured in the field.

Additional data were obtained from Alyeska which were used in this evaluation of the rock slope stability at the VMT site. This report has been prepared to determine the

safety of the rock slopes under different conditions including seismic shaking. It is not intended to be the basis of a design document, but instead its intent is to point out any concerns for the long term stability of rock slopes on the VMT facility.

4. SITE GEOLOGY

The Valdez Marine Terminal is a 1,000 acre site on the 11 mile long fiord near the northeast corner of Prince William Sound. It is located on the south shore of the Port Valdez Fiord about 5 miles south of the town of Valdez, Alaska along the Valdez Arm of the Prince William Sound. The bedrock formations comprise a part of the Valdez Group of the Chugach Terrane. Metamorphosed, marine sedimentary rocks consisting of several thousand feet of interbedded slates, graywackes, phyllites, argillites and greenstones (metabasalt) are present. These were formed in late Cretaceous time near the edge of the continental shelf. Rocks that crop out at VMT have undergone greenschist facies metamorphism (Connor and O'Hare, 1988; Verigin and Harder, 1989; Bukovansky, 1990).

Folding in the rocks is intense and accompanied by recrystallization resulting in development of cleavage and schistosity. The significant rock hardness is due to thorough impregnation by siliceous solutions. Numerous openings have been filled and sealed with quartz so that quartz stringers are prevalent. The rocks have a well developed foliation which strikes east-west and dips steeply to the north. Rocks are strongly jointed with the most prominent ones being a vertical set oriented perpendicular to the foliation. These major joints are prominently exposed along the south side of the Valdez Arm where water courses commonly follow them. These two structural features, foliation (or bedding)

and the perpendicular joints effectively control the topographic grain of the region. The perpendicular joints also form release planes that can isolate rock blocks that subsequently undergo failure.

5. SEISMIC SETTING

Southern Alaska is one of the most seismically active regions in the world. This is due to the northward, underthrusting of the Pacific crustal plate below the North American crustal plate, all along the Aleutian trench, the southern limit of the Aleutian Megathrust Zone.

Great earthquakes have occurred historically throughout this region and can be expected to continue in the future. Davies (1985) indicated that three of the ten largest earthquakes in the world have occurred in Alaska and that Alaska may experience as many as six times the number of moderate and greater earthquakes than does California. Davies et al. (1979) has suggested that the Megathrust Zone in this area produces earthquakes of the size of the 1964 Alaska earthquake ($M_s = 8.5$, $M_w = 9.2$) approximately every 160 years. This is in contrast to the 2500 year return cycle suggested by others. The straight line distance from the epicenter of the March 27, 1964 earthquake to the VMT is approximately 38 miles. Several points of interest were noted in the report by Bukovansky (1990). The Power and Vapor Recovery (PVR) cut is located within poor quality phyllites and the west portion of this cut is where the 1975 failure occurred. He claimed that the slope was cut back to 45° after failure. The BWT by contrast is located in hard competent greenstone, the best quality rock of any of the bedrock on the site. The West Manifold Cut, is located partly in phyllite and partly in greenstone.

6. FIELD INVESTIGATION

6-1 First Visit - July 2006

Dr. West and leadership personnel for the VMT site met in the VMT office, along with Bucky Tart from Golder Associates and Jim Roddick from the Alyeska office in Anchorage. Also in attendance was Dr. Thomas Kuckertz, project manager for RCAC. During an early discussion the Alyeska team suggested that pore pressures in rock fractures would be dissipated by minor movements of the rock mass and not cause further stability problems. Dr. West disagreed with this concept which is contrary to basic analysis procedures for rock slopes. Pore pressures act in two ways to reduce slope stability, they increase the driving force and decrease the resistance force.

The group visited slopes on the site, and the reinforced earthwall. They observed the Power and Vapor Recovery Cut, Ballast Water Treatment Cut, West Manifold Cut, West Tank Farm Cuts, East Tank Farm Cuts, Tea Shelter Slope and the rock quarry. The locations of these slopes are shown in Figure 6.1. During this visit Dr. West noted the nature of the rock mass and the stabilization techniques employed. This included rock bolts, rock fill berms, mechanically stabilized earth (MSE) walls, drain holes and piezometer instrumentation. Dr. West later concluded, based on field observation, that the MSE walls were in a stable condition. No detailed measurements of the rock discontinuities were accomplished. Later in the week Dr. West examined the soil slopes on the east side of the terminal property and the hydroelectric dam further to the east, the Solomon Gulch rock fill dam. The foliated, metasedimentary rock at the dam site was more massive than that found on most of the VMT site.

Figure 6.1 Slope Location Map



Two types of rock prevailed at the dam site: 1) a very hard, fine-grained, dark gray, argillite lacking well-developed cleavage, with some interbedded slate or slaty argillite and 2) a fine-grained blue-black slate interbedded with argillite.

The slate has well developed cleavage, but there is little or no cleavage in the argillite (Verign and Harder, 1989). Massive rock is exposed in the outlet channel for the dam. It consists of steeply dipping, foliated argillite striking parallel to the slope and dipping outward at about 60°. The trend is much like that observed at several locations on the VMT property.

6-2. Second Visit - August 2006

A three man team spent five days at the VMT site obtaining rock discontinuity data on the rock cuts. Detailed line mapping of fractures was accomplished by the team led by Dr. T. R. West with Dr. Kyu Ho Cho and another field assistant working as well. More than 300 strike and dip measurements were made on the primary rock slopes on the site. This detailed field work became necessary after it was determined that no discontinuity data from previous studies on the VMT site would be made available for analysis. It had been assumed by Dr. West when the study was proposed to RCAC, that abundant rock slope data were available and would be provided by Alyeska. The report by Bokovansky (1990) indicates that significant slope design work was accomplished for the VMT site prior to completion of the rock cuts in 1977. It was also suggested that seismic effects were included in this analysis as well. This rock slope discontinuity data and slope design analysis were not made available for Dr. West's study.

At the close of the five day field investigation Dr. West and his team met with the leaders of the senior staff of VMT. In an exit discussion he noted that based on a

preliminary evaluation, a combination of high pore pressures and some seismic activity, that the rock slopes may become unstable. Also it was expressed that the rock slopes were designed and constructed 30 years ago and the standard of practice for rock slope engineering has become more stringent since that time. As an example, catchment ditches have been increased in size both in width and depth. Concerning item e) of the list of objectives it was determined that the CRSP evaluation was not feasible for the VMT slopes. A stability evaluation of the higher reaches of the mountainous terrain would be evaluated instead, using air-photo interpretation.

7. DATA ANALYSIS

7-1. Rock Slope Stability Analysis

For practical purposes, the analysis of rock slope stability consists of a two-part process. The first step is to analyze the structural fabric of the slope to determine if the orientation of the discontinuities could result in instability of the slope under consideration. This determination is usually accomplished by means of stereographic analysis of the structural discontinuities such as bedding planes, joints, foliations, and faults, and is commonly referred to as kinematic analysis.

Once it has been determined that a kinematically possible failure mode is present, the second step requires a limit-equilibrium stability analysis to compare the forces resisting failure to those forces causing failure. The ratio between these two sets of forces is called the factor of safety (FS). This analytical method is called also as “kinetic analysis”. In the FS analysis, all input parameters are applied as fixed values despite the fact that all parameters and even the FS show a degree of variability. This method is also referred to as the deterministic procedure. Because of this limitation of the deterministic

method, probability methods using a reliability index and a probability of failure have been considered for rock slope stability analysis as an alternative method. For comparison, both the FS and probability of failure methods were used to evaluate the stability of the VMT slopes in this study.

7-1-1. Types of Rock Slope Failure

Most slope failures can be classified into one of four categories depending on the geometrical and mechanical nature of the discontinuity and the conditions of the rock masses as shown in Figure 7.1. Planar failures occur when a discontinuity strikes parallel or nearly parallel to the slope face and dips into the excavation at an angle greater than the friction angle. Slope failure during construction of the PVR slope was caused by planar failure. Wedge failures involve a rock mass defined by two discontinuities with a line of intersection that is inclined out from the slope face where the inclination of the intersection line is significantly greater than the angle of friction. Circular failures occur when rock masses are highly fractured or composed of very weak material. Toppling failures involve rock slabs or columns defined by discontinuities that dip steeply into the slope face.

7-1-2. Kinematic Analysis

The kinematic analysis is performed using the stereographic projection method which is a strong tool to use for systematic data collection and presentation. Data required to perform the stereographic projection method are dip and dip direction of each discontinuity. The dip is defined as the maximum inclination of a structural discontinuity plane measured from the horizontal. The dip direction is the direction of the horizontal trace of the line of dip measured clockwise from north. The definition of the dip and dip

direction are illustrated in Figure 7.2. The discontinuity can be also represented using strike and dip. Strike is the compass bearing of the line formed by the intersection of a discontinuity plane and a horizontal plane. The discontinuity data measured at VMT are presented using strike, dip, and dip direction in tabular form in this report.

The discontinuity data were recorded as dip and dip direction using a Bronton Compass, for example 30/150, where 30 is the dip and 150 is the dip direction. In the kinematic analysis, the dip and dip direction were plotted by a software package Dips 2.2 (Rocscience) using the stereographic equal-angle projection method.

The kinematic conditions for each of the rock slope failure modes are as follows:

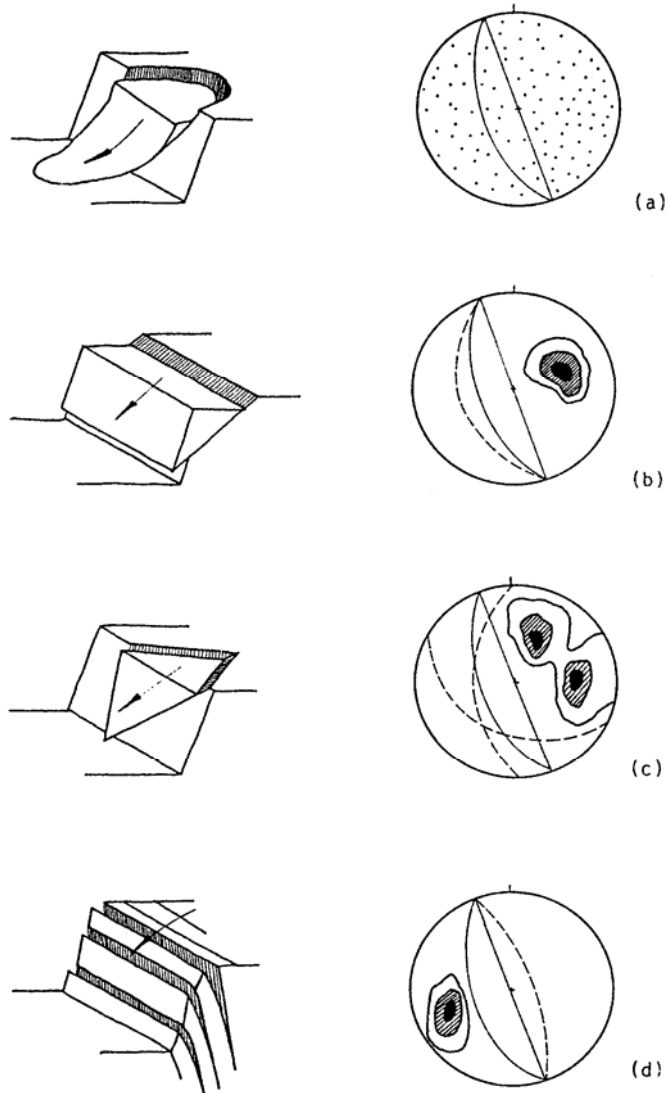
A. Planar Failure

Planar failure is a relatively rare occurrence in rock slopes because only occasionally do all the geometrical conditions required to produce planar failure actually occur. Wedge-type failures are more common and in fact rock engineers commonly consider that planar failure is a special case of the wedge failure analysis where the wedge angle between the two planes goes to 180° . The four structural conditions required for planar failure are shown in Figure 7.3 and explained below:

- The dip direction of the planar discontinuity must be within 20 degrees of the dip direction of the slope face.
- The dip of the planar discontinuity must be less than the dip of the slope face (daylights in the slope)
- The dip of the planar discontinuity must be greater than the angle of friction of the failure plane.

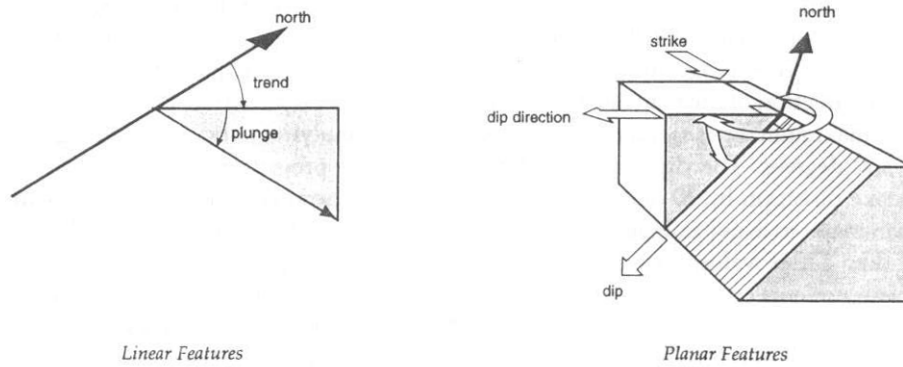
- The lateral extent of the potential failure mass must be isolated by lateral release surfaces which free a block for sliding. This is the requirement that reduces the likelihood of planar failure occurrence.

Figure 7.1 Four types of rock slope failures (After Hoek and Bray, 1981)

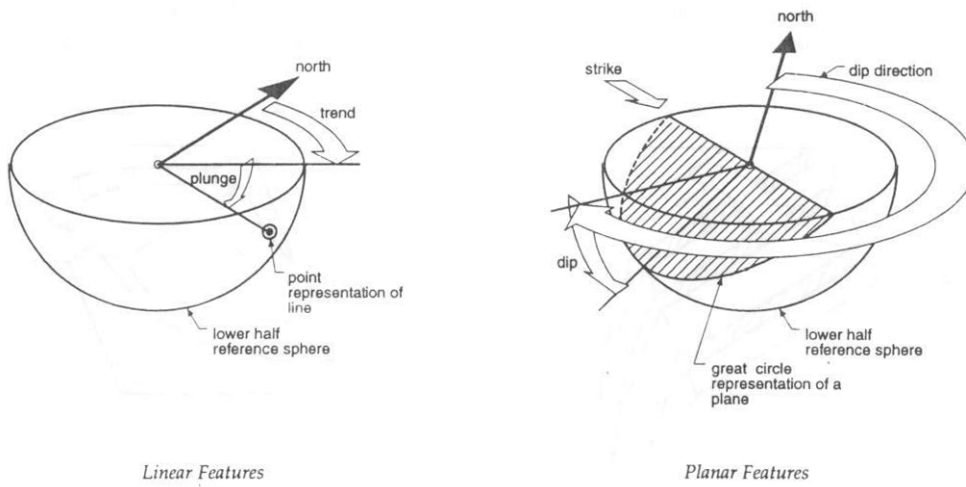


(a) Circular Failure (b) Planar Failure (c) Wedge Failure (d) Toppling

Figure 7.2 Dip and Dip Direction



(a) Definition of terms



(b) Representation on reference sphere

If structural analysis indicates that the orientation of the slope is unstable, that is, kinematically unstable, then stability is evaluated using a limit equilibrium procedure.

B. Wedge Failure

Wedge failures result when a rock mass slides along two intersecting discontinuities both of which dip out of the cut slope at an oblique angle to the cut face, forming a wedge-shaped block. For wedge failures to occur, three conditions are required as shown in Figure 7.4:

- The trend of the line of intersection must be similar to the dip direction of the slope face.
- The plunge (dip angle) of the line of intersection must be less than the dip angle of the slope face (daylights on slope).
- The plunge (dip angle) of the line of intersection must be greater than the angle of friction of the failure plane.

On the stereographic projection, the point of intersection of the two great circles representing the intersecting planes must plot within the shaded area, which is called the daylight zone, and lies on the convex side of the cut slope. If the structural analysis of wedge stability using stereographic methods indicates the possibility of a wedge failure, kinetic analysis is performed.

C. Circular Failure

Circular failures occur along circular slip paths which are commonly associated with highly weathered and decomposed, highly fractured or weak rock masses. In general, structural discontinuities such as joints and bedding planes do not form distinctive patterns that lead to a circular failure path and develop into kinematical failure condition. For the VMT, it is unlikely that circular failures would be a major concern in the rock cut areas.

Figure 7.3 Kinematic conditions for planar failure (After Norrish and Wyllie, 1996)

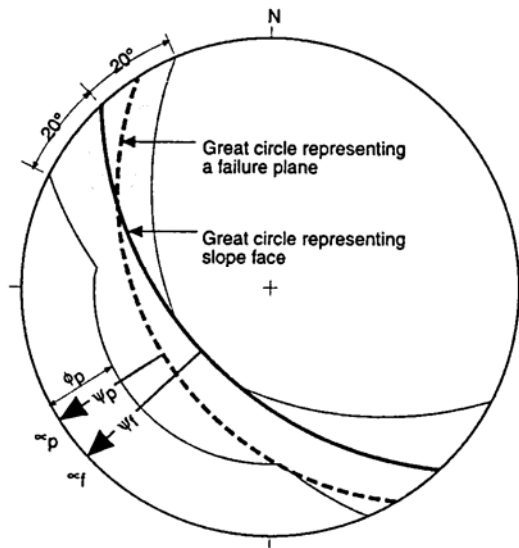
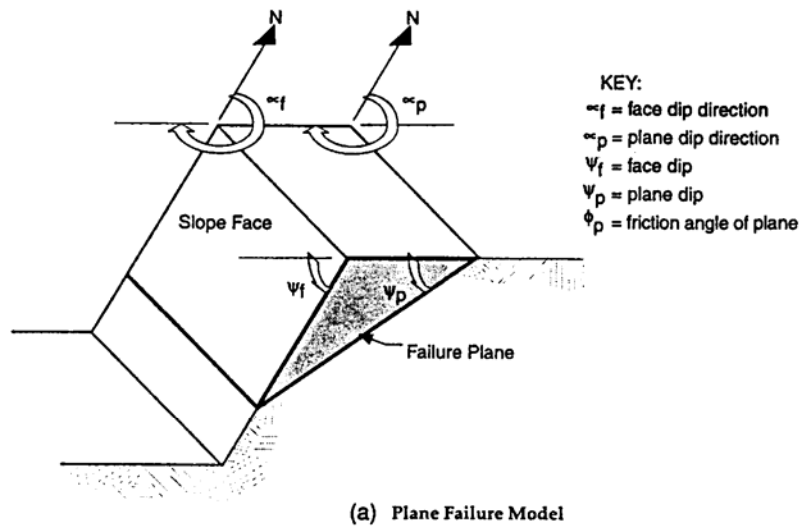
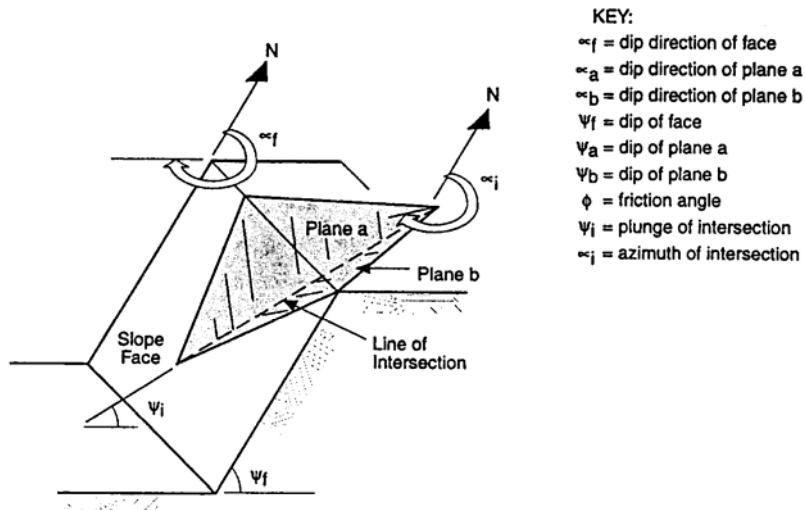
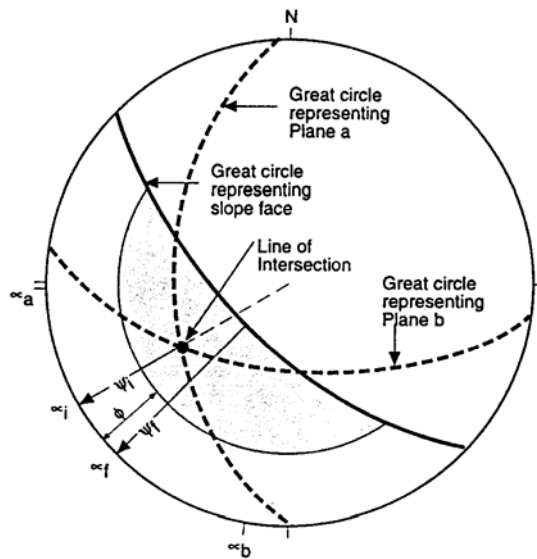


Figure 7.4 Kinematic conditions for wedge failure (After Norrish and Wyllie, 1996)



(a) Wedge Failure Model



(b) Great Circle Representation

D. Toppling

The necessary conditions for toppling failure can be summarized as follows:

- The strike of the layers must be approximately parallel to the slope face. Differences in these orientations of 20 degrees or less are required based on references in the literature.
- The dip of the layers must be into the slope face.
- The discontinuity condition must satisfy the following equation.

$$[90^\circ - \phi_p (\text{dip of plane}) \leq \phi_f (\text{dip of slope face}) - \phi_p (\text{friction angle along plane})]$$

- Analogous to planar failure, some limitation to the lateral extent of the toppling failure is a fourth condition for a kinematically possible failure.

Based on our field investigations, the planar and wedge failures are the prevalent failure modes in the VMT slopes rather than are circular or toppling. Therefore, potential planar and wedge failures are considered in the following kinetic analysis.

7-1-3. Kinetic Analysis

A. Factor of Safety in Planar Failure

The factor of safety in planar failure can be calculated using the following equation (modified from Cho, 2002).

$$FS = \frac{cA + \{W [(1 - k_v) \cos \theta - k_h \sin \theta] - U\} \tan \phi + T}{W [(1 - k_v) \sin \theta + k_h \cos \theta]}$$

c = Cohesion

ϕ = Friction angle of failure surface

A = Area of failure plane

W = Weight of block

- T = Tension in bolts or cables
- U = Water pressure
- k_h = Horizontal pseudostatic coefficient
- k_v = Vertical pseudostatic coefficient
- θ = Inclination (dip) of failure plane

In the equation, the earthquake forces are considered as a static force equal to the product of the design acceleration and the weight of the block. This force is usually applied horizontally so as to decrease stability, but two directions of the forces can be considered as shown in Figure 7.5. The water pressure applied to planar failure mode is shown in Figure 7.6. The water pressure (U) increases from zero at the water surface to a maximum value at half the groundwater surface height ($H_w/2$) and then decreases to zero at the daylight point where the failure plane intersects with the slope face shown in Figure 7.6. The water force can be evaluated as follows:

$$U = \frac{\gamma_w H_w^2 \operatorname{cosec}\theta}{4}$$

H_w = Height of water

γ_w = Unit weight of water (62.4 pcf)

It should be noted that the force T is assumed to increase the resisting force only. When the force T is applied both to increase the resisting force and to decrease the driving force, the driving force becomes a negative value for high T values. Therefore, in this project, the T force is applied only to increase the resisting force based on a fundamental reference (Hoek and Bray, 1981). For the kinematically unstable slope in the planar failure mode, the FS is calculated using the above equation under various water pressure and earthquake loading conditions.

Figure 7.5 Planar failure model

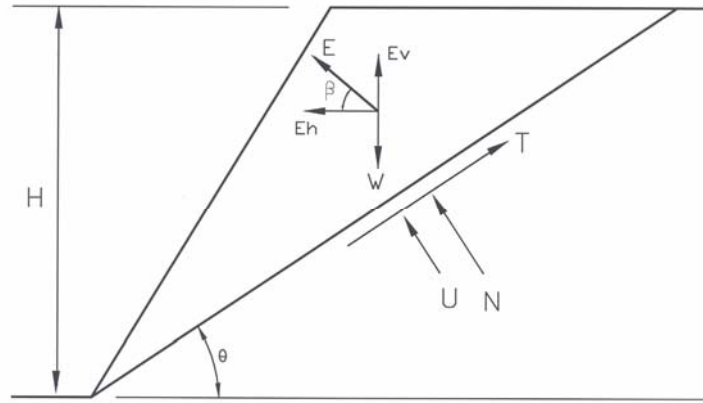
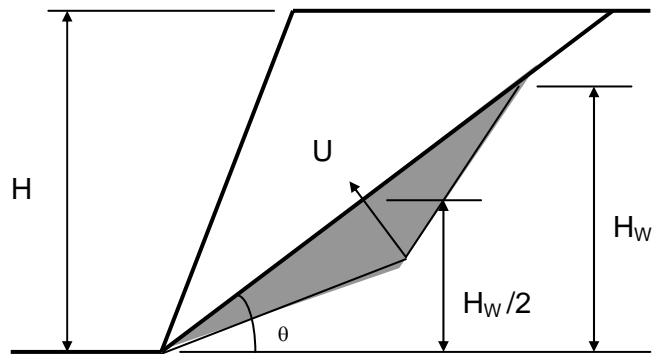


Figure 7.6 Water pressure in planar failure mode (After Hoek and Bray, 1981)



B. Factor of Safety in Wedge Failure

The factor of safety in wedge failure can be calculated using the following equation (modified from Cho, 2002).

$$FS = \frac{c_1 A_1 + c_2 A_2 + \left\{ \frac{\cos \omega_2}{\sin(\omega_1 + \omega_2)} [W(1 - k_v) \cos \theta - k_h \sin \theta] - U_1 \right\} \tan \phi_1 + \left\{ \frac{\cos \omega_1}{\sin(\omega_1 + \omega_2)} [W(1 - k_v) \cos \theta - k_h \sin \theta] - U_2 \right\} \tan \phi_2 + T}{W[(1 - k_v) \sin \theta + k_h \cos \theta]}$$

$$U_1 = \frac{1}{6} \gamma_w H_w A_{w1}, U_2 = \frac{1}{6} \gamma_w H_w A_{w2}$$

c_1 and c_2 = Cohesions for failure planes A and B, respectively

ϕ_1 and ϕ_2 = Friction angle of failure planes A and B, respectively

W = Weight of block

T = Tension in bolts or cables

U_1 and U_2 = Water pressure on failure planes A and B, respectively

k_h = Horizontal pseudostatic coefficient

k_v = Vertical pseudostatic coefficient

θ = Inclination (dip) of failure plane

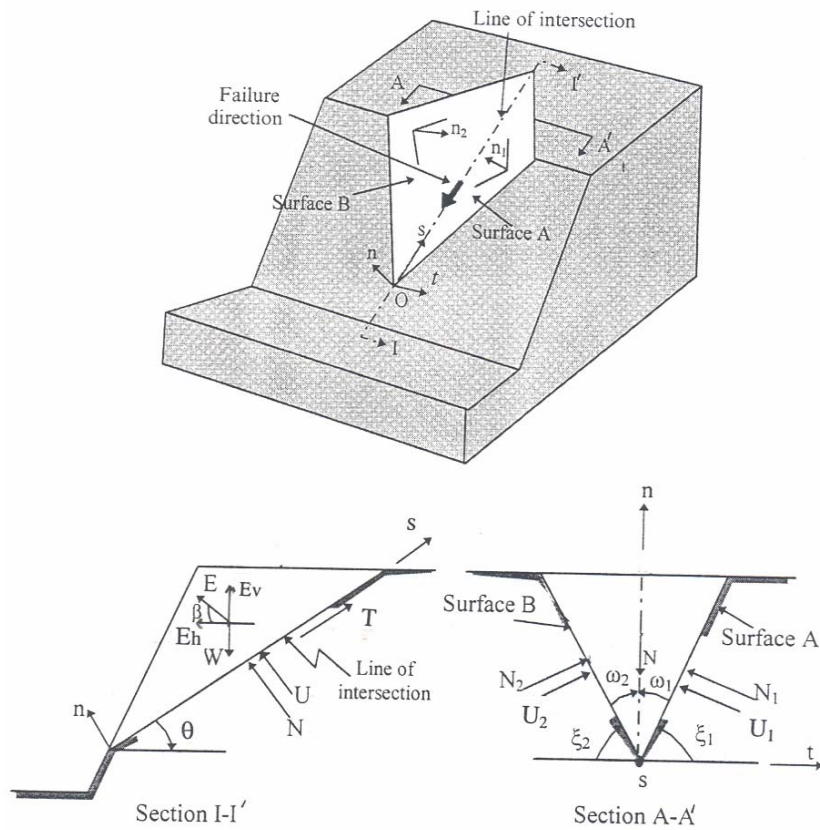
ω_1 = Angles between failure plane A and the vertical line

ω_2 = Angles between failure plane B and the vertical line

Effects of earthquake forces on wedge failures in rock slopes can be considered in the same manner as considered for the planar failure using limit equilibrium analysis. The wedge failure model can be illustrated as shown in Figure 7.7. The force T is assumed only to increase the resisting force as explained previously for the planar failure mode.

The factor of safety for a kinematically unstable slope in the wedge failure mode is calculated using the above equation under various water pressure and earthquake loading conditions.

Figure 7.7 Wedge failure model (modified from Kumsar et al., 2000)



7-1-4. Probability of Failure

The probability of failure (P_f) is defined in this study as the probability that the factor of safety is less than 1.0. To calculate the probability of failure, the mean and standard deviation of the factor of safety (FS) are needed. The mean FS can be calculated from each mean value of the input parameters and the standard deviation can be calculated from each variation of the input parameters using the Taylor's series expansion. The approach for computing the uncertainty in the factor of safety, then finding the reliability index and probability of failure is explained in the following discussion:

A. Identification of Variables

All variables (x_i) that affect the stability of a particular slope should be identified. For planar and wedge failures in this analysis, the slope geometry is fixed. The variables are unit weight (γ) of unstable blocks and shear strength parameters (c , ϕ). The pore pressure conditions are assumed to be dry ($H_w/H_{slope} = 0$), partially saturated ($H_w/H_{slope} = 0.3$ and 0.7), and/or fully saturated ($H_w/H_{slope} = 1$).

B. Mean of Variables

To determine the best estimate of the factor of safety, the best estimates, which are usually the mean values of variables, $\mu(x_i)$, should be selected in advance. In this project, the mean unit weight and mean strength parameters were obtained based on our experience regarding similar rock types and on the literature.

C. Standard Deviation of Variables

To evaluate uncertainty of variables, the standard deviation ($\sigma(x_i)$) should be considered in the reliability analysis. The $\sigma(x_i)$ can be evaluated from measurements.

Also the standard deviation can be determined from the coefficient of variance (cov) after the mean is determined because $cov = \sigma(x_i)/\mu(x_i)$. The values of cov used in this analysis are listed in Table 7.1.

Table 7.1 Values of coefficient of variation (After Duncan, 2000)

Parameters	Coefficient of Variation
Unit weight (γ)	3 – 7 %
Effective stress friction angle (ϕ')	2 – 13 %
Cohesion (c)	13 – 40 %

D. Sensitivity Analysis

Sensitivity analysis is accomplished by calculating the change in factor of safety due to changing each variable and computing $\Delta FS/\Delta x_i$. In this study, $\Delta FS/\Delta \gamma$, $\Delta FS/\Delta \phi$ and $\Delta FS/\Delta c$ were determined.

E. Standard Deviation of Factor of Safety

Uncertainty in the factor of safety can be measured by its variance or standard deviation using the Taylor series expansion. Assuming each variable is independent, the equation for $\sigma(FS)$ is given below:

$$\sigma(FS) = \sqrt{\sum_{i=1}^n \left(\left. \frac{\partial g}{\partial x_i} \right|_{x=\mu} \right)^2 \sigma(x_i)^2} = \sqrt{\left(\frac{\Delta FS}{\Delta \gamma} \right)^2 \sigma(\gamma)^2 + \left(\frac{\Delta FS}{\Delta \tan \phi} \right)^2 \sigma(\tan \phi)^2 + \left(\frac{\Delta FS}{\Delta c} \right)^2 \sigma(c)^2}$$

F. Reliability Index and Probability of Failure

Reliability index (β) describes the factor of safety using the number of standard deviations that separate the best estimate of FS from its defined failure value of 1.0.

It can also be considered as a way to normalize the factor of safety with respect to its standard deviation. When the shape of the probability distribution of the factor of safety is known, the reliability index can be related to the probability of failure (P_f). Reliability index (β) can be calculated from the factor of safety (FS) as follows:

$$\beta = \frac{\mu(FS) - 1.0}{\sigma(FS)} = \frac{\mu(FS) - 1.0}{\mu(FS) \cdot \text{cov}(FS)}$$

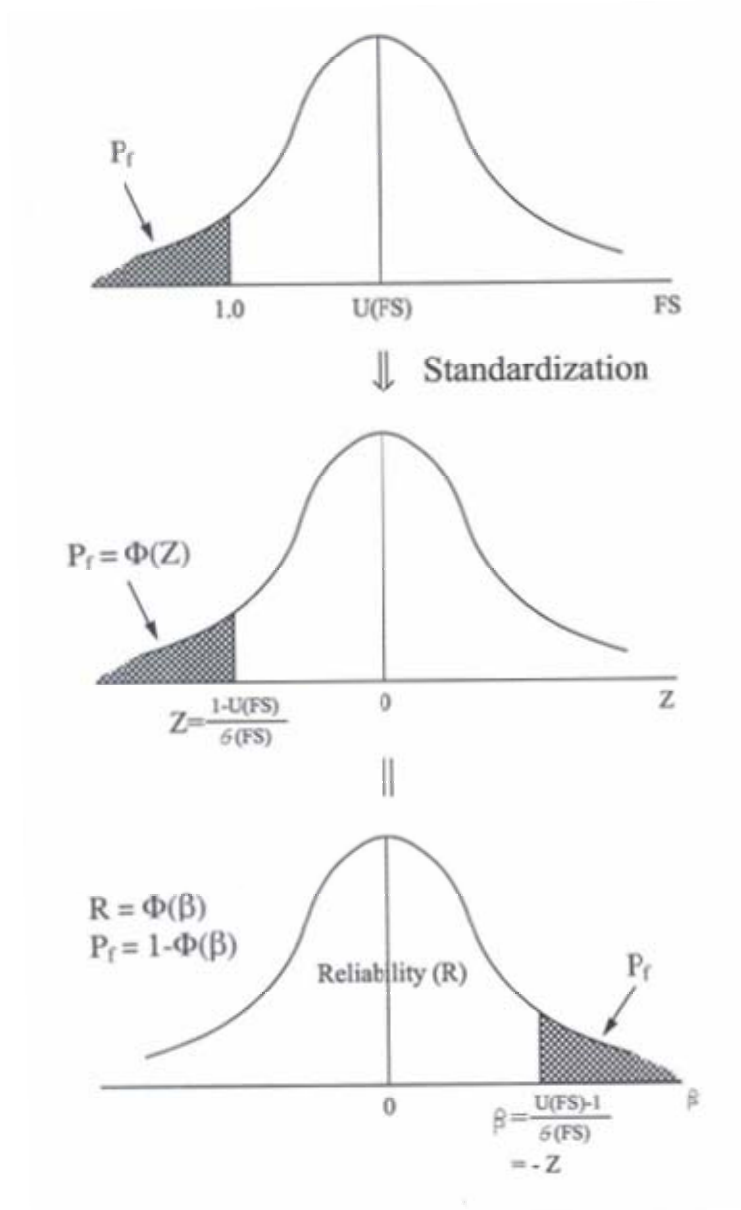
In the analysis, the probability of failure (P_f) is calculated assuming that the FS follows the normal distribution as shown in Figure 7.8. The probabilities of failure [$P(FS < 1.0)$] for planar and wedge failures in the VMT slopes are calculated.

7-2. Rock Slopes in VMT

7-2-1. Limitations of This Analysis

During the field investigations, discontinuity data were measured on those relatively critical slopes located adjacent to the existing VMT facilities. These include the Ballast Water Treatment Plant (“BWT Slope”), the Power House and Vapor Recovery Plant (“PVR Slope”), the West Manifold Building (“WM Slope”), the West Tank Farm Slope (“WTF Slope”), and the East Tank Farm Slope (“ETF Slope”). Discontinuity data were also obtained from the less critical slopes located adjacent to the existing facilities. These include the Power House Road Slope, the Tea Shelter Slope, and the rock quarries located on the southern portion of the VMT site.

Figure 7.8 Probability of failure (P_f) (Cho, 2002)



During the field investigations, in most of the critical slopes, it was difficult to gain access to the higher portions of the cut slopes so most of the data were obtained along the base of the slopes. Therefore, the data measured for the site may not be fully representative of the entire rock slope.

It was observed that the critical slopes have been reinforced with rock bolts in the BWT Slope, PVR Slope, and the first tier of WM Slope. It appears that the slopes have a minimum of four rock bolts per unit width extending up the slope. Due to the limited information available, tension values equal to 400 kips per rock block to be analyzed was assumed, yielding conservative analyses. Rock bolts were originally tensioned to 100 kips per bolt as indicated in the reference document (Bukovansky, 1990).

In the FS analysis, it was also assumed that the discontinuity planes involved were through-going, meaning that the fracture is continuous through out the block as shown in Figures 7.5 and 7.7. The concept of a through-going fracture is commonly accepted in the engineering practice. However, if the discontinuity is not through-going, the FS becomes higher than that determined assuming a through-going fracture. Fracture continuity is one of the most important parameters that affect the rock mass strength, and it is also very difficult to quantify.

The mechanical properties of the rock slope discontinuities include unit weight, friction angle of the potential failure plane, and cohesion. These were also assumed based on a literature review. In this analysis, cohesion was assumed to be zero and the friction angles of 30 degrees and 45 degrees were assumed for foliations and joints, respectively. Unit weight of the rock was assumed to be 160 pcf.

In the factor of safety calculations involving earthquake loading conditions, the slope is considered to be stable if the FS is greater than 1.0. In the same manner, the slope is considered to be unstable if the FS is less than 1.0.

7-2-2. BWT Slope

A. Site Observations

The BWT slope is located immediately south of the Ballast Water Treatment facilities. Based on the topographic map provided, the height of the slope ranges approximately from 120 feet to 160 feet.

The BWT slope consists of hard, competent greenstone. The major discontinuities are foliations, joints, and a fault located in the west end of this slope. It appears that the strike and dip of the fault are approximately N20W and 62SW, respectively. It rises higher toward the road above the slope.

Rock bolts have been installed in this slope using both random and systematic patterns. Based upon available information (Bukovansky, 1990), the bolts were installed using 5 to 10 foot staggered patterns, whereas, some bolts were installed in an approximately 20 foot pattern.

During the site visit, it was observed that a number of blocks of various sizes, most of them less than about one foot in diameter, have fallen from the cut slopes.

B. Kinematic Analysis

The major discontinuities measured in this slope are listed in Table 7.2 and the pole plot of these data is illustrated in Figure 7.9. Based on the kinematic analysis shown in Figures 7.10A and 7.10B, and Figures 7.12A and 7.12B, it is anticipated that wedge failures are most prominent with planar failure and toppling being less prominent for the

major cut slope behind the BWT facilities. It is also anticipated that local planar and wedge failures and toppling can occur along the cut slope located west of the BWT facilities. However, it appears that the slope west of the BWT facilities is not a major concern due to its low height ranging approximately from 30 feet to 40 feet and the significant distance from the facilities.

For the BWT slope, the major joints which were kinematically unstable are J2 (62/037), J3 (80/292), and J4 (85/086). These joints were considered in the subsequent kinetic analysis. Results of the kinematic analysis are summarized in Table 7.3.

C. Kinetic Analysis

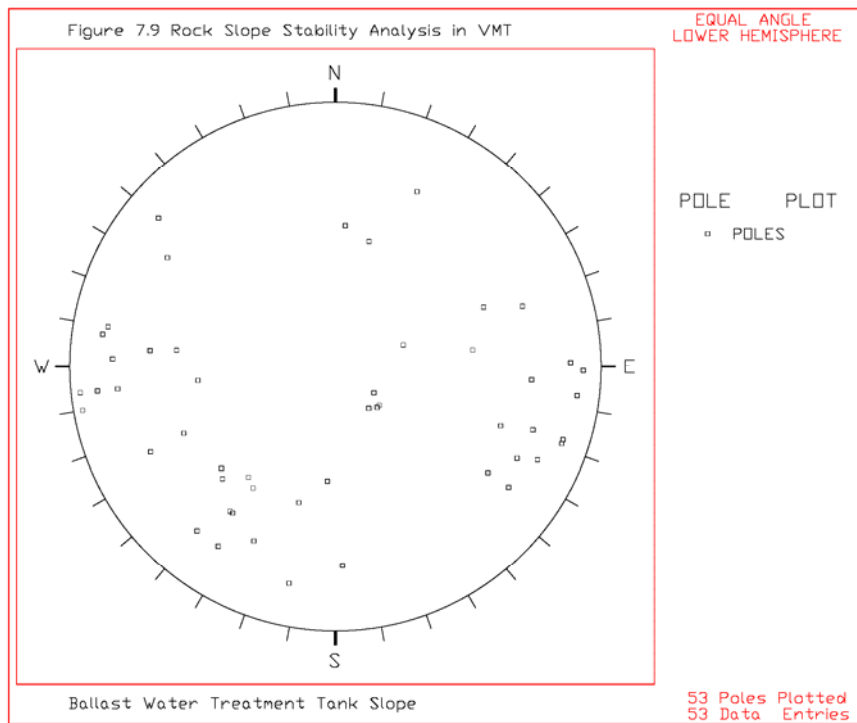
Based on the kinetic analysis of joint set J2 that was kinematically unstable in the planar failure mode, the factor of safety (FS) ranged from 1.27 to 0.95 under the pore pressure conditions of dry to fully saturated conditions without earthquake loading conditions. Under earthquake loading conditions using a range from 0.1g to 0.7g and when adding pore pressure conditions, the FS ranges from 1.11 to 0.33. Under the earthquake conditions considering both horizontal and vertical accelerations and dry conditions ($H_w/H_{\text{slope}} = 0$), the FS ranges from 1.11 to 0.52. For this planar failure mode, the minimum external loading condition that can cause the planar failure is the pore pressure equal to $0.9H_w/H_{\text{slope}}$. If both earthquake and pore pressure loadings are considered, the $0.6H_w/H_{\text{slope}}$ with 0.1g of horizontal acceleration will cause the planar failure to occur. The results of the kinetic analysis for planar failure conditions are shown in Figures 7.11A through 7.11C.

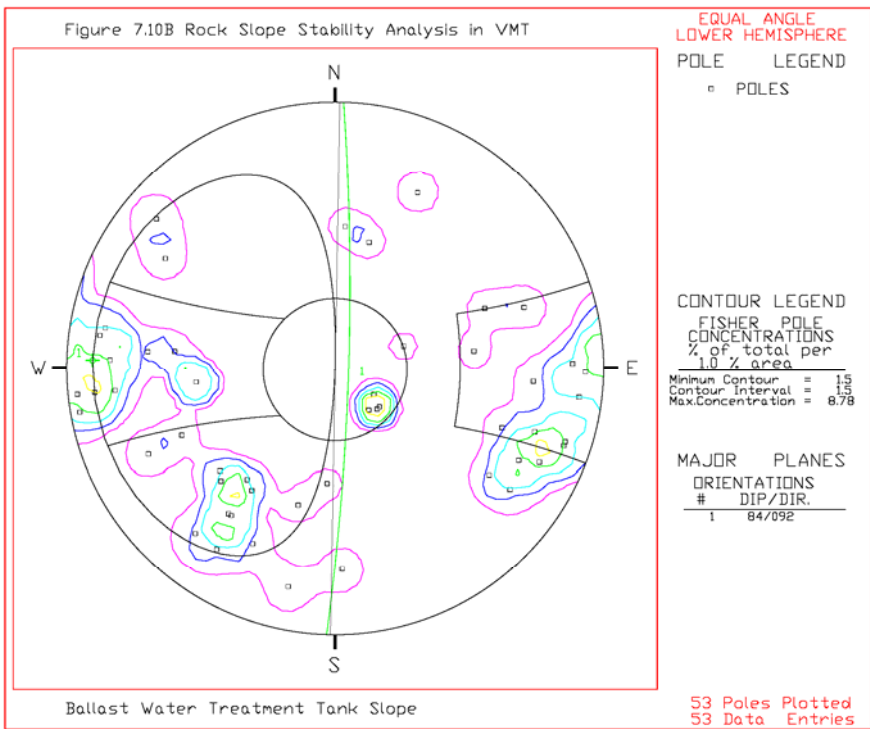
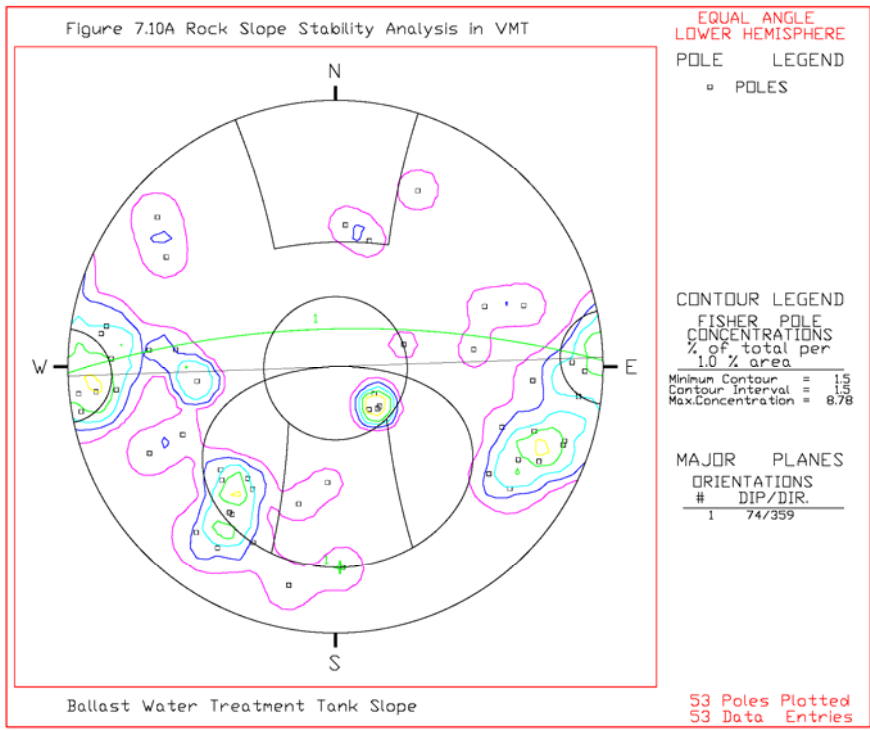
Table 7.2 Discontinuities in the BWT Slope

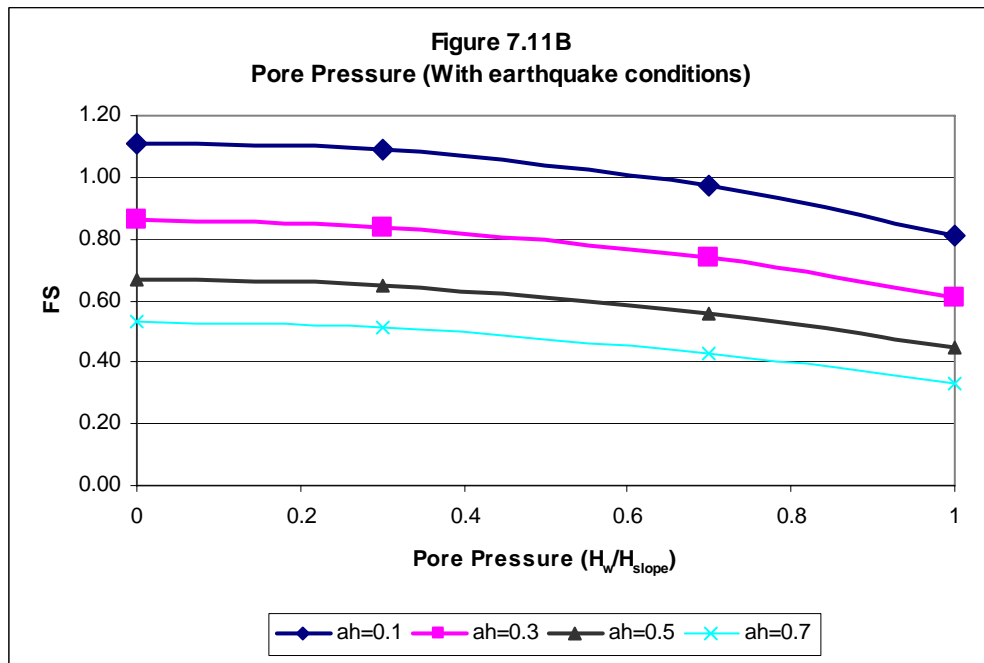
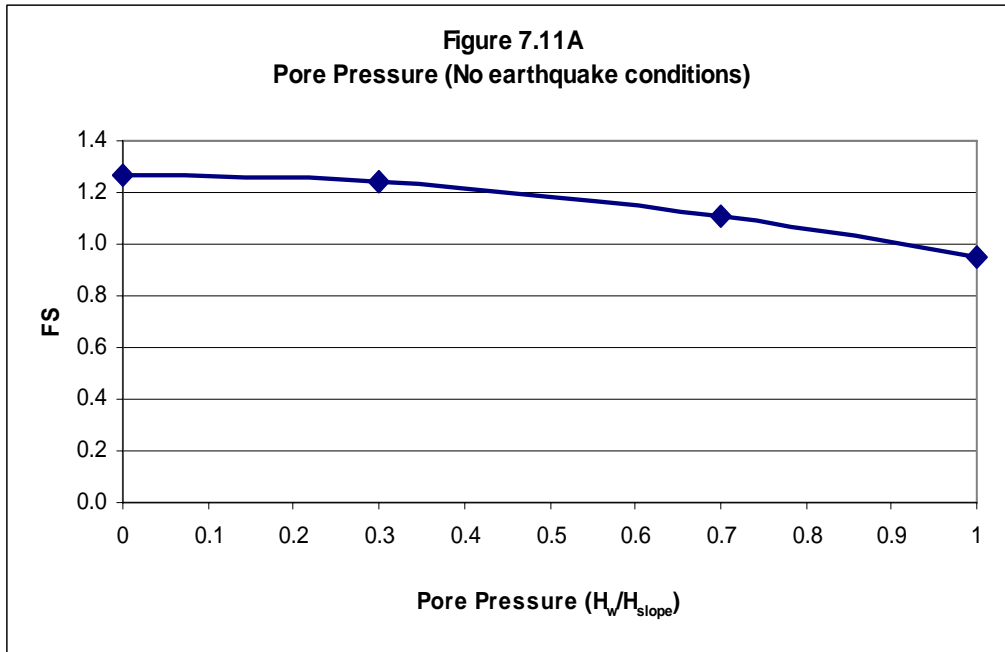
Slope Face	Trend= Face Angle=	N88E 74NW	Dip Dir=	358
No.	Strike	Dip (+/-)	Dip	Dip Direction
1	N88E	74-	74NW	358
2	N4E	73-	73NW	274
3	N6E	62+	62SE	96
4	N6W	84+	84NE	84
5	N24W	64+	64NE	66
6	N33E	74+	74SE	123
7	N7E	85-	85NW	277
8	N6W	55+	55NE	84
9	N6W	55+	55NE	84
10	N6W	55+	55NE	84
11	N6W	88+	88NE	84
12	N50W	78+	78NE	40
13	N6W	79+	79NE	84
14	N19E	84-	84NW	289
15	N27E	75-	75NW	297
16	N52W	56+	56NE	38
17	N35E	70-	70NW	305
18	N55W	68+	68NE	35
19	N40E	82+	82SE	130
20	N2E	80+	80SE	92
21	N35E	77-	77NW	305
22	N1E	86-	86NW	271
23	N35E	20-	20NW	305
24	N78W	80+	80NE	12
25	N18E	76-	76NW	288
26	N18E	84-	84NW	288
27	N22W	62-	62SW	248
28	N54W	68+	68NE	36
29	N75W	56+	56NE	15
30	N45W	62+	62NE	45
31	N57W	78+	78NE	33
32	N25E	80-	80NW	295
33	N65W	72+	72NE	25
34	N25W	75+	75NE	65
35	N5E	70+	70SE	95
36	N20E	67-	67NW	290
37	N52E	23-	23NW	322
38	N42W	60+	60NE	48
39	N18W	73-	73SW	252
40	N45E	25-	25NW	315

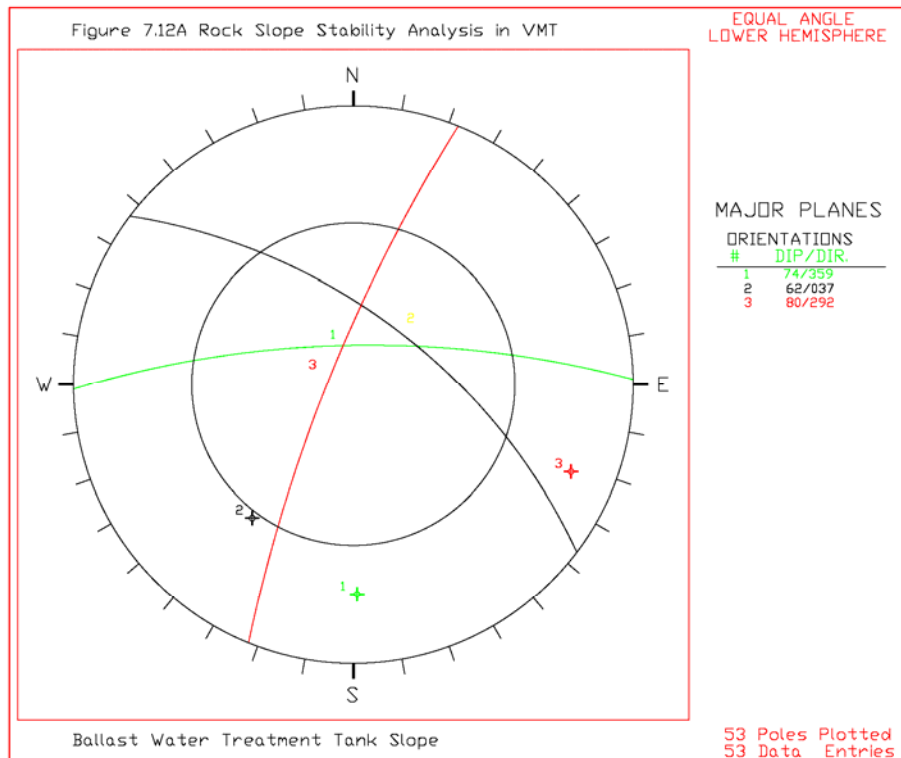
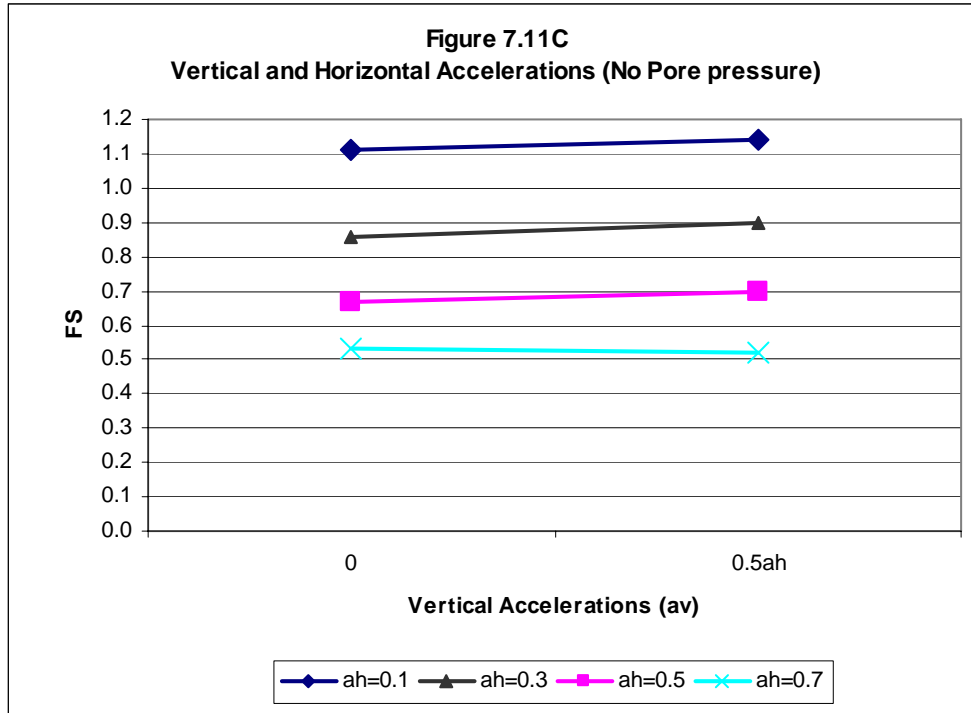
Table 7.2 Discontinuities in the BWT Slope (Continued.)

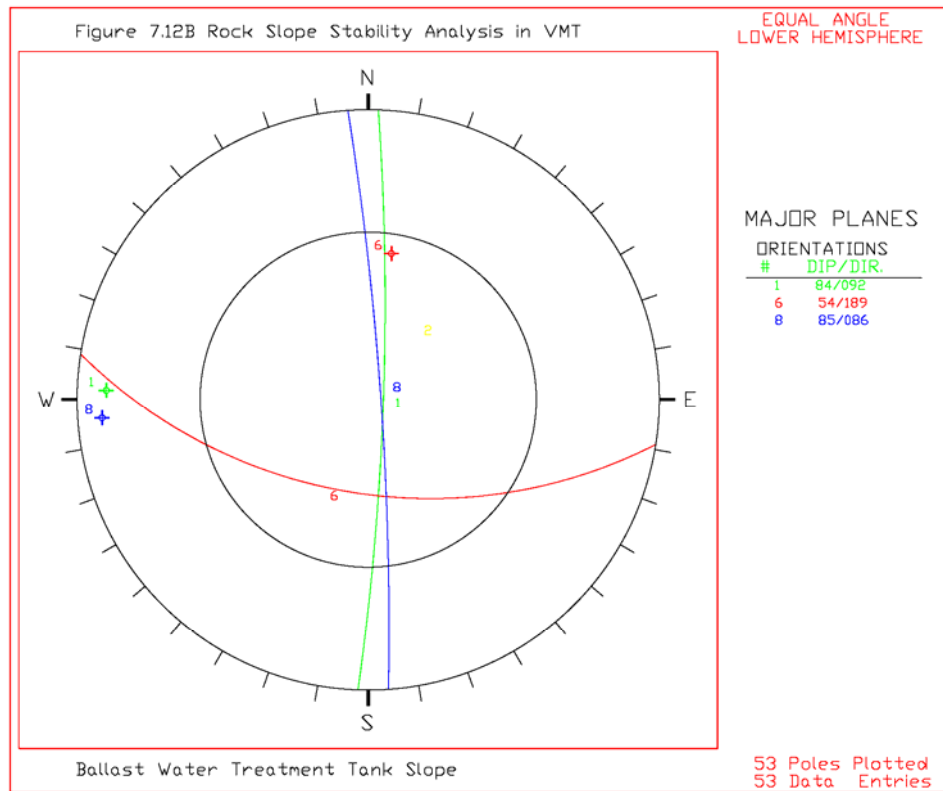
41	N42E	25-	25NW	312
42	N42E	25-	25NW	312
43	N10E	82+	82SE	100
44	N1W	83-	83SW	269
45	N56W	58+	58NE	34
46	N10W	88+	88NE	80
47	N86W	47+	47NE	4
48	N18W	30-	30SW	252
Slope Face	Trend= Face Angle=	N1E 84SE	Dip Dir=	91
49	N65W	72-	72SW	205
50	N8E	83+	83SE	98
51	N7W	55-	55SW	263
52	N86W	56-	56SW	184
53	N75W	52-	52SW	195











The kinetic analysis was also performed on the joint sets that form the most unfavorable wedge failure. Based on the kinetic analysis of the intersection of joint sets J2 and J3 that were kinematically unstable in the wedge failure mode, the factor of safety (FS) ranges from 1.38 to 0.51 under the pore pressures of dry to fully saturated conditions without earthquake loading conditions. Under earthquake loading conditions ranging from 0.1g to 0.7g, adding pore pressure conditions, the FS ranges from 1.21 to zero. Under the earthquake conditions considering both horizontal and vertical accelerations and dry conditions ($H_w/H_{slope} = 0$), the FS ranges from 1.21 to 0.31.

Table 7.3 Kinematic Analysis for the BWT Slope

1. Orientation of slope face

E-W trend slope face south of BWT: 74/359 (Dip/Dip Direction)
 N-S trend slope face west of BWT: 84/092 (Dip/Dip Direction)

2. Major Discontinuities

Joint Set	J1	J2	J3	J4	J5	J6
Type	Joint	Foliation	Joint	Joint	Joint	Foliation
Dip	78	62	80	85	54	23
Dip Direction	126	037	292	086	189	313

3. Kinematic analysis for E-W trend slope face:

A. Potential joint or joint sets for plane failure

Joint Sets:	Joint in J2:	47/004
-------------	--------------	--------

B. Potential joint or joint sets for wedge failure

2 joint sets	J2 & J3	J3 & J4
--------------	---------	---------

C. Potential joint or joint sets for toppling

Joint Sets:	J5
-------------	----

4. Kinematic analysis for N-S trend slope face:

A. Potential joint or joint sets for plane failure

Joint Sets:	Joint in J4:	55/084
-------------	--------------	--------

B. Potential joint or joint sets for wedge failure

2 joint sets	J4 & J5
--------------	---------

C. Potential joint or joint sets for toppling

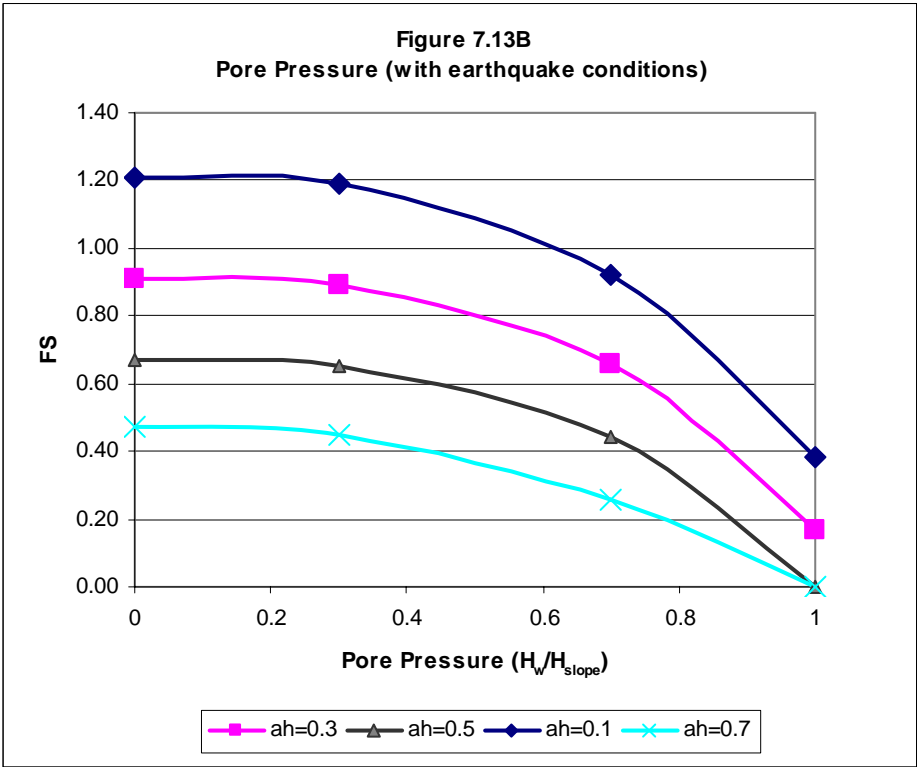
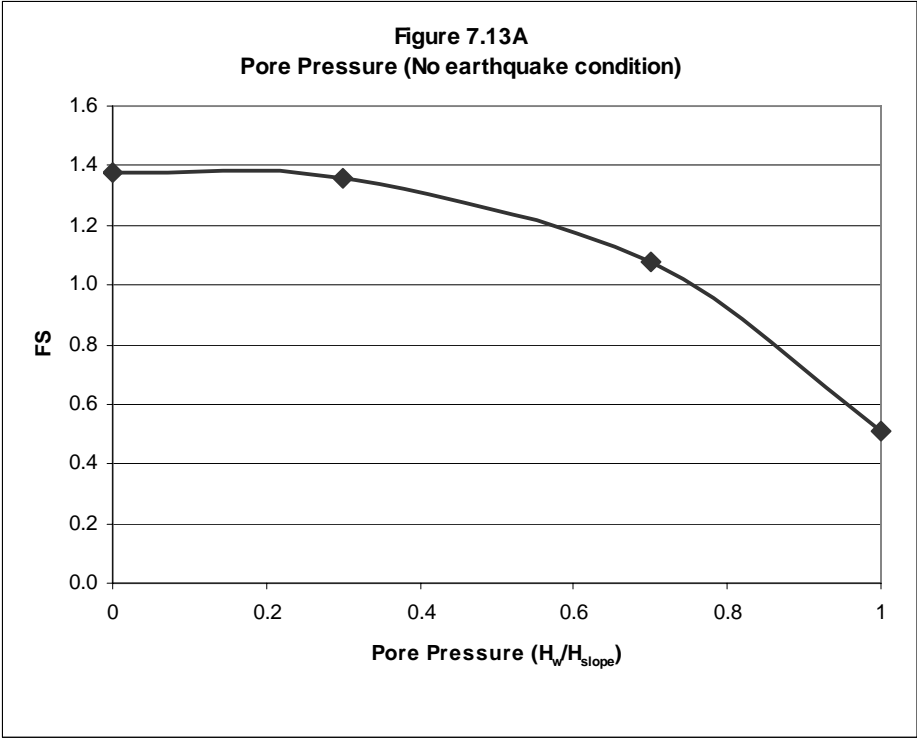
Joint Sets:	J3
-------------	----

For this wedge failure mode, the minimum external loading condition that can cause wedge failure is the pore pressure equal to $0.7H_w/H_{\text{slope}}$. If both earthquake and pore pressure loadings are considered together, the $0.6H_w/H_{\text{slope}}$ with 0.1g of horizontal acceleration will cause the wedge failure to occur. The results of the kinetic analysis for the wedge failure conditions are shown in Figures 7.13A through 7.13C.

Therefore, it is anticipated that a slope failure in the BWT is likely to occur, depending upon the imposed conditions on the slope. Therefore, it should be anticipated that a wedge failure is likely to occur in the BWT slope with a small increase in pore pressure and/or small magnitude earthquake.

D. Probability of Failure

The probability of failure (P_f) calculated using the planar failure mode in kinetic analysis ranges from 0.2 to 100%, depending upon the imposed loading conditions (Tables 7.4A and 7.4B). The probability of failure (P_f) calculated using the wedge failure mode in kinetic analysis ranges from zero to 100%, depending upon the imposed loading conditions (Tables 7.5A and 7.5B).



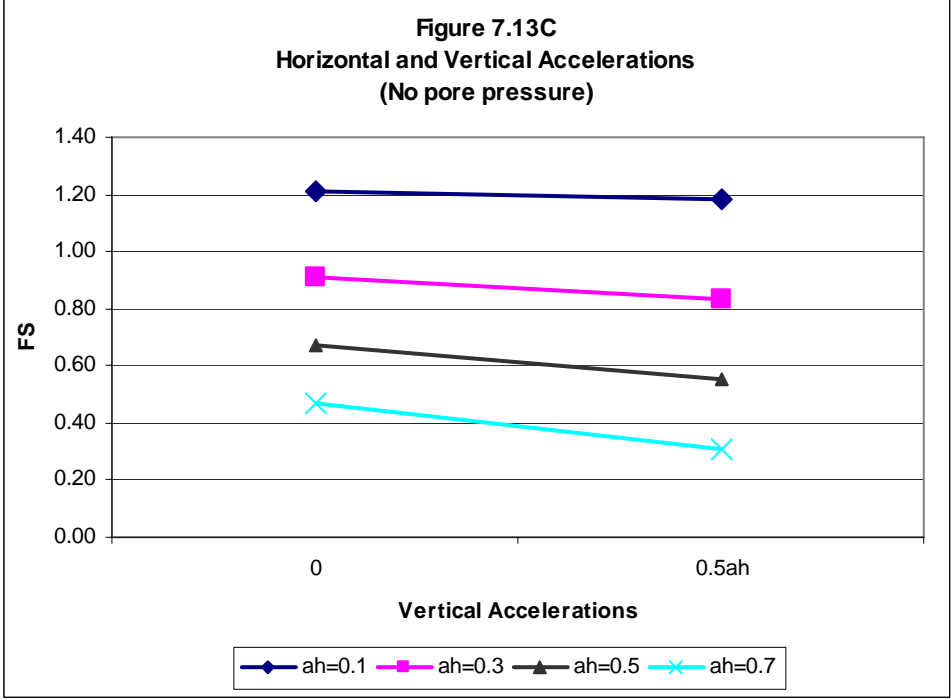


Table 7.4A Probability of failure for J2 in BWT Slope

Parameters		$H_w/H_{\text{slope}}=0$				
		$a_h=0.0$	$a_h=0.1$	$a_h=0.3$	$a_h=0.5$	$a_h=0.7$
Unit weight (γ , pcf)	Mean	160	160	160	160	160
	Stdev	8.0	8.0	8.0	8.0	8.0
	FS(γ) -	1.31	1.15	0.89	0.70	0.55
	FS(γ) +	1.24	1.08	0.83	0.65	0.50
	$d(\text{FS})/d(\gamma)$	-0.004	-0.004	-0.004	-0.003	-0.003
Tangent of Friction Angle	Mean	0.577	0.577	0.577	0.577	0.577
	Stdev	0.070	0.070	0.070	0.070	0.070
	FS(ϕ) -	1.19	1.04	0.82	0.65	0.51
	FS(ϕ) +	1.36	1.19	0.91	0.70	0.54
	$d(\text{FS})/d(\tan\phi)$	1.216	1.073	0.644	0.358	0.215
Cohesion (psf)	Mean	0	0	0	0	0
	Stdev	0	0	0	0	0
	FS(C) -	1.27	1.11	0.86	0.67	0.53
	FS(C) +	1.27	1.11	0.86	0.67	0.53
	$d(\text{FS})/d(c)$	0.000	0.000	0.000	0.000	0.000
Factor of Safety (FS)	Mean FS	1.27	1.11	0.86	0.67	0.53
	Stdev(FS)	0.092	0.083	0.054	0.035	0.029
	COV(FS)	0.072	0.075	0.063	0.053	0.055
Reliability Index	β	2.937	1.329	-2.589	-9.334	-16.121
Probability of Failure ($P(\text{FS}<1.0)$)	P(f)	0.001656	0.091913	0.995182	1.000000	1.000000

Note :

1. "FS (i) - and FS (i) +" are FS values from "mean - std and mean + std" of i parameter
2. cov (γ) = 3-7 %, 5 % (8 pcf) is assumed in this analysis.
3. cov (ϕ) = 2-13 %, But 13 % (4 degree) is assumed in this analysis.
4. cov (c) = 13-40 %, 24 % is assumed in this study.

Table 7.4B Probability of failure for J2 in BWT Slope

Parameters		$H_w/H_{slope}=1$				
		$a_h=0.0$	$a_h=0.1$	$a_h=0.3$	$a_h=0.5$	$a_h=0.7$
Unit weight (γ , pcf)	Mean	160	160	160	160	160
	Stdev	8.0	8.0	8.0	8.0	8.0
	FS(γ) -	0.97	0.83	0.62	0.46	0.34
	FS(γ) +	0.93	0.80	0.59	0.44	0.32
	d(FS)/d(γ)	-0.003	-0.002	-0.002	-0.001	-0.001
Tangent of Friction Angle	Mean	0.577	0.577	0.577	0.577	0.577
	Stdev	0.070	0.070	0.070	0.070	0.070
	FS(ϕ) -	0.91	0.79	0.60	0.46	0.35
	FS(ϕ) +	0.98	0.84	0.61	0.44	0.31
	d(FS)/d($\tan\phi$)	0.501	0.358	0.072	-0.143	-0.286
Cohesion (psf)	Mean	0	0	0	0	0
	Stdev	0	0	0	0	0
	FS(C) -	0.95	0.81	0.61	0.45	0.33
	FS(C) +	0.95	0.81	0.61	0.45	0.33
	d(FS)/d(c)	0.000	0.000	0.000	0.000	0.000
Factor of Safety (FS)	Mean FS	0.95	0.81	0.61	0.45	0.33
	Stdev(FS)	0.040	0.029	0.016	0.014	0.022
	COV(FS)	0.042	0.036	0.026	0.031	0.068
Reliability Index	β	-1.240	-6.517	-24.666	-38.891	-29.963
Probability of Failure (P(FS<1.0))	P(f)	0.89258	1.00000	1.00000	1.00000	1.00000

Note :

1. "FS (i) - and FS (i) +" are FS values from "mean - std and mean + std" of i parameter
2. cov (γ) = 3-7 %, 5 % (8 pcf) is assumed in this analysis.
3. cov (ϕ) = 2-13 %, But 13 % (4 degree) is assumed in this analysis.
4. cov (c) = 13-40 %, 24 % is assumed in this study.

Table 7.5A Probability of failure for wedge of J2 and J3 in the BWT Slope

Parameters		$H_w/H_{\text{slope}}=0$				
		$a_h=0.0$	$a_h=0.1$	$a_h=0.3$	$a_h=0.5$	$a_h=0.7$
Unit weight (γ , pcf)	Mean	160	160	160	160	160
	Stdev	8.0	8.0	8.0	8.0	8.0
	FS(γ) -	1.42	1.24	0.94	0.70	0.50
	FS(γ) +	1.35	1.17	0.88	0.64	0.44
	d(FS)/d(γ)	-0.004	-0.004	-0.004	-0.004	-0.004
Tangent of Friction Angle	Mean	0.789	0.789	0.789	0.789	0.789
	Stdev	0.088	0.088	0.088	0.088	0.088
	FS(ϕ) -	1.28	1.12	0.86	0.65	0.48
	FS(ϕ) +	1.51	1.31	0.96	0.69	0.46
	d(FS)/d($\tan\phi$)	1.314	1.086	0.571	0.229	-0.114
Cohesion (psf)	Mean	0	0	0	0	0
	Stdev	0	0	0	0	0
	FS(C) -	1.38	1.21	0.91	0.67	0.47
	FS(C) +	1.38	1.21	0.91	0.67	0.47
	d(FS)/d(c)	0.000	0.000	0.000	0.000	0.000
Factor of Safety (FS)	Mean FS	1.38	1.21	0.91	0.67	0.47
	Stdev(FS)	0.120	0.101	0.058	0.036	0.032
	COV(FS)	0.087	0.084	0.064	0.054	0.067
Reliability Index	β	3.161	2.074	-1.543	-9.153	-16.760
Probability of Failure (P(FS<1.0))	P(f)	0.000786	0.019029	0.938644	1.000000	1.000000

Note :

1. "FS (i) - and FS (i) +" are FS values from "mean - std and mean + std" of i parameter

2. cov (γ) = 3-7 %, 5 % (8 pcf) is assumed in this analysis.

3. cov (ϕ) = 2-13 %, But 13 % (4 degree for J2 and 6 degree for J3) is assumed in this analysis.

4. cov (c) = 13-40 %, 24 % is assumed in this study.

Table 7.5B Probability of failure for wedge of J2 and J3 in the BWT Slope

Parameters		$H_w/H_{\text{slope}}=0.7$				
		$a_h=0.0$	$a_h=0.1$	$a_h=0.3$	$a_h=0.5$	$a_h=0.7$
Unit weight (γ , pcf)	Mean	160	160	160	160	160
	Stdev	8.0	8.0	8.0	8.0	8.0
	FS(γ) -	1.11	0.95	0.68	0.46	0.28
	FS(γ) +	1.06	0.90	0.64	0.42	0.24
	d(FS)/d(γ)	-0.003	-0.003	-0.003	-0.003	-0.003
Tangent of Friction Angle	Mean	0.789	0.789	0.789	0.789	0.789
	Stdev	0.088	0.088	0.088	0.088	0.088
	FS(ϕ) -	1.03	0.89	0.65	0.46	0.30
	FS(ϕ) +	1.15	0.93	0.66	0.41	0.21
	d(FS)/d($\tan\phi$)	0.686	0.229	0.057	-0.286	-0.514
Cohesion (psf)	Mean	0	0	0	0	0
	Stdev	0	0	0	0	0
	FS(C) -	1.08	0.92	0.66	0.44	0.26
	FS(C) +	1.08	0.92	0.66	0.44	0.26
	d(FS)/d(c)	0.000	0.000	0.000	0.000	0.000
Factor of Safety (FS)	Mean FS	1.08	0.92	0.66	0.44	0.26
	Stdev(FS)	0.065	0.032	0.021	0.032	0.049
	COV(FS)	0.060	0.035	0.031	0.073	0.189
Reliability Index	β	1.231	-2.499	-16.492	-17.491	-15.027
Probability of Failure (P(FS<1.0))	P(f)	0.10920	0.99377	1.00000	1.00000	1.00000

Note :

1. "FS (i) - and FS (i) +" are FS values from "mean - std and mean + std" of i parameter

2. cov (γ) = 3-7 %, 5 % (8 pcf) is assumed in this analysis.

3. cov (ϕ) = 2-13 %, But 13 % (4 degree for J2 and 6 degree for J3) is assumed in this analysis.

4. cov (c) = 13-40 %, 24 % is assumed in this study.

7-2-3. PVR Slope

A. Site Observations

The PVR slope is located immediately south of the Power and Vapor Recovery facilities. Based on the topographic map provided, the height of the slope ranges approximately from 110 feet to 130 feet.

The PVR slope consists of weathered phyllite. The slope is flatter in the western portion of the slope than the eastern slope because after the western slope failed in 1975 during construction, the slope was reduced to about 45 degrees. Subsequent stabilization measures were implemented, including rock bolting, dewatering, rock buttress construction at the toe and placement of an impermeable liner at the crest (Bukovansky, 1990). During the site visit, it was observed that there had been rock slab failures along the phyllite foliation. Dewatering of rock slopes is accomplished by the installation of horizontal drain holes drilled into the rock mass. Removing pore pressures from a slope can be a challenging process with conditions not unlike those when wells are drilled for water supply (Santi et al., 2001).

The major discontinuities observed in this slope are foliations and joints. Also, a fault was observed trending 20/285 (dip/dip direction). Based on the available information (Bukovansky, 1990), the bolts were installed in 5 foot to 10 foot staggered patterns.

B. Kinematic Analysis

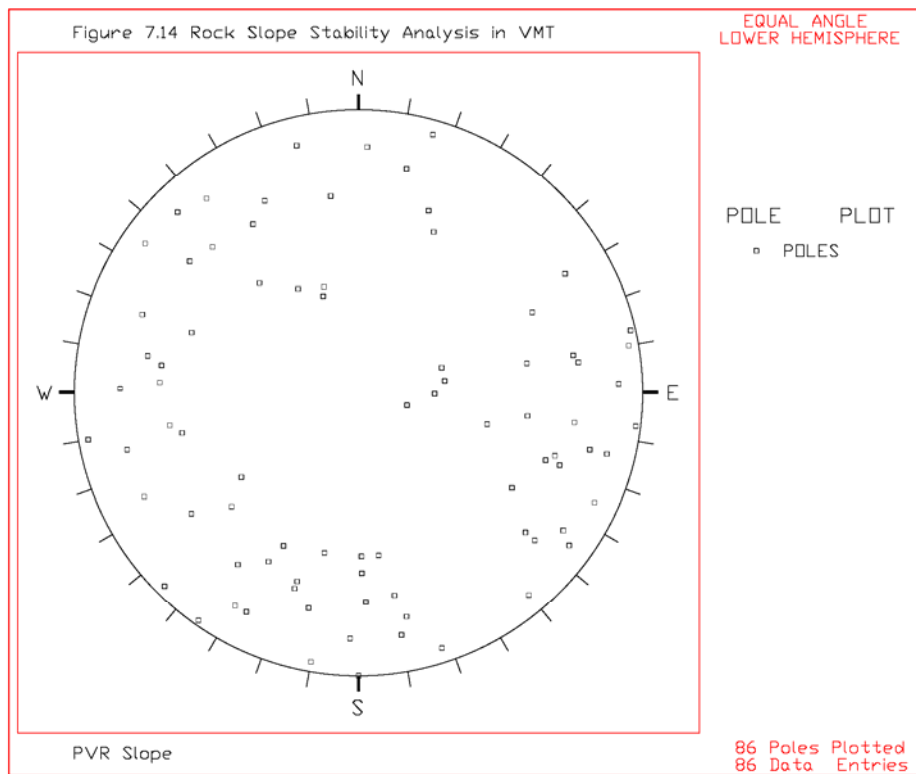
The major discontinuities measured in this slope are listed in Table 7.6 and the pole plot of these data is illustrated in Figure 7.14.

Table 7.6 Discontinuities in the PVR Slope

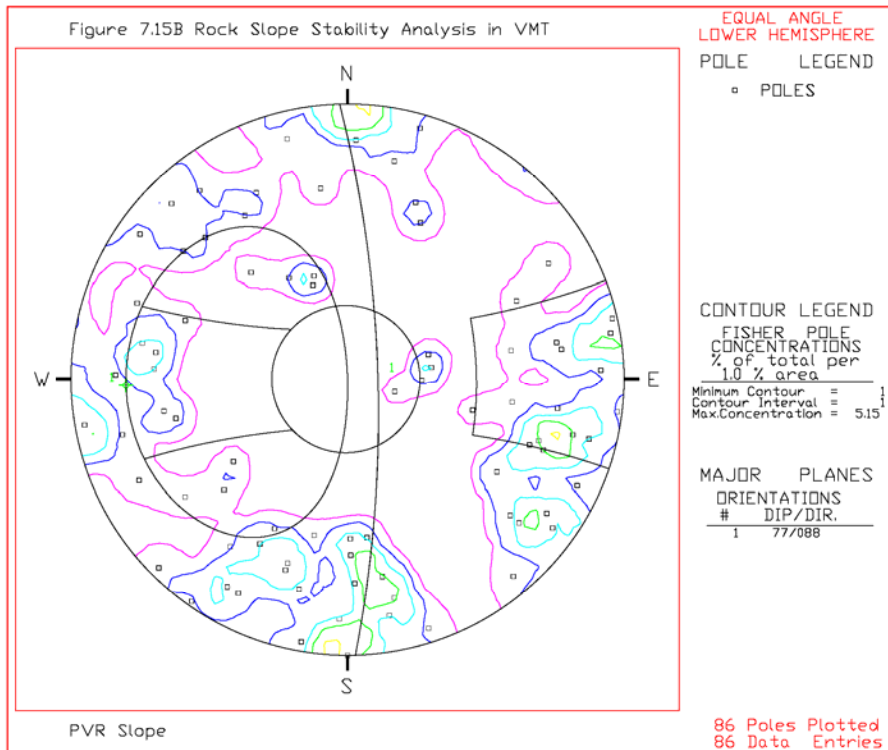
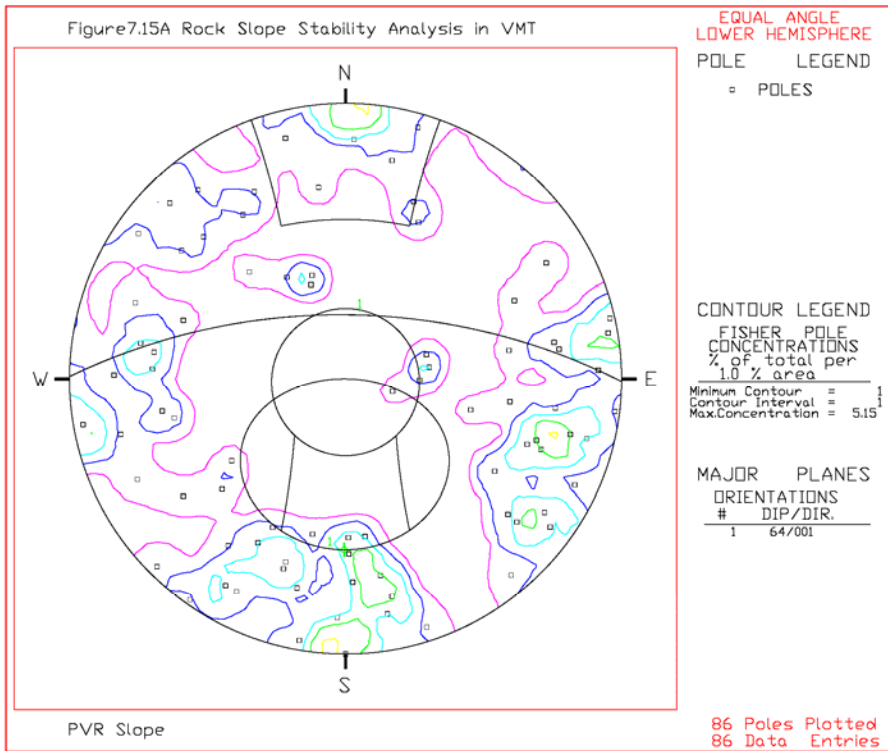
Slope Face	Trend= Face Angle=	E-W 64N	Dip Dir=	1
No.	Strike	Dip (+/-)	Dip	Dip Direction
1	N17W	34-	34SW	253
2	N40E	75-	75NW	310
3	N1E	80+	80SE	91
4	N50E	86-	86NW	320
5	N8W	76-	76SW	262
6	N32E	65-	65NW	302
7	N32E	65-	65NW	302
8	N76E	84+	84SE	166
9	N14E	84-	84NW	284
10	N1E	30-	30NW	271
11	N8E	75-	75NW	278
12	N74W	87-	87SW	196
13	N10W	75-	75SW	260
14	N34E	82-	82NW	304
15	N20E	74-	74NW	290
16	N82E	70+	70SE	172
17	N20E	70-	70NW	290
18	N18E	72-	72NW	288
19	N8E	70+	70SE	98
20	N10W	88+	88NE	80
21	N54E	90	90	Vertical
22	N36W	72+	72NE	54
23	N20E	78+	78SE	110
24	N3E	70+	70SE	93
25	N43W	90	90	Vertical
26	N13W	89-	89SW	257
27	N45E	84+	84SE	135
28	N78W	78-	78SW	192
29	N14E	80-	80NW	284
30	N87W	69-	69SW	201
31	N76E	90	90	Vertical
32	N20E	64+	64SE	110
33	N8W	34-	34SW	262
34	N10E	74+	74SE	100
35	N72E	43+	43SE	162
36	N88W	82-	82SW	182
37	N80E	82-	82NW	350
38	N8E	62-	62NW	278
39	N2W	85-	85SW	268
40	N15E	20-	20NW	285
41	N60E	46+	46SE	150

Table 7.6 Discontinuities in the PVR Slope (Continued.)

42	N45W	88+	88NE	45
43	N80W	88+	88NE	10
44	N36E	85-	85NW	306
45	N10W	88-	88SW	260
46	N25E	85-	85NW	295
47	N72E	87-	87NW	342
48	N14W	80+	80NE	76
49	N58E	70+	70SE	148
50	N30W	80-	80SW	240
51	N48E	55+	55SE	138
52	N7E	89-	89NW	277
53	N52E	82+	82SE	142
54	N70E	40+	40SE	160
55	N64W	62+	62NE	26
	Slope Face	Trend= Face Angle=	N1W 77NE	Dip Dir= 88
56	N40E	78-	78NW	310
57	N88E	73-	73NW	358
58	N65W	64-	64SW	205
59	N78E	78-	78NW	348
60	N55W	73+	73NE	35
61	N55W	89+	89NE	35
62	N10W	68+	68NE	80
63	N42W	62+	62NE	48
64	N77W	76+	76NE	13
65	N72W	72+	72NE	18
66	N36W	54+	54NE	54
67	N72W	70+	70NE	18
68	N62W	68+	68NE	28
69	N25W	68-	68SW	245
70	N60W	82+	82NE	30
71	N45E	72+	72SE	135
72	N88W	82+	82NE	2
73	N63W	82+	82NE	27
74	N13W	65+	65NE	77
75	N89E	60-	60NW	359
76	N64E	74+	74SE	154
77	N78W	60+	60NE	12
78	N35E	85+	85SE	125
79	N89E	65-	65NW	359
80	N80E	72-	72NW	350
81	N80E	72-	72NW	350
82	N14E	50-	50NW	284
83	N10W	62-	62SW	260
84	N83E	60-	60NW	353
85	N38E	74+	74SE	128
86	N26W	80+	80NE	64



Based on the kinematic analysis shown in Figures 7.15A and 7.15B, and Figures 7.17A and 7.17B, it is anticipated that joint J5 (88/003) and the intersection of joint sets J3 (80/307) and J4 (73/096) are kinematically unstable with regard to planar and wedge failures along the slope south of the PVR facilities. It is also anticipated that local toppling along the south and west sides of the facilities and the local planar and wedge failures along the slope west of the facilities, can occur for this slope. However, it appears that toppling is not a major concern due to the lower height of the slope and the great distance to the facilities.

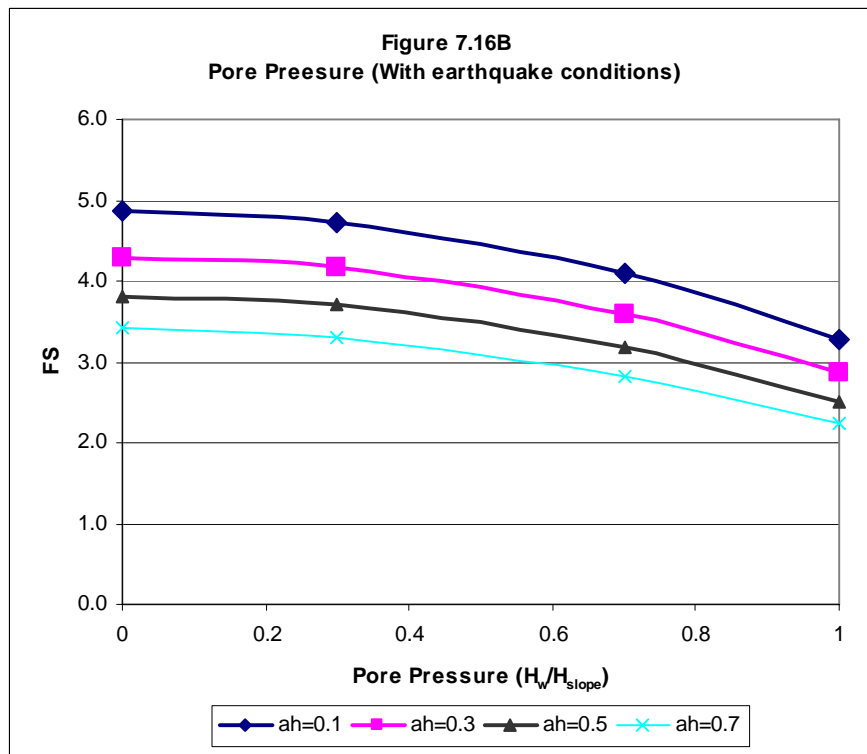
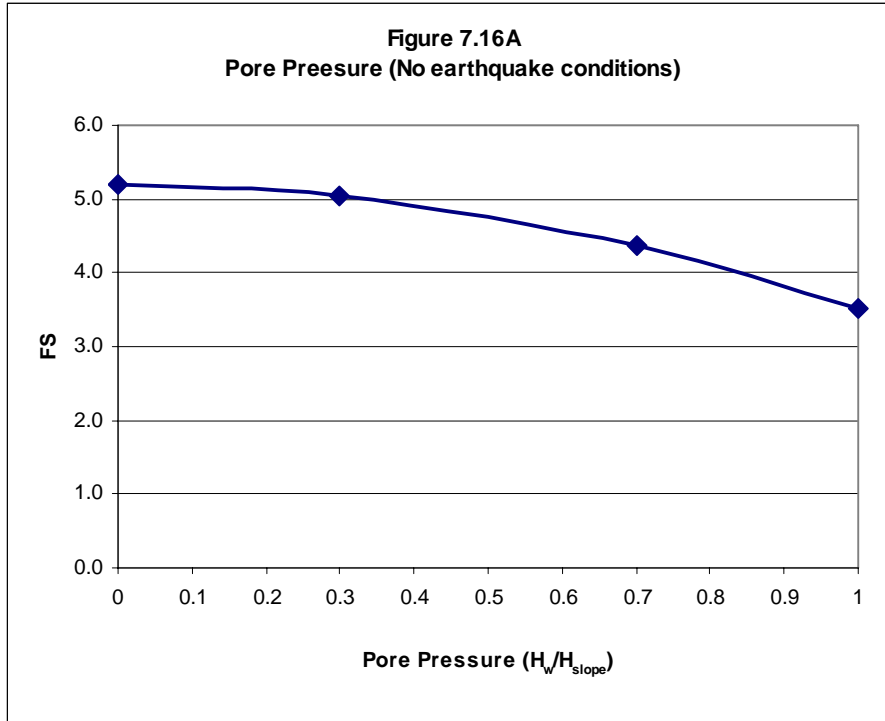


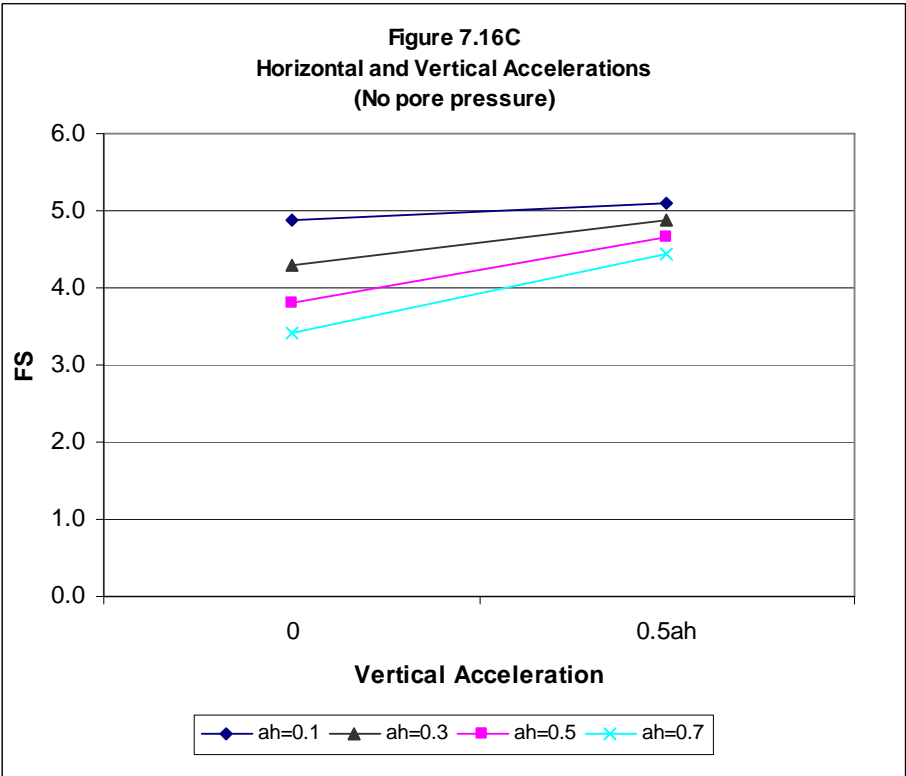
The major joints sets which can cause planar or wedge failures in the PVR slope were used for the subsequent kinetic analysis. Results of the kinematic analysis are summarized in Table 7.7.

C. Kinetic Analysis

Based on the kinetic analysis on joint set J2 that was kinematically unstable in the planar failure mode, the factor of safety (FS) ranges from 5.20 to 3.53 under the pore pressure conditions of zero to saturated condition ($H_w/H_{\text{slope}} = 1$) without earthquake loading conditions. Under earthquake loading conditions ranging from 0.1g to 0.7g in addition to the pore pressure conditions, the FS ranges from 4.87 to 2.23 under various pore pressure conditions. Under the earthquake conditions considering both horizontal and vertical accelerations and dry conditions ($H_w/H_{\text{slope}} = 0$), the FS ranges from 5.09 to 3.42 under earthquake loading conditions ranging from 0.1g to 0.7g.

It appears that the PVR slope is stable with regards to the planar failure based on the parameters considered. The results of the kinetic analysis of the planar failure are shown in Figures 7.16A through 7.16C.





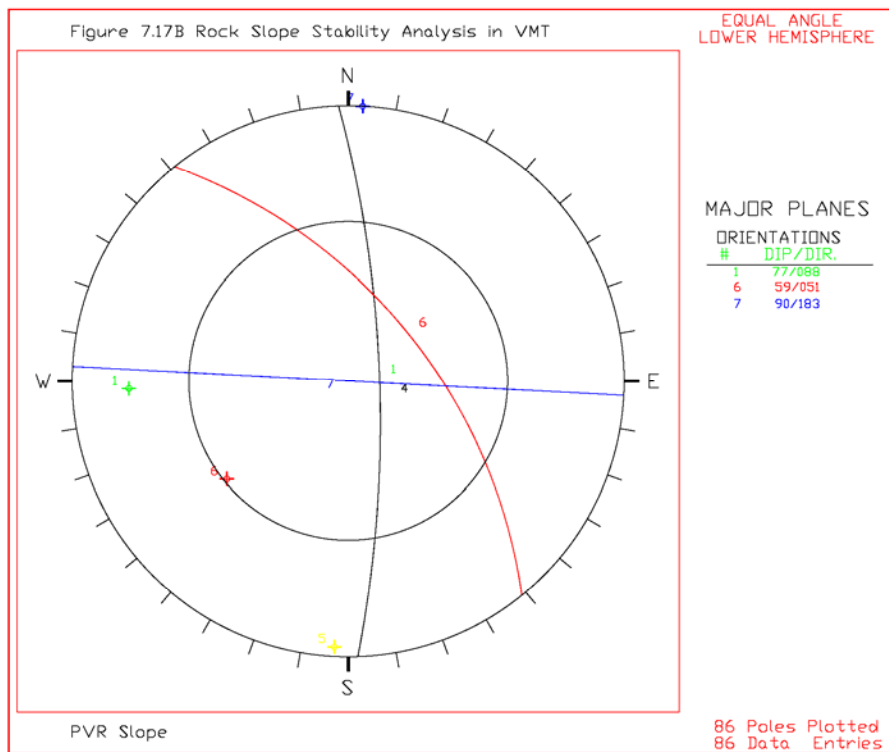
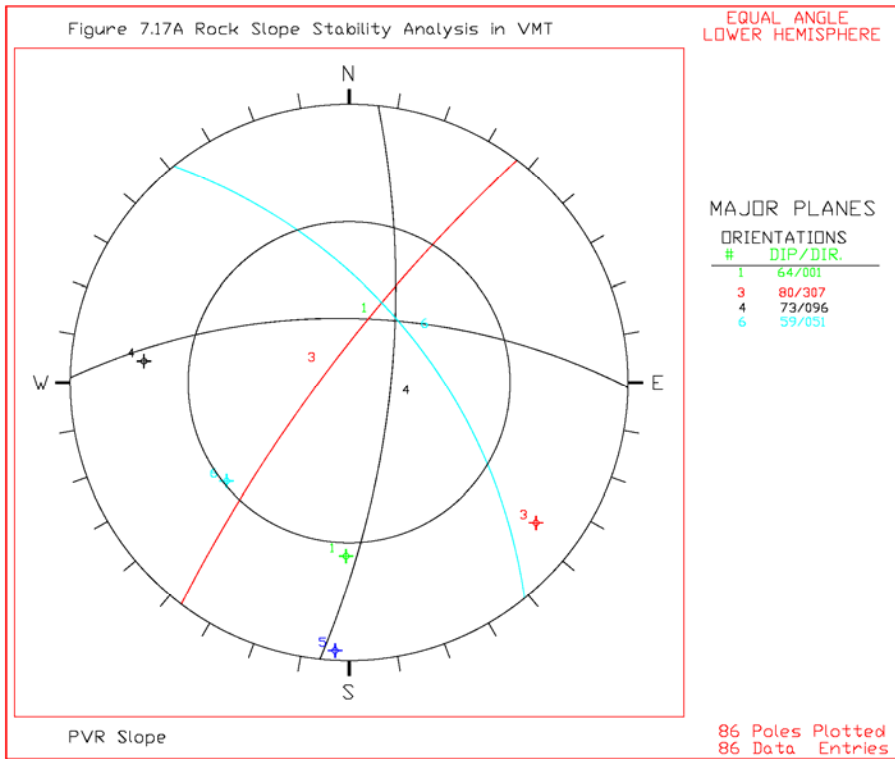


Table 7.7 Kinematic Analysis for the PVR Slope

1. Orientation of slope face

E-W trend slope face: 64/001 (Dip/Dip Direction)
 N-S trend slope face: 77/088 (Dip/Dip Direction)

2. Major Discontinuities

Joint Set	J1	J2	J3	J4	J5	J6	J7
Type	Joint	Foliation	Joint	Joint	Foliation	Joint	Joint
Dip	87	77	80	73	88	59	90
Dip Direction	261	285	307	096	003	051	183

3. Kinematic analysis for E-W trend slope face:

A. Typical joint or joint sets for plane failure

Joint Sets:	Some joints in J5:		60/012
-------------	--------------------	--	--------

B. Typical joint or joint sets for wedge failure

2 joint sets	J3 & J4
--------------	---------

C. Typical joint or joint sets for toppling

Joint Sets:	J7
-------------	----

4. Kinematic analysis for N-S trend slope face:

A. Typical joint or joint sets for plane failure

Joint Sets:	J4
-------------	----

B. Typical joint or joint sets for wedge failure

2 joint sets	J6 & J7
--------------	---------

C. Typical joint or joint sets for toppling

Joint Sets:	J1
-------------	----

A kinetic analysis was performed on the joint sets of joints J3 and J4 that were kinematically unstable in the wedge failure mode. The FS ranges from 2.77 to zero under the pore pressure conditions of zero to saturated condition ($H_w/H_{slope} = 1$) without earthquake loading conditions. Under earthquake loading conditions ranging from 0.1g to 0.7g in addition to the pore pressure conditions, the FS ranges from 2.28 to zero under various pore pressure conditions. Under the earthquake conditions considering both horizontal and vertical accelerations and dry conditions ($H_w/H_{slope} = 0$), the FS ranges from 2.28 to zero under earthquake loading conditions ranging from 0.1g to 0.7g. For this wedge failure mode, the minimum external loading condition that can cause wedge failure is the pore pressure equal to $0.85H_w/H_{slope}$. If earthquake and pore pressure loadings are considered together, the $0.8H_w/H_{slope}$ with 0.1g of horizontal acceleration and the $0.55H_w/H_{slope}$ with 0.2g of horizontal acceleration will cause wedge failure to occur. The results of the kinetic analysis of the wedge failure are shown in Figures 7.18A through 7.18C.

D. Probability of Failure

The probability of failure (P_f) calculated using the planar failure mode in kinetic analysis was zero percent under the pore pressure ranging from dry to saturated conditions (Tables 7.8A and 7.8B). However, the P_f for the wedge failure ranges from zero to 100%, depending upon the imposed loading conditions. The P_f under dry and 0.7 (H_w/H_{slope}) conditions and various earthquake loading conditions for the wedge failure are listed in Tables 7.9A and 7.9B.

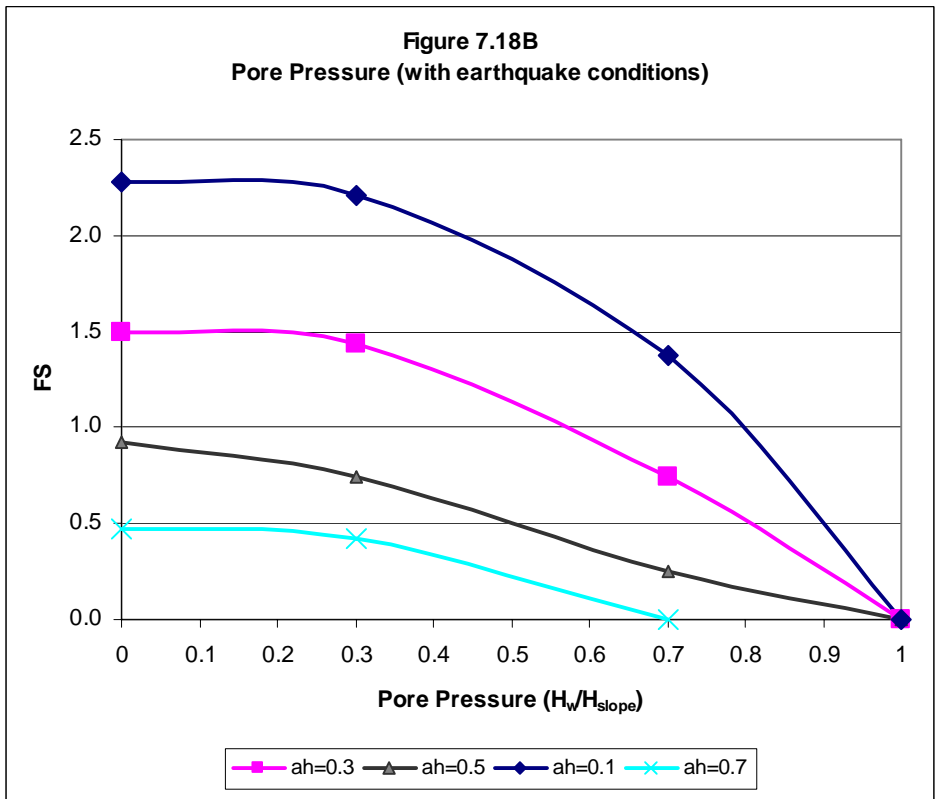
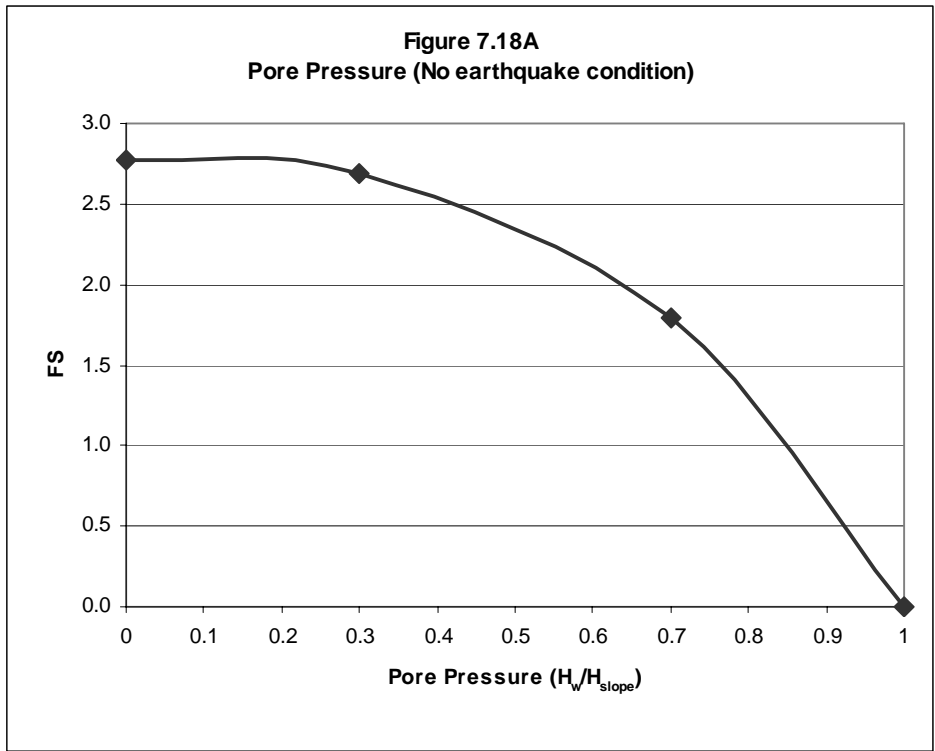


Figure 7.18C
Horizontal and Vertical Accelerations
(No pore pressure)

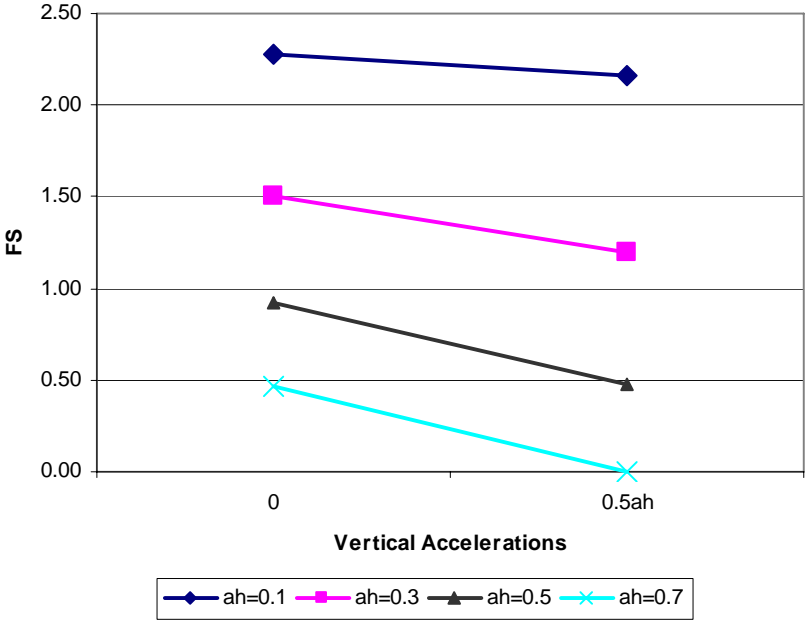


Table 7.8A Probability of failure for J5 in the PVR Slope

Parameters		H _w /H _{slope} =0				
		a _h =0.0	a _h =0.1	a _h =0.3	a _h =0.5	a _h =0.7
Unit weight (γ , pcf)	Mean	160	160	160	160	160
	Stdev	8.0	8.0	8.0	8.0	8.0
	FS(γ) -	5.46	5.11	4.51	4.01	3.60
	FS(γ) +	4.97	4.65	4.09	3.63	3.25
	d(FS)/d(γ)	-0.031	-0.029	-0.026	-0.024	-0.022
Tangent of Friction Angle	Mean	0.577	0.577	0.577	0.577	0.577
	Stdev	0.070	0.070	0.070	0.070	0.070
	FS(ϕ) -	5.15	4.83	4.27	3.81	3.43
	FS(ϕ) +	5.26	4.91	4.31	3.82	3.41
	d(FS)/d(tan ϕ)	0.787	0.572	0.286	0.072	-0.143
Cohesion (psf)	Mean	0	0	0	0	0
	Stdev	0	0	0	0	0
	FS(C) -	5.20	4.87	4.29	3.81	3.42
	FS(C) +	5.20	4.87	4.29	3.81	3.42
	d(FS)/d(c)	0.000	0.000	0.000	0.000	0.000
Factor of Safety (FS)	Mean FS	5.20	4.87	4.29	3.81	3.42
	Stdev(FS)	0.251	0.233	0.211	0.190	0.175
	COV(FS)	0.048	0.048	0.049	0.050	0.051
Reliability Index	β	16.727	16.577	15.596	14.784	13.806
Probability of Failure (P(FS<1.0))	P(f)	0.000000	0.000000	0.000000	0.000000	0.000000

Note :

1. "FS (i) - and FS (i) +" are FS values from "mean - std and mean + std" of i parameter
2. cov (γ) = 3-7 %, 5 % (8 pcf) is assumed in this analysis.
3. cov (ϕ) = 2-13 %, But 13 % (4 degree) is assumed in this analysis.
4. cov (c) = 13-40 %, 24 % is assumed in this study.

Table 7.8B Probability of failure for J5 in the PVR Slope

Parameters		$H_w/H_{slope}=1$				
		$a_h=0.0$	$a_h=0.1$	$a_h=0.3$	$a_h=0.5$	$a_h=0.7$
Unit weight (γ , pcf)	Mean	160	160	160	160	160
	Stdev	8.0	8.0	8.0	8.0	8.0
	FS(γ) -	3.70	3.44	3.00	2.65	2.35
	FS(γ) +	3.38	3.14	2.73	2.40	2.12
	d(FS)/d(γ)	-0.020	-0.019	-0.017	-0.016	-0.014
Tangent of Friction Angle	Mean	0.577	0.577	0.577	0.577	0.577
	Stdev	0.070	0.070	0.070	0.070	0.070
	FS(ϕ) -	3.74	3.49	3.06	2.71	2.42
	FS(ϕ) +	3.30	3.06	2.64	2.30	2.02
	d(FS)/d($\tan\phi$)	-3.146	-3.075	-3.003	-2.932	-2.860
Cohesion (psf)	Mean	0	0	0	0	0
	Stdev	0	0	0	0	0
	FS(C) -	3.53	3.28	2.86	2.51	2.23
	FS(C) +	3.53	3.28	2.86	2.51	2.23
	d(FS)/d(c)	0.000	0.000	0.000	0.000	0.000
Factor of Safety (FS)	Mean FS	3.53	3.28	2.86	2.51	2.23
	Stdev(FS)	0.272	0.262	0.250	0.240	0.231
	COV(FS)	0.077	0.080	0.087	0.096	0.103
Reliability Index	β	9.300	8.697	7.450	6.289	5.331
Probability of Failure (P(FS<1.0))	P(f)	0.00000	0.00000	0.00000	0.00000	0.00000

Note :

1. "FS (i) - and FS (i) +" are FS values from "mean - std and mean + std" of i parameter
2. cov (γ) = 3-7 %, 5 % (8 pcf) is assumed in this analysis.
3. cov (ϕ) = 2-13 %, But 13 % (4 degree) is assumed in this analysis.
4. cov (c) = 13-40 %, 24 % is assumed in this study.

Table 7.9A Probability of failure for wedge J3 & J4 in the PVR Slope

Parameters		$H_w/H_{slope}=0$				
		$a_h=0.0$	$a_h=0.1$	$a_h=0.3$	$a_h=0.5$	$a_h=0.7$
Unit weight (γ , pcf)	Mean	160	160	160	160	160
	Stdev	8.0	8.0	8.0	8.0	8.0
	FS(γ) -	2.78	2.29	1.51	0.93	0.48
	FS(γ) +	2.76	2.27	1.50	0.92	0.47
	d(FS)/d(γ)	-0.001	-0.001	-0.001	-0.001	-0.001
Tangent of Friction Angle	Mean	1.000	1.000	1.000	1.000	1.000
	Stdev	0.105	0.105	0.105	0.105	0.105
	FS(ϕ) -	2.28	1.88	1.25	0.77	0.40
	FS(ϕ) +	3.37	2.77	1.82	1.11	0.56
	d(FS)/d($\tan\phi$)	5.185	4.234	2.712	1.617	0.761
Cohesion (psf)	Mean	0	0	0	0	0
	Stdev	0	0	0	0	0
	FS(C) -	2.77	2.28	1.50	0.92	0.47
	FS(C) +	2.77	2.28	1.50	0.92	0.47
	d(FS)/d(c)	0.000	0.000	0.000	0.000	0.000
Factor of Safety (FS)	Mean FS	2.77	2.28	1.50	0.92	0.47
	Stdev(FS)	0.545	0.445	0.285	0.170	0.080
	COV(FS)	0.197	0.195	0.190	0.185	0.171
Reliability Index	β	3.247	2.876	1.754	-0.470	-6.612
Probability of Failure ($P(FS < 1.0)$)	P(f)	0.000583	0.002016	0.039705	0.680960	1.000000

Note :

1. "FS (i) - and FS (i) +" are FS values from "mean - std and mean + std" of i parameter
2. cov (γ) = 3-7 %, 5 % (8 pcf) is assumed in this analysis.
3. cov (ϕ) = 2-13 %, But 13 % (6 degree) is assumed in this analysis.
4. cov (c) = 13-40 %, 24 % is assumed in this study.

Table 7.9B Probability of failure for wedge J3 & J4 in the PVR Slope

$H_w/H_{slope}=0.7$

Parameters		$a_h=0.0$	$a_h=0.1$	$a_h=0.3$	$a_h=0.5$
Unit weight (γ , pcf)	Mean	160	160	160	160
	Stdev	8.0	8.0	8.0	8.0
	FS(γ) -	1.75	1.34	0.70	0.22
	FS(γ) +	1.83	1.42	0.77	0.28
	$d(FS)/d(\gamma)$	0.005	0.005	0.004	0.004
Tangent of Friction Angle	Mean	1.000	1.000	1.000	1.000
	Stdev	0.105	0.105	0.105	0.105
	FS(ϕ) -	1.49	1.15	0.62	0.23
	FS(ϕ) +	2.17	1.67	0.87	0.28
	$d(FS)/d(\tan\phi)$	3.235	2.474	1.189	0.238
Cohesion (psf)	Mean	0	0	0	0
	Stdev	0	0	0	0
	FS(C) -	1.79	1.38	0.74	0.25
	FS(C) +	1.79	1.38	0.74	0.25
	$d(FS)/d(c)$	0.000	0.000	0.000	0.000
Factor of Safety (FS)	Mean FS	1.79	1.38	0.74	0.25
	Stdev(FS)	0.342	0.263	0.130	0.039
	COV(FS)	0.191	0.191	0.175	0.156
Reliability Index	β	2.308	1.445	-2.003	-19.206
Probability of Failure (P(FS<1.0))	P(f)	0.01051	0.07429	0.97741	1.00000

Note :

1. "FS (i) - and FS (i) +" are FS values from "mean - std and mean + std" of i parameter
2. cov (γ) = 3-7 %, 5 % (8 pcf) is assumed in this analysis.
3. cov (ϕ) = 2-13 %, But 13 % (6 degree) is assumed in this analysis.
4. cov (c) = 13-40 %, 24 % is assumed in this study.

7-2-4. West Manifold Slope

A. Site Observations

The West Manifold Building slope is located immediately on the south and west sides of the West Manifold Building. The slope consists of both phyllite and greenstone. Based upon available information (Bukovansky, 1990), a portion of the slope failed during construction so that stabilizing measures had to be implemented. These included rock bolting, dewatering, shotcrete placement, and buttress construction at the toe.

The WM slope was excavated in a series of cuts and most discontinuity measurements at this time were performed on the bench above the first cut slope. Based on the topographic map provided, the height of the second slope that we investigated has an approximate range from 40 feet to 60 feet plus a small bench above the third slope. The slope continues to the West Farm Tank Area.

The major discontinuities are foliations and joints. It appears that the exposed rocks are relatively stronger than other slopes in VMT. Rock bolts were installed in the first slope, but the slope we investigated was not rock-bolted.

During the site visit, it was observed that various sizes of the rock fragments had fallen loose to accumulate along the ditch. Individual fragments measured less than one foot diameter.

B. Kinematic Analysis

The major discontinuities measured in this slope are listed in Table 7.10 and the pole plot of these data is illustrated in Figure 7.19. Based on the kinematic analysis shown in Figures 7.20A through 7.20D, wedge failure is more prevalent than the planar failure and toppling at the slope located south of the West Manifold building.

However, it appears that the slope located west of the West Manifold building is kinematically stable.

Major joint sets of J1 (64/103) and J2 (63/008) which may cause wedge failures in the WM slope located south of the WM building were considered for the subsequent kinetic analysis. Results of the kinematic analysis are summarized in Table 7.11.

C. Kinetic Analysis

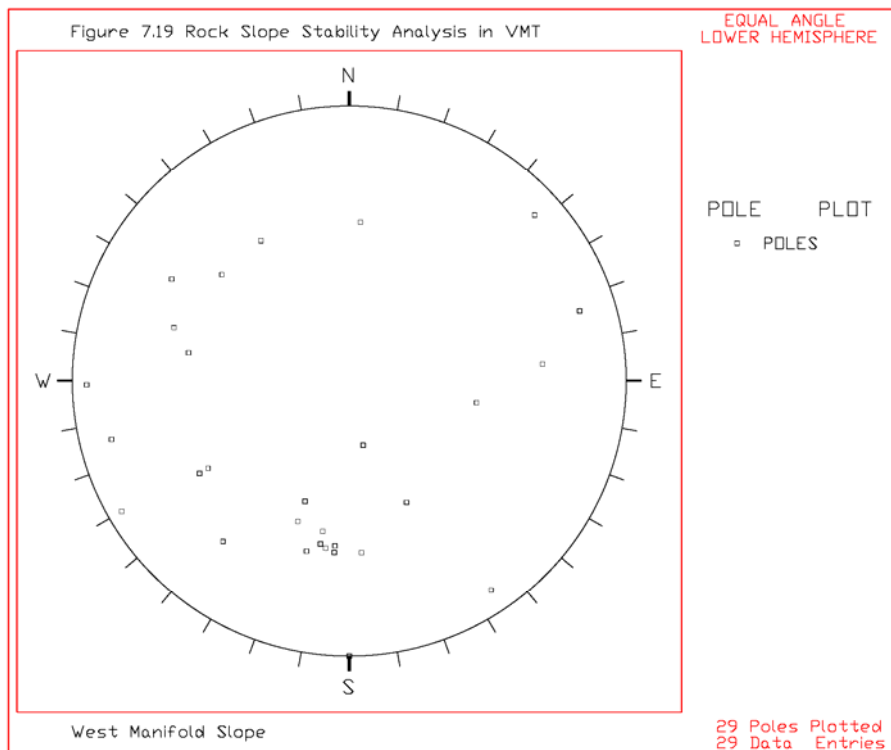
It appears that the slope is stable under current conditions at the time of our field investigations except for local sloughing of small rock fragments. Based on back calculations using the current slope conditions, the 45 and 60 degrees of internal friction angles of foliation and joints, respectively, were used for the slope stabilization analysis. The factor of safety (FS) for the potential wedge failure ranges from 0.0 to 1.33 under different pore pressure conditions ranging from saturated conditions ($H_w/H_{slope} = 1$) to dry conditions ($H_w/H_{slope} = 0$) without any earthquake loading. Under earthquake loading conditions ranging from 0.1g to 0.5g in addition to the pore pressure conditions, the FS ranges from 1.07 to zero. When vertical acceleration ($0.5a_h$) was imposed in addition to the horizontal accelerations, the FS reduced significantly as shown in Figure 7.21C. For this wedge failure mode, the minimum external loading condition that causes a wedge failure is a pore pressure equal to $0.35H_w/H_{slope}$. If both earthquake and pore pressure loadings are considered, the $0.15H_w/H_{slope}$ with 0.1g of horizontal acceleration will cause a wedge failure. The results of the kinetic analysis of the wedge failure are shown in Figures 7.21A through 7.21C.

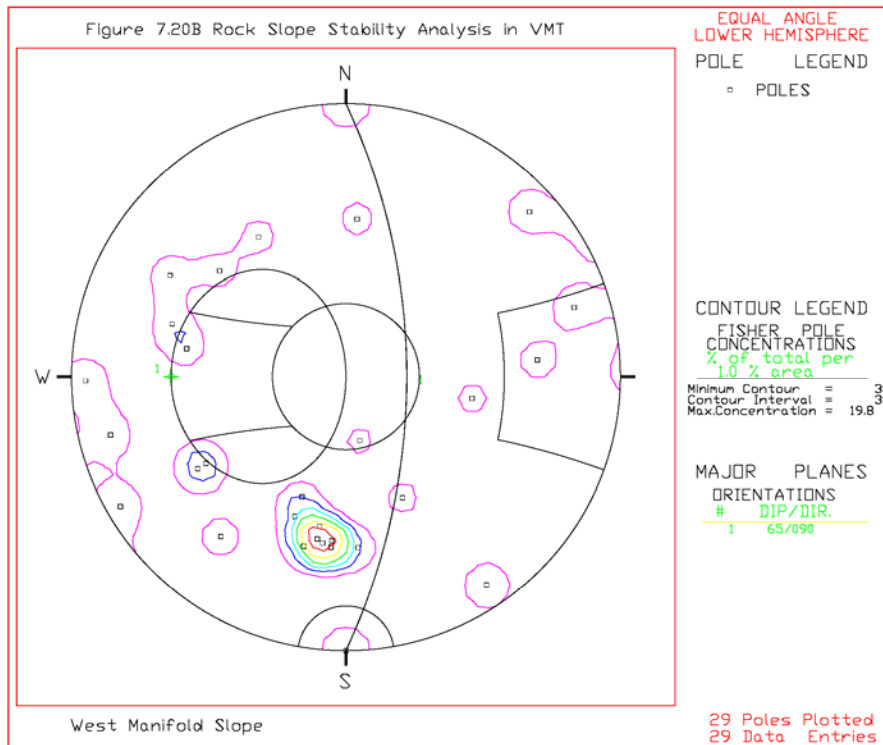
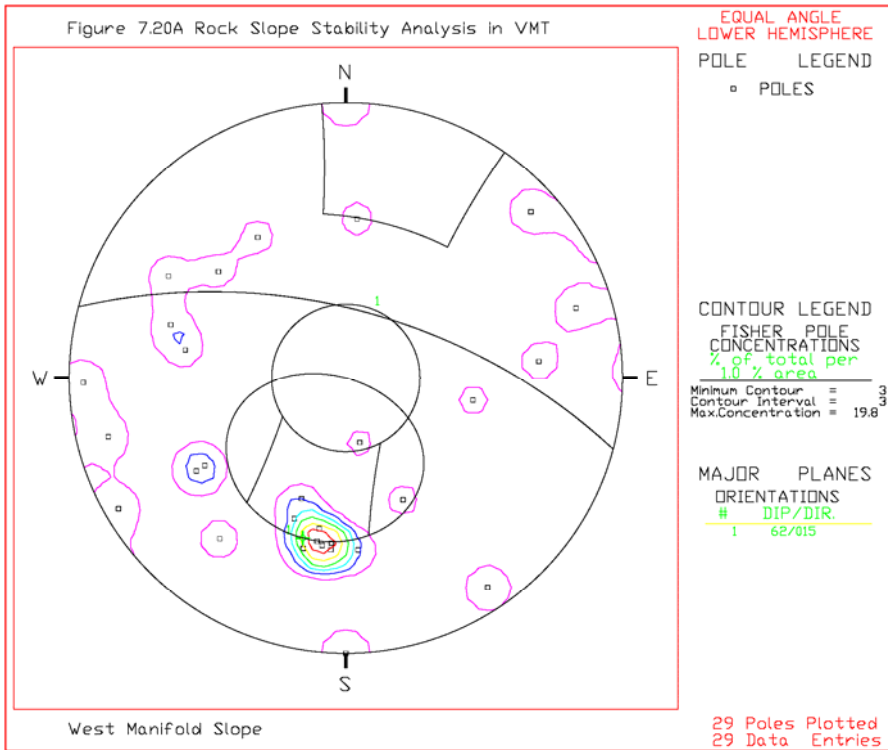
Therefore, it appears that the WM Slope investigated is likely to fail, depending upon the imposed conditions on the slope. Based on this, it should be anticipated that a

wedge failure is likely to occur in the West Manifold slope under a small amount of pore pressure and/or small magnitude of earthquake.

D. Probability of Failure

The probability of failure (P_f) calculated using the wedge failure mode in kinetic analysis ranges from 20% to 100%, depending upon the imposed loading conditions. The P_f values under dry and partially saturated ($H_w/H_{slope}=0.3$) conditions and various earthquake loading conditions are listed in Tables 7.12A and 7.12B.





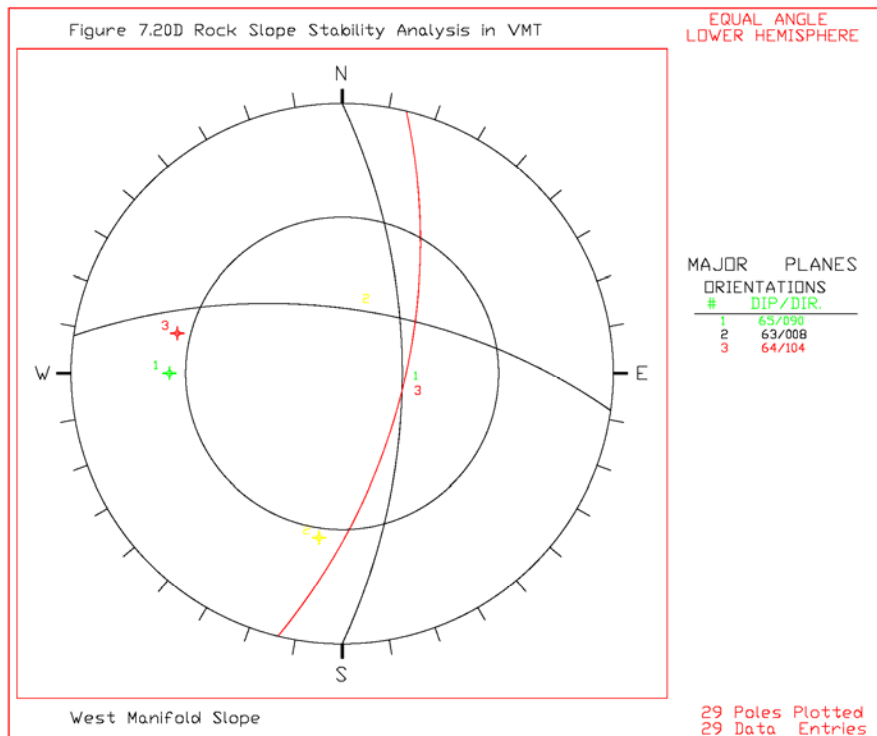
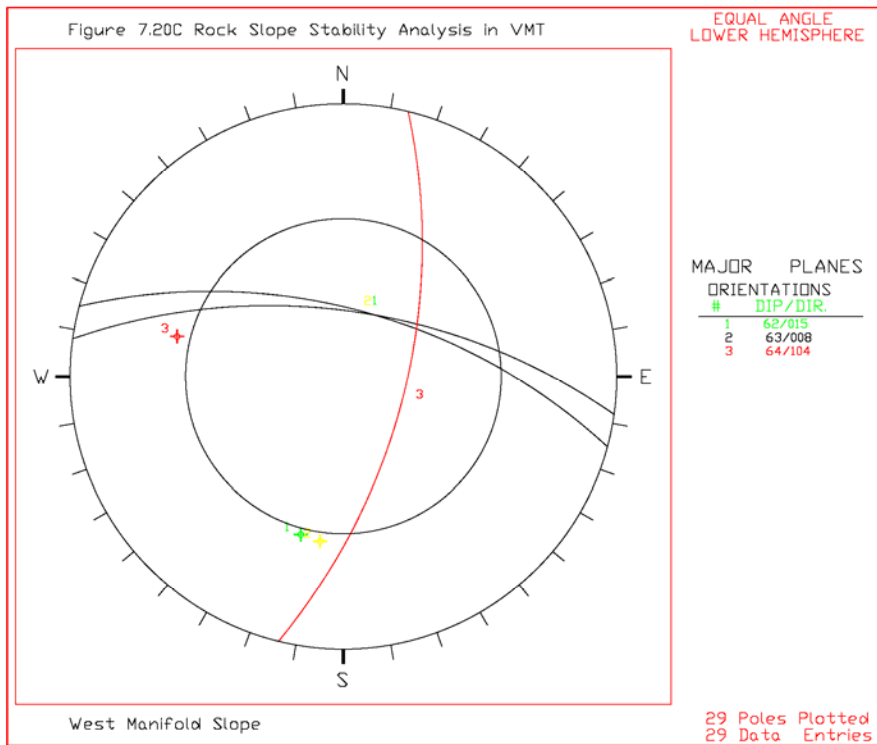


Table 7.10 Discontinuities in the WM Slope

Slope Face	Trend= Face Angle=	N75W 62NE	Dip Dir=	15
No.	Strike	Dip (+/-)	Dip	Dip Direction
1	N70W	57+	57NE	20
2	N65E	52-	52NW	335
3	N5W	70-	70SW	265
4	N82W	63+	63NE	8
5	N42W	84-	84SW	228
6	N78E	27-	27NW	348
7	N70W	50+	50NE	20
8	N17W	82-	82SW	253
9	N10E	61+	61SE	100
10	N76W	65+	65NE	14
11	N14W	83+	83NE	76
12	N80W	58+	58NE	10
13	N30W	87+	87NE	60
14	N40E	62+	62SE	130
15	N56E	85-	85NW	326
16	N17E	67+	67SE	107
17	N80W	62+	62NE	10
18	N85W	64+	64NE	5
19	N32W	62+	62NE	58
20	N32W	65+	65NE	58
21	N85W	62+	62NE	5
22	N52W	73+	73NE	38
23	N10E	50-	50NW	280
Slope Face	Trend= Face Angle=	NS 65E	Dip Dir=	90
24	N1W	87+	87NE	89
25	N30E	73+	73SE	120
26	N86W	60-	60SW	184
27	N58E	62+	62SE	148
28	N30W		90 vertical	vertical
29	N86E	64-	64NW	356

Table 7.11 Kinematic Analysis for the WM Slope

1. Orientation of slope face

E-W trend slope 62/015 (Dip/Dip Direction)
 N-S trend slope 65/090 (Dip/Dip Direction)

2. Major Discontinuities

Joint Set	J1	J2	J3
Type	Joint	Foliation	Foliation
Dip	64	63	65
Dip Direction	103	008	058

3. Kinematic analysis for E-W trend slope face:

A. Potential joint or joint sets for plane failure
 : Major plane failure is not likely to occur in this slope

B. Potential joint or joint sets for wedge failure

2 joint sets	J1 & J2
--------------	---------

C. Potential joint or joint sets for toppling
 : Major toppling is not likely to occur in this slope

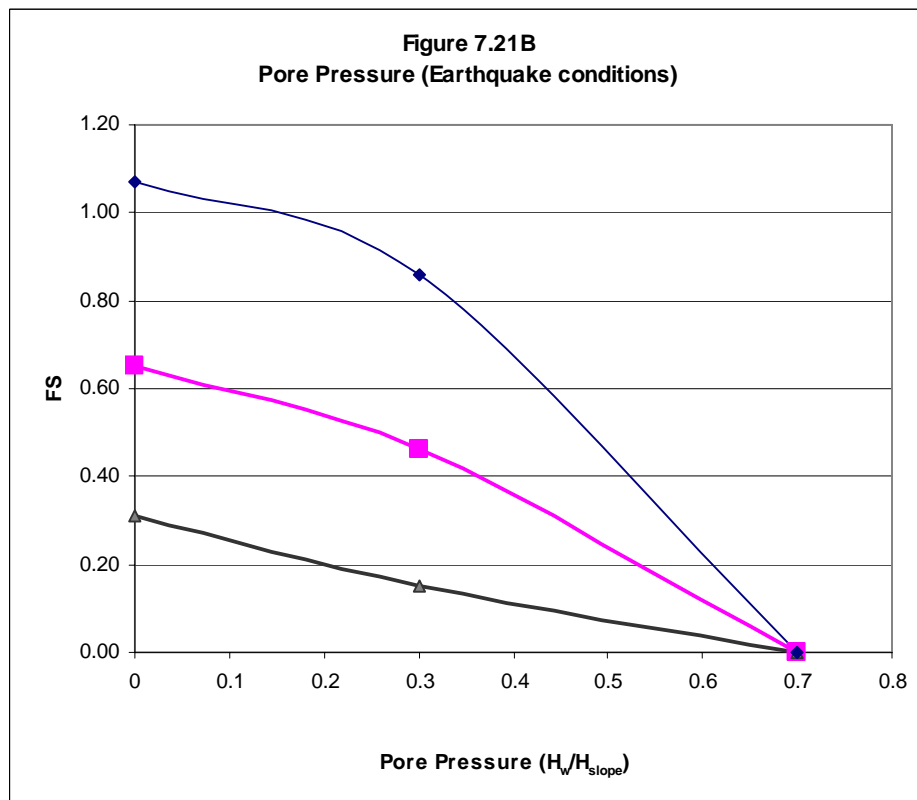
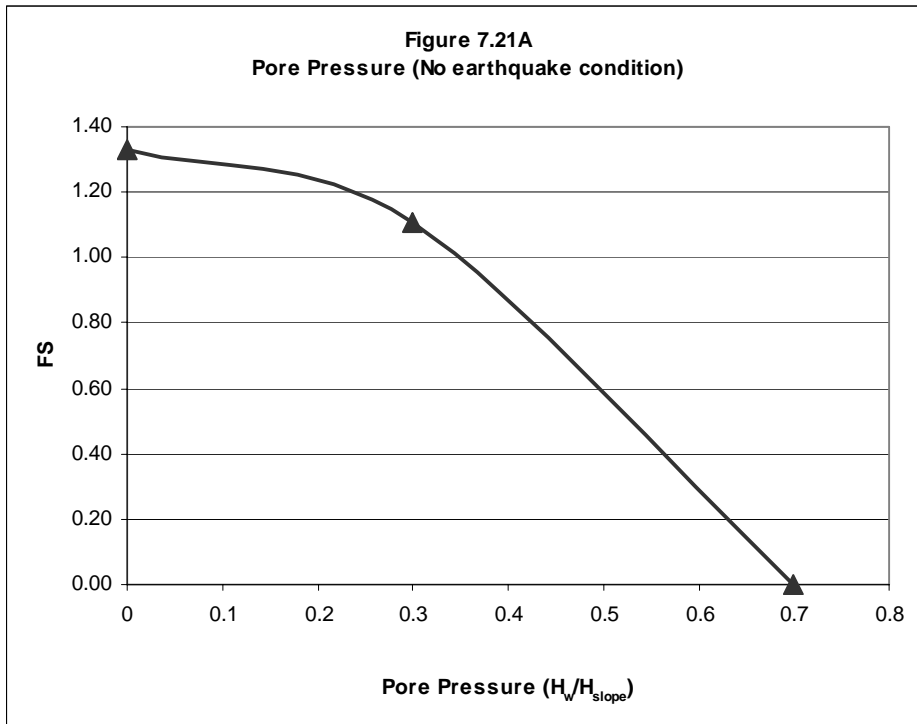
4. Kinematic analysis for N-S trend slope face:

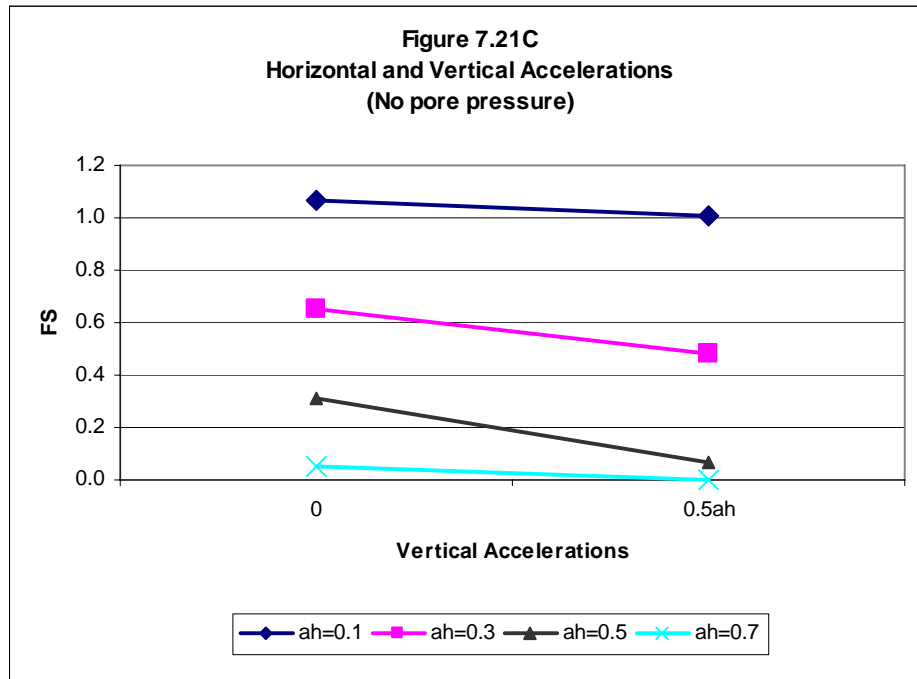
A. Potential joint or joint sets for plane failure
 : Major plane failure is not likely to occur in this slope

B. Potential joint or joint sets for wedge failure

2 joint sets	J1 & J2
--------------	---------

C. Potential joint or joint sets for toppling
 : Major toppling is not likely to occur in this slope





7-2-5 West Tank Farm Slope

A. Site Conditions

The West Tank Farm Slope is located immediately south of the West Tank Farm with an approximate height of 100 feet to 120 feet.

The major discontinuities are foliations and joints. A large, vertical joint trending 90/080 (dip/dip direction) was also observed in this slope. Rock bolts were not implemented on this slope.

Table 7.12A Probability of failure for wedge of J1 and J2 in the WM Slope

Parameters		H _w /H _{slope} =0			
		a _h =0.0	a _h =0.1	a _h =0.3	a _h =0.5
Unit weight (γ , pcf)	Mean	160	160	160	160
	Stdev	8.0	8.0	8.0	8.0
	FS(γ) -	1.33	1.07	0.65	0.31
	FS(γ) +	1.33	1.07	0.65	0.31
	d(FS)/d(γ)	0.000	0.000	0.000	0.000
Tangent of Friction Angle	Mean	1.366	1.366	1.366	1.366
	Stdev	0.123	0.123	0.123	0.123
	FS(ϕ) -	1.02	0.82	0.50	0.24
	FS(ϕ) +	1.81	1.46	0.88	0.43
	d(FS)/d(tan ϕ)	3.216	2.605	1.547	0.773
Cohesion (psf)	Mean	0	0	0	0
	Stdev	0	0	0	0
	FS(C) -	1.33	1.07	0.65	0.31
	FS(C) +	1.33	1.07	0.65	0.31
	d(FS)/d(c)	0.000	0.000	0.000	0.000
Factor of Safety (FS)	Mean FS	1.33	1.07	0.65	0.31
	Stdev(FS)	0.395	0.320	0.190	0.095
	COV(FS)	0.297	0.299	0.292	0.306
Reliability Index	β	0.835	0.219	-1.842	-7.263
Probability of Failure (P(FS<1.0))	P(f)	0.201734	0.413422	0.967270	1.000000

Note :

1. "FS (i) - and FS (i) +" are FS values from "mean - std and mean + std" of i parameter
2. cov (γ) = 3-7 %, 5 % (8 pcf) is assumed in this analysis.
3. cov (ϕ) = 2-13 %, But 13 % (8 degree for J1 and 6 degree for J2) is assumed in this analysis.
4. cov (c) = 13-40 %, 24 % is assumed in this study.

Table 7.12B Probability of failure for wedge of J1 and J2 in the WM Slope

$H_w/H_{slope}=0.3$

Parameters		$a_h=0.0$	$a_h=0.1$	$a_h=0.3$	$a_h=0.5$
Unit weight (γ , pcf)	Mean	160	160	160	160
	Stdev	8.0	8.0	8.0	8.0
	FS(γ) -	1.09	0.85	0.45	0.14
	FS(γ) +	1.12	0.87	0.47	0.16
	d(FS)/d(γ)	0.002	0.001	0.001	0.001
Tangent of Friction Angle	Mean	1.366	1.366	1.366	1.366
	Stdev	0.123	0.123	0.123	0.123
	FS(ϕ) -	0.84	0.65	0.35	0.11
	FS(ϕ) +	1.52	1.19	0.64	0.22
	d(FS)/d($\tan\phi$)	2.768	2.198	1.181	0.448
Cohesion (psf)	Mean	0	0	0	0
	Stdev	0	0	0	0
	FS(C) -	1.11	0.86	0.46	0.15
	FS(C) +	1.11	0.86	0.46	0.15
	d(FS)/d(c)	0.000	0.000	0.000	0.000
Factor of Safety (FS)	Mean FS	1.11	0.86	0.46	0.15
	Stdev(FS)	0.340	0.270	0.145	0.056
	COV(FS)	0.307	0.314	0.316	0.373
Reliability Index	β	0.323	-0.518	-3.715	-15.205
Probability of Failure (P(FS<1.0))	P(f)	0.37327	0.69783	0.99990	1.00000

Note :

1. "FS (i) - and FS (i) +" are FS values from "mean - std and mean + std" of i parameter
2. cov (γ) = 3-7 %, 5 % (8 pcf) is assumed in this analysis.
3. cov (ϕ) = 2-13 %, But 13 % (8 degree for J1 and 6 degree for J2) is assumed in this analysis.
4. cov (c) = 13-40 %, 24 % is assumed in this study.

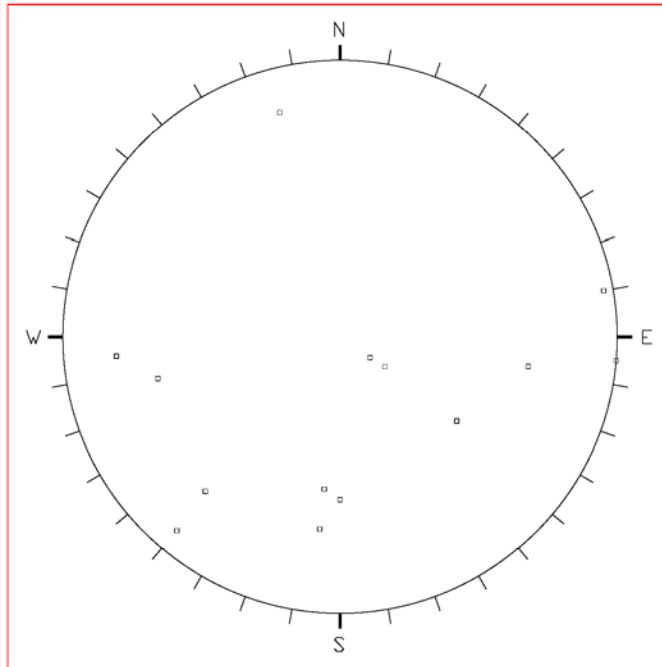
B. Kinematic Analysis

The major discontinuities observed in this slope are listed in Table 7.13 and the pole plot of these data is illustrated in Figure 7.22. Based on the kinematic analysis shown in Figures 7.23A and 7.23B, it is anticipated that wedge failures along the intersection of joints J3 (90/080) and J4 (55/306), and J3 and J5 (69/279) are likely. The results of the kinematic analysis are summarized in Table 7.14. The wedge failure caused by J3 and J4 was selected for analysis due to its more unfavorable conditions to the slope orientation than the other wedge intersection of J3 and J5.

Table 7.13 Discontinuities in the WTF Slope

Slope Face	Trend= Face Angle=	N78W 58NE	Dip Dir=	12
No.	Strike	Dip (+/-)	Dip	Dip Direction
1	N5W	78+	78NE	85
2	N84W	58+	58NE	6
3	N13W	68+	68NE	77
4	N84W	70+	70NE	6
5	EW	61+	61N	0
6	N34E	22-	22NW	304
7	N75E	80+	80SE	165
8	N50W	85+	85NE	40
9	N49W	73+	73NE	41
10	N9E	69-	69NW	279
11	N10W	88-	88SW	260
12	N10W	88-	88SW	260
13	N10W	88-	88SW	260
14	N5E	90-		275
15	N35E	15-	15NW	305
16	N36E	55-	55NW	306

Figure 7.22 Rock Slope Stability Analysis in VMT



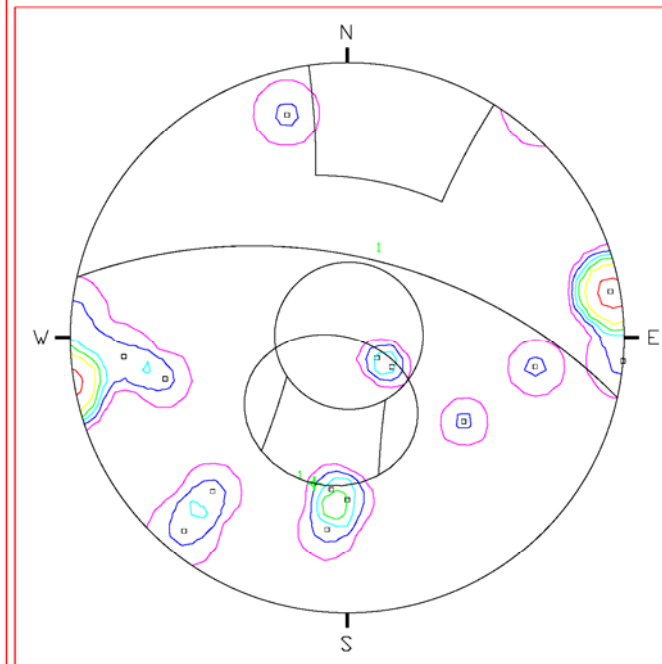
West Tank Farm Slope

EQUAL ANGLE
LOWER HEMISPHERE

POLE PLOT
◻ POLES

16 Poles Plotted
16 Data Entries

Figure 7.23A Rock Slope Stability Analysis in VMT



West Tank Farm Slope

EQUAL ANGLE
LOWER HEMISPHERE

POLE LEGEND
◻ POLES

CONTOUR LEGEND
FISHER POLE
CONCENTRATIONS
% of total per
10% area

Minimum Contour = 3
Contour Interval = 3
Max. Concentration = 18.7

MAJOR PLANES
ORIENTATIONS
DIP/DIR.

1 57/013

16 Poles Plotted
16 Data Entries

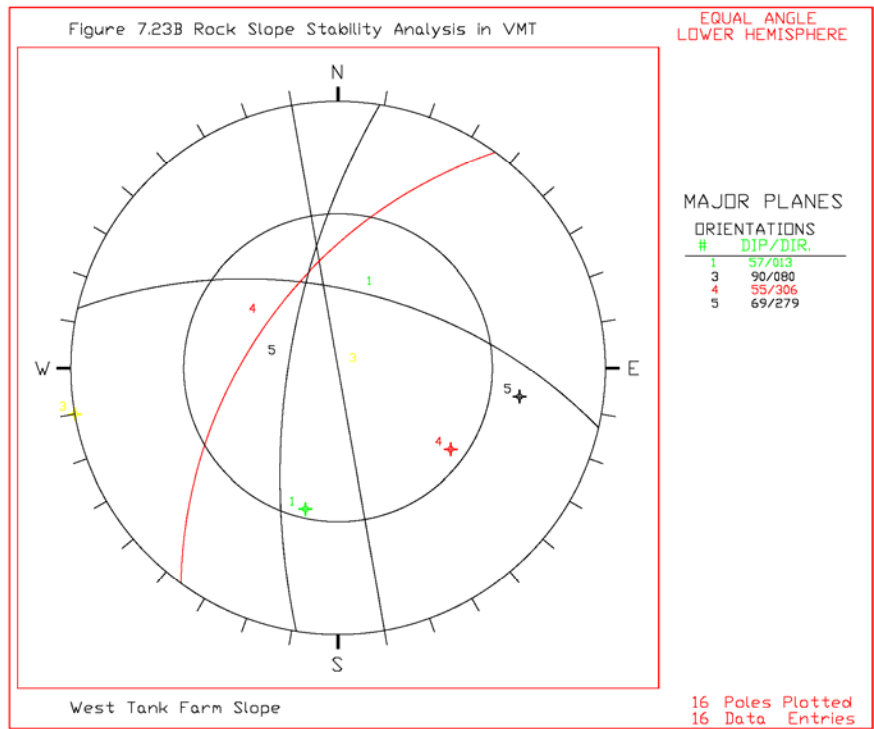


Table 7.14 Kinematic Analysis for the WTF Slope

1. Orientation of slope face

57/013 (Dip/Dip Direction)

2. Major Discontinuities

Joint Set	J1	J2	J3	J4	J5
Type	Joint	Foliation	Joint	Joint	Joint
Dip	88	63	90	55	69
Dip Direction	260	004	080	306	279

3. Kinematic analysis for north slope face:

A. Potential joint or joint sets for plane failure
: Major plane failure is not likely to occur in this slope

B. Potential joint or joint sets for wedge failure

2 joint sets	J3 & J4	J3 & J5
--------------	---------	---------

C. Potential joint or joint sets for toppling
: Major toppling is not likely to occur in this slope

C. Kinetic Analysis

It appears that the slope is stable under current conditions at the time of our field investigations. However, The FS for the potential wedge failure ranges from 1.87 to zero under the pore pressure conditions of dry condition ($H_w/H_{\text{slope}} = 0$) to saturated condition ($H_w/H_{\text{slope}} = 1$) without earthquake loading. Under earthquake loading, ranging from 0.1g to 0.7g in addition to the pore pressure conditions, the FS ranges from 1.53 to zero. When vertical acceleration ($0.5a_h$) was imposed in addition to the horizontal acceleration, the FS is reduced somewhat as shown in Figure 7.24C. For this wedge failure mode, the minimum external loading condition that can cause wedge failure is the pore pressure equal to $0.65H_w/H_{\text{slope}}$. If both earthquake and pore pressure loadings are considered, the $0.5H_w/H_{\text{slope}}$ with 0.1g of horizontal acceleration will cause wedge failure to occur. The results of the kinetic analysis of the wedge failure are shown in Figures 7.24A through 7.24C.

D. Probability of Failure

The probability of failure (P_f) calculated using the wedge failure mode in the kinetic analysis ranges from 1% to 100% under dry conditions and various earthquake loading conditions. The P_f under partially saturated conditions ($H_w/H_{\text{slope}} = 0.7$) and various earthquake loading conditions ranges from 80% to 100%. The results of the P_f analysis are listed in Tables 7.15A and 7.15B.

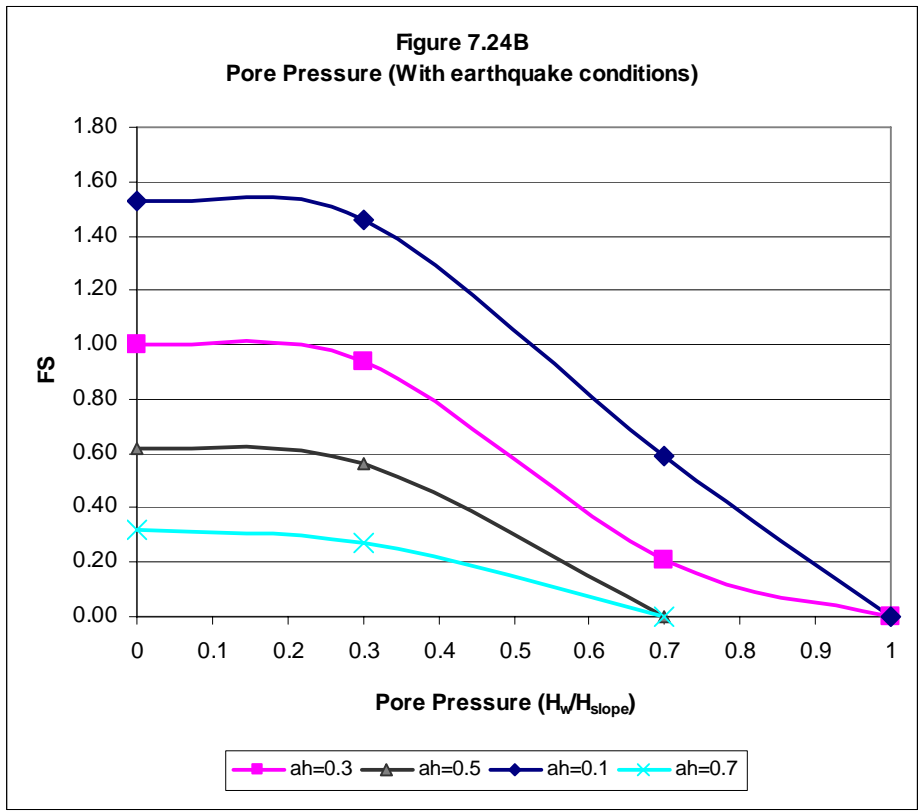
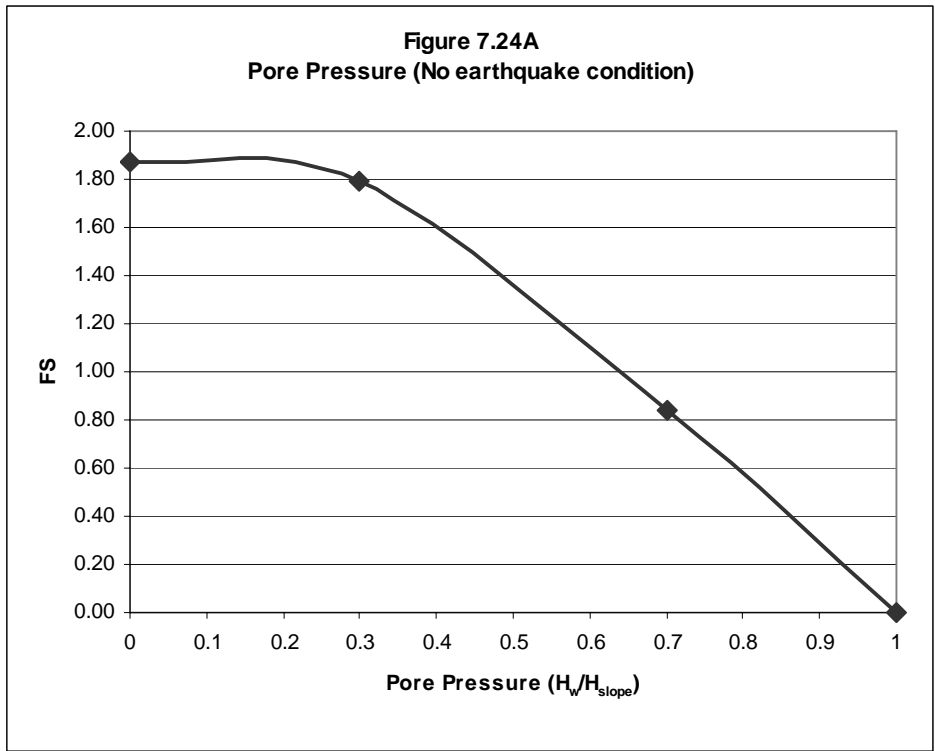


Figure 7.24C
Horizontal and Vertical Accelerations
(No pore pressure)

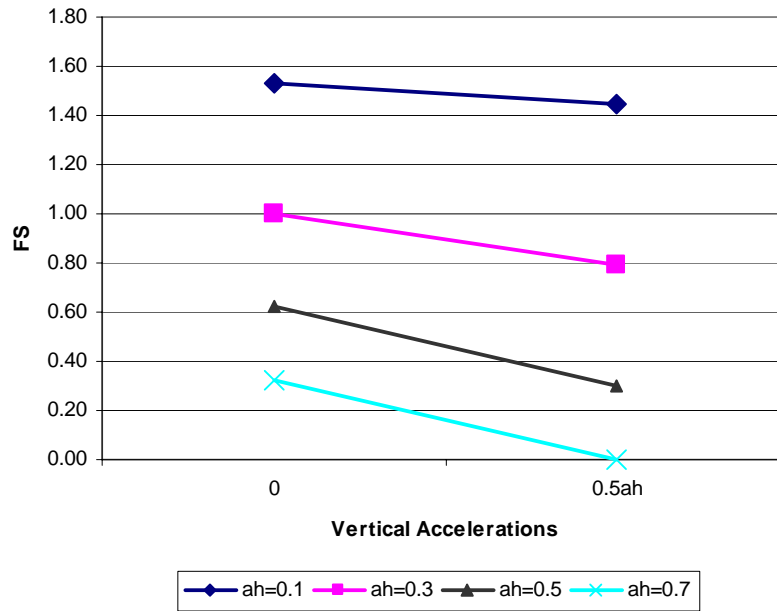


Table 7.15A Probability of failure for wedge J3 & J4 in the WTF Slope

$H_w/H_{slope}=0$

Parameters		$a_h=0.0$	$a_h=0.1$	$a_h=0.3$	$a_h=0.5$	$a_h=0.7$
Unit weight (γ , pcf)	Mean	160	160	160	160	160
	Stdev	8.0	8.0	8.0	8.0	8.0
	FS(γ) -	1.87	1.33	1.00	0.62	0.32
	FS(γ) +	1.87	1.33	1.00	0.62	0.32
	d(FS)/d(γ)	0.000	0.000	0.000	0.000	0.000
Tangent of Friction Angle	Mean	1.000	1.000	1.000	1.000	1.000
	Stdev	0.105	0.105	0.105	0.105	0.105
	FS(ϕ) -	1.52	1.24	0.81	0.50	0.26
	FS(ϕ) +	2.31	1.89	1.24	0.76	0.39
	d(FS)/d($\tan\phi$)	3.758	3.092	2.046	1.237	0.618
Cohesion (psf)	Mean	0	0	0	0	0
	Stdev	0	0	0	0	0
	FS(C) -	1.87	1.53	1.00	0.62	0.32
	FS(C) +	1.87	1.53	1.00	0.62	0.32
	d(FS)/d(c)	0.000	0.000	0.000	0.000	0.000
Factor of Safety (FS)	Mean FS	1.87	1.53	1.00	0.62	0.32
	Stdev(FS)	0.395	0.325	0.215	0.130	0.065
	COV(FS)	0.211	0.212	0.215	0.210	0.203
Reliability Index	β	2.203	1.631	0.000	-2.923	-10.462
Probability of Failure (P(FS<1.0))	P(f)	0.013814	0.051470	0.500000	0.998267	1.000000

Note :

1. "FS (i) - and FS (i) +" are FS values from "mean - std and mean + std" of i parameter
2. cov (γ) = 3-7 %, 5 % (8 pcf) is assumed in this analysis.
3. cov (ϕ) = 2-13 %, But 13 % (6 degree) is assumed in this analysis.
4. cov (c) = 13-40 %, 24 % is assumed in this study.

Table 7.15B Probability of failure for wedge J3 & J4 in the WTF Slope

$H_w/H_{\text{slope}}=0.7$

Parameters		$a_h=0.0$	$a_h=0.1$	$a_h=0.3$
Unit weight (γ , pcf)	Mean	160	160	160
	Stdev	8.0	8.0	8.0
	FS(γ) -	0.78	0.54	0.16
	FS(γ) +	0.89	0.63	0.24
	d(FS)/d(γ)	0.007	0.006	0.005
Tangent of Friction Angle	Mean	1.000	1.000	1.000
	Stdev	0.105	0.105	0.105
	FS(ϕ) -	0.68	0.48	0.17
	FS(ϕ) +	1.04	0.73	0.25
	d(FS)/d($\tan\phi$)	1.713	1.189	0.381
Cohesion (psf)	Mean	0	0	0
	Stdev	0	0	0
	FS(C) -	0.84	0.59	0.21
	FS(C) +	0.84	0.59	0.21
	d(FS)/d(c)	0.000	0.000	0.000
Factor of Safety (FS)	Mean FS	0.84	0.59	0.21
	Stdev(FS)	0.188	0.133	0.057
	COV(FS)	0.224	0.225	0.269
Reliability Index	β	-0.850	-3.086	-13.965
Probability of Failure (P(FS<1.0))	P(f)	0.80236	0.99899	1.00000

Note :

1. "FS (i) - and FS (i) +" are FS values from "mean - std and mean + std" of i parameter
2. cov (γ) = 3-7 %, 5 % (8 pcf) is assumed in this analysis.
3. cov (ϕ) = 2-13 %, But 13 % (6 degree) is assumed in this analysis.
4. cov (c) = 13-40 %, 24 % is assumed in this study.

7-2-6 East Tank Farm Slope

A. Site Conditions

The East Tank Farm Slope is located immediately south of the East Tank Farm along the East Tank Loop Road. The slope extends approximately 100 to over 400 feet to the west.

Based on available information (Bukovansky, 1990), no stabilization measures were taken here because of the significant distance (approximately 400 feet) from the slope to the nearest tank. Blocks that had fallen from this slope were found in the ditch located between the slope and the road.

B. Kinematic Analysis

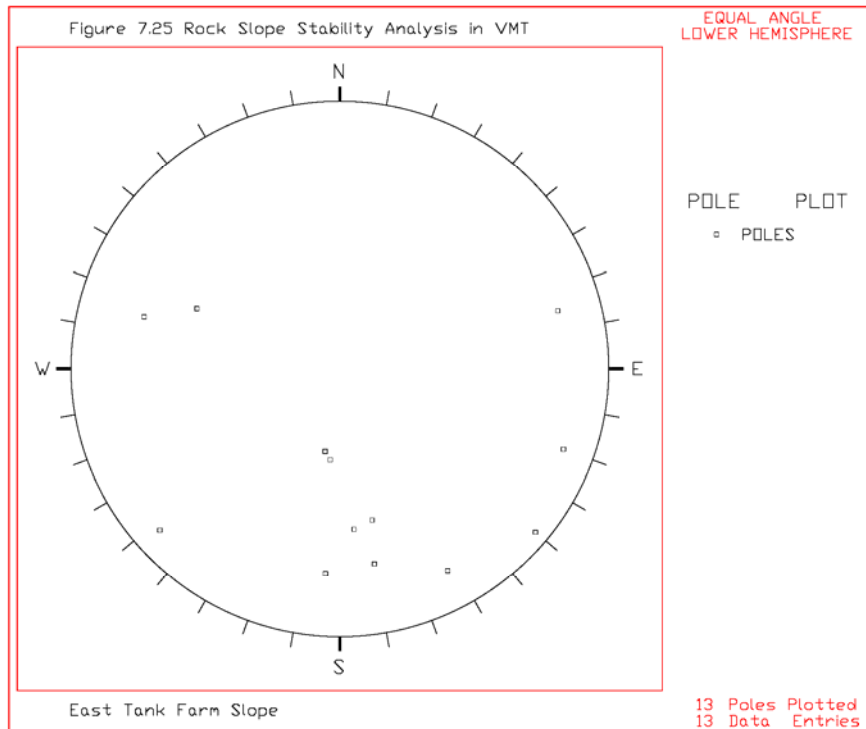
The major discontinuities measured in this slope are listed in Table 7.16 and the pole plot of these data is illustrated in Figure 7.25. Based on the kinematic analysis shown in Figure 7.26 and Figure 7.28, it is anticipated that a planar failure by foliation J3 (90/080) and a wedge failure by the intersection of joints J1 (65/351) and J2 (60/113) may occur. The results of the kinematic analysis are summarized in Table 7.17.

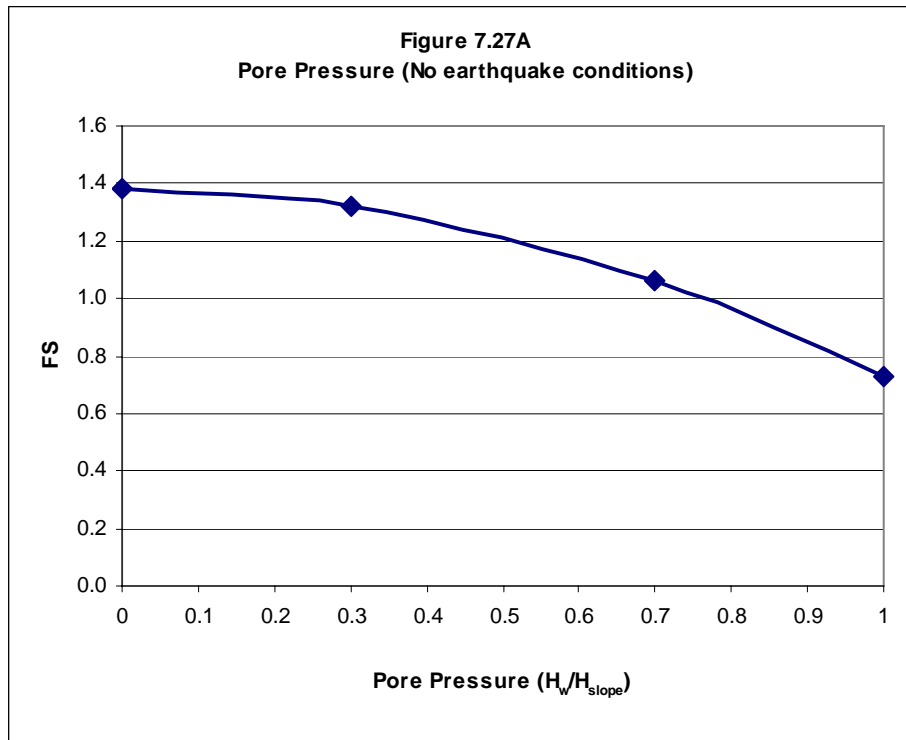
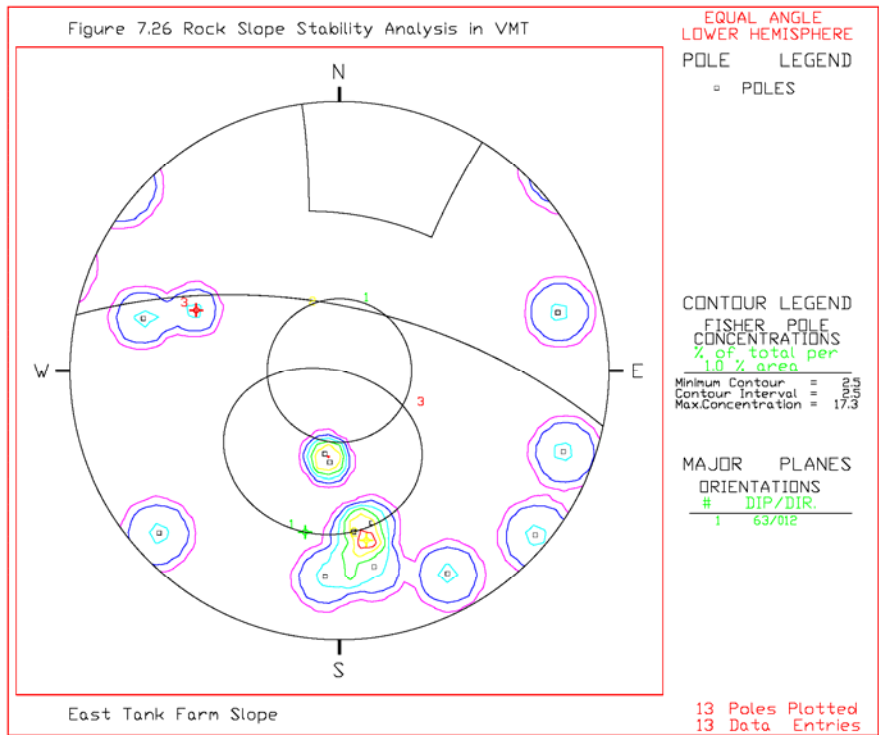
C. Kinetic Analysis

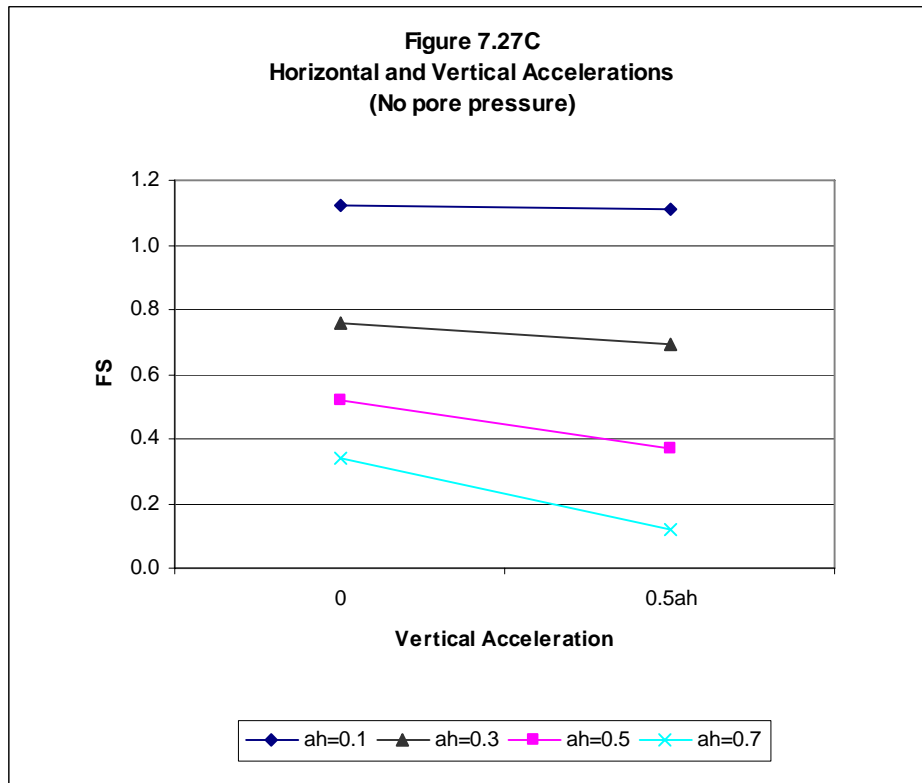
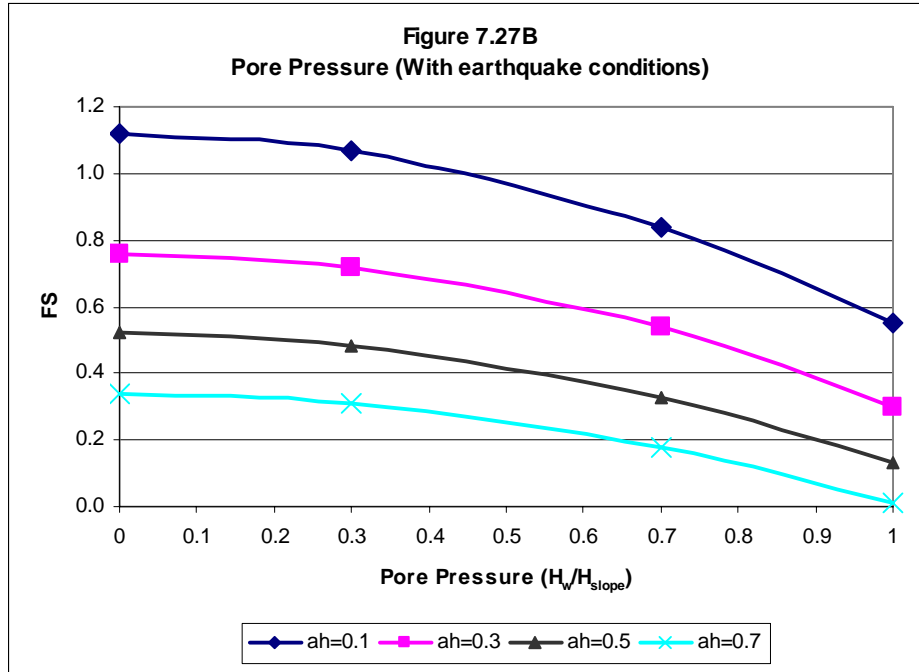
Based on the kinetic analysis on the joint sets that were kinematically unstable in the planar failure mode, the factor of safety (FS) ranges from 1.38 to 0.73 under pore pressure conditions of zero to a saturated condition ($H_w/H_{\text{slope}} = 1$) without earthquake loading effects. Under earthquake loading conditions ranging from 0.1g to 0.7g in addition to the pore pressure effects, FS ranges from 1.12 to 0.01 under various pore pressure conditions.

Table 7.16 Discontinuities in the ETF Slope

Slope Face	Trend= Face Angle=	N78W 62-63NE	Dip Dir=	12
No.	Strike	Dip (+/-)	Dip	Dip Direction
1	N85E	62-	62NW	355
2	N86W	75+	75NE	4
3	N40E	87-	87NW	310
4	N23E	60+	60SE	113
5	N20E	83-	83NW	290
6	N15W	80-	80SW	255
7	N84W	38+	38NE	6
8	N62E	81-	81NW	332
9	N42W	84+	84NE	48
10	N80W	35+	35NE	10
11	N15E	74+	74SE	105
12	N78E	60-	60NW	348
13	N80E	73-	73NW	350







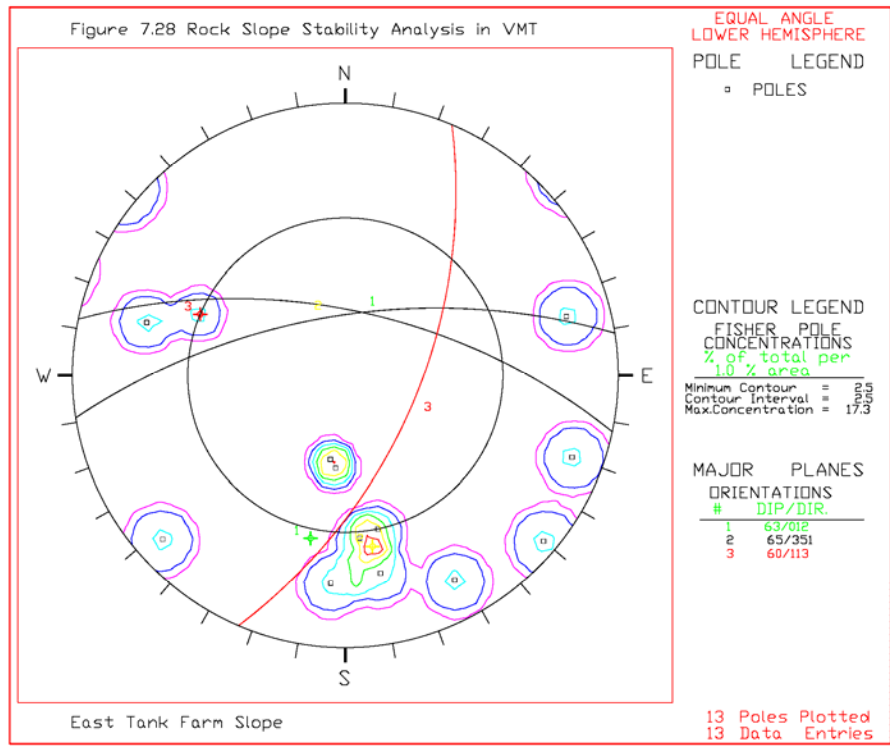


Table 7.17 Kinematic Analysis for ETF Slope

1. Orientation of slope face
63/012 (Dip/Dip Direction)

2. Major Discontinuities

Joint Set	J1	J2	J3	J4
Type	Foliation	Joint	Foliation	Joint
Dip	65	60	36	84
Dip Direction	351	113	007	048

3. Kinematic analysis

A. Typical joint or joint sets for plane failure

Joint Sets:	J3
-------------	----

B. Typical joint sets for wedge failure

2 joint sets	J1 & J2
--------------	---------

C. Potential joint or joint sets for toppling
: Major toppling is not likely to occur in this slope

For the earthquake conditions considering both horizontal and vertical accelerations and dry conditions ($H_w/H_{\text{slope}} = 0$), FS ranges from 1.12 to 0.12 for the earthquake loading conditions ranging from 0.1g to 0.7g. For the planar failure mode, the minimum external loading condition that can cause a planar failure is a pore pressure equal to $0.75H_w/H_{\text{slope}}$. If both earthquake and pore pressure loadings are considered, the $0.45H_w/H_{\text{slope}}$ with 0.1g of horizontal acceleration will cause a wedge failure to occur. The results of the kinetic analysis for the planar failure are shown in Figures 7.27A through 7.27C.

A kinetic analysis was performed on the joint sets of joints J3 and J4 that were kinematically unstable in the wedge failure mode. The FS ranges from 1.71 to 0.44 under the pore pressure conditions of zero to saturated condition ($H_w/H_{\text{slope}} = 1$) without an earthquake loading condition. Under earthquake loading effects ranging from 0.1g to 0.7g in addition to the pore pressure effects, FS ranges from 1.40 to zero under various pore pressure conditions. Under the earthquake conditions considering both horizontal and vertical accelerations and dry conditions ($H_w/H_{\text{slope}} = 0$), FS ranges from 1.40 to zero under earthquake loading conditions ranging from 0.1g to 0.7g. For this wedge failure mode, the minimum external loading condition that can cause a wedge failure is a pore pressure equal to $0.7H_w/H_{\text{slope}}$. If both earthquake and pore pressure loadings are considered together, the $0.6H_w/H_{\text{slope}}$ with 0.1g of horizontal acceleration will cause the wedge failure to occur. The results of the kinetic analysis of the wedge failure are shown in Figures 7.29A through 7.29C.

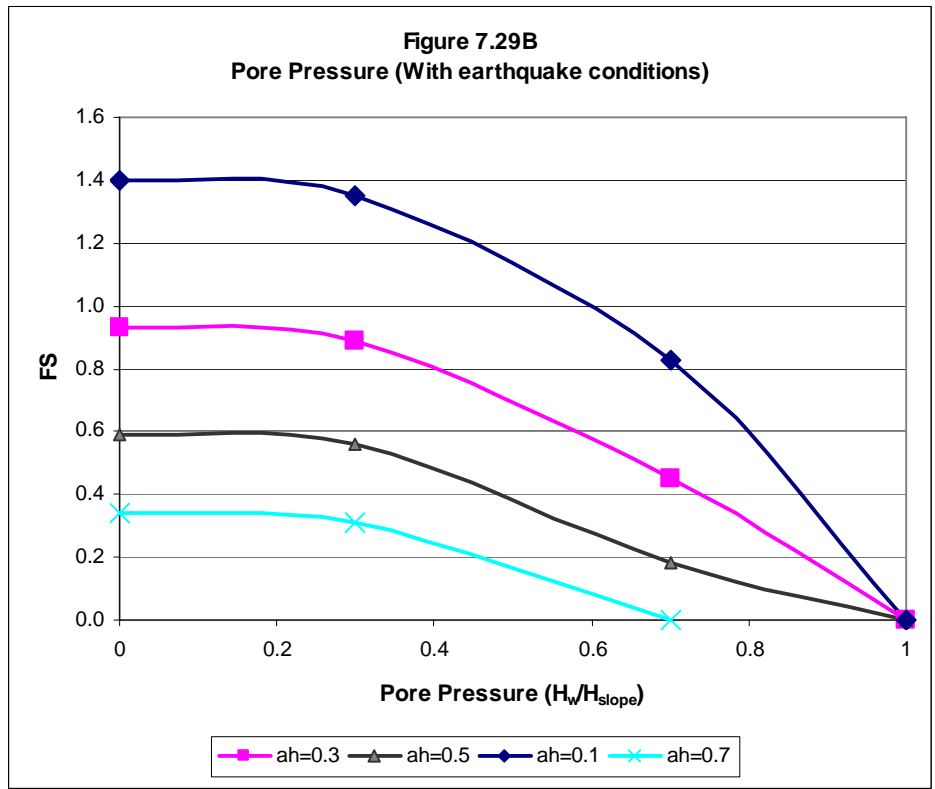
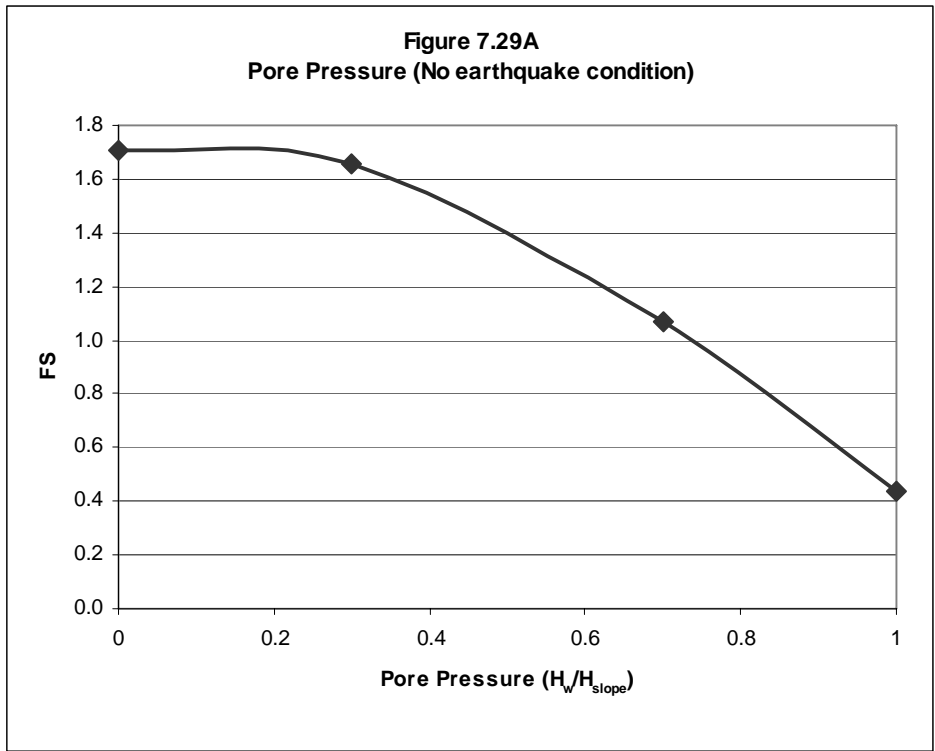
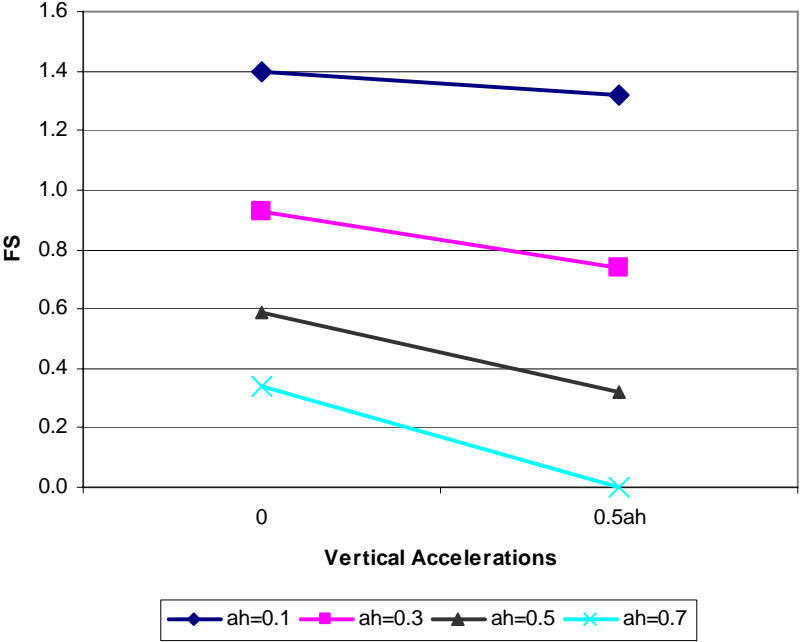


Figure 7.29C
Horizontal and Vertical Accelerations
(No pore pressure)



D. Probability of Failure

The probability of failure (P_f) calculated using the planar failure mode in kinetic analysis ranges from 10% to 100% under dry conditions with the earthquake loading ranging from zero to 0.7g. The P_f under the partially saturated conditions ($H_w/H_{\text{slope}} = 0.7$) ranges from 40% to 100% (Tables 7.18A and 7.18B). However, the P_f for the wedge failure ranges from 3% to 100% under dry conditions with the earthquake loading conditions ranging from zero to 0.7g. The P_f under the partially saturated conditions ($H_w/H_{\text{slope}}=0.7$) ranges from 4% to 100%. Results of the probability of failure analysis for the wedge failure are listed in Tables 7.19A and 7.19B.

7-2-7 Other Slopes

During the field investigation, additional data were obtained from the slopes deemed to be of less significance, including the Tea Shelter Slope, the Power House Road Slope and the rock quarry. It appears that the discontinuities observed in these areas would not cause critical damage to the existing facilities due to their lower height and significant distance from the facilities.

The data for the discontinuities measured in these slopes are included in Tables 7.20 through 7.22 and Figures 7.30 through 7.32.

7-3 Analysis of Aerial Photographs above VMT

Another concern for rock slope stability was considered. This included an area which extends beyond the 1000 acre site itself and involves the stability of the large rock mass at the top of the mountain to the south. Viewed from the water in the Valdez arm, the mass of glaciated rock slopes extend high above the VMT facilities.

The rock mass is an extensive cirque feature where a massive ice field had existed prior to the current melt-back of glaciers in southern Alaska. Because of this concern, stereo pairs of air photos were examined by Dr. West to evaluate the potential for massive rock failures that could yield large blocks of rock tumbling down upon the VMT facilities. This is not an inconsequential concern because it is well documented that massive rock slides occur in proximity to high magnitude earthquakes (Keefer, 1984). Rockslides and rock falls are abundant occurrence in close proximities to high magnitude earthquake.

Examination of the air photos indicated that a large valley exists between the high peaks and the slopes directly above the VMT site. This was the route of the descending glacier from this high cirque area. Based on this evaluation, it is concluded that if a major rock fall or slide occurs on the high slope during a major earthquake near the VMT site, that the rock mass would not be directed toward the site but be routed into another lower area.

Table 7.18A Probability of failure for J3 in the ETF Slope

Parameters		$H_w/H_{slope}=0$				
		$a_h=0.0$	$a_h=0.1$	$a_h=0.3$	$a_h=0.5$	$a_h=0.7$
Unit weight (γ , pcf)	Mean	160	160	160	160	160
	Stdev	8.0	8.0	8.0	8.0	8.0
	FS(γ) -	1.38	1.12	0.76	0.52	0.34
	FS(γ) +	1.38	1.12	0.76	0.52	0.34
	d(FS)/d(γ)	0.000	0.000	0.000	0.000	0.000
Tangent of Friction Angle	Mean	1.000	1.000	1.000	1.000	1.000
	Stdev	0.105	0.105	0.105	0.105	0.105
	FS(ϕ) -	1.11	0.91	0.62	0.42	0.28
	FS(ϕ) +	1.70	1.39	0.94	0.64	0.43
	d(FS)/d($\tan\phi$)	2.807	2.283	1.522	1.047	0.714
Cohesion (psf)	Mean	0	0	0	0	0
	Stdev	0	0	0	0	0
	FS(C) -	1.38	1.12	0.76	0.52	0.34
	FS(C) +	1.38	1.12	0.76	0.52	0.34
	d(FS)/d(c)	0.000	0.000	0.000	0.000	0.000
Factor of Safety (FS)	Mean FS	1.38	1.12	0.76	0.52	0.34
	Stdev(FS)	0.295	0.240	0.160	0.110	0.075
	COV(FS)	0.214	0.214	0.211	0.212	0.221
Reliability Index	β	1.288	0.500	-1.500	-4.364	-8.800
Probability of Failure ($P(FS < 1.0)$)	P(f)	0.098849	0.308538	0.933193	0.999994	1.000000

Note :

1. "FS (i) - and FS (i) +" are FS values from "mean - std and mean + std" of i parameter

2. cov (γ) = 3-7 %, 5 % (8 pcf) is assumed in this analysis.

3. cov (ϕ) = 2-13 %, But 13 % (6 degree) is assumed in this analysis.

4. cov (c) = 13-40 %, 24 % is assumed in this study.

Table 7.18B Probability of failure for J3 in the ETF Slope

$H_w/H_{slope}=0.7$

Parameters		$a_h=0.0$	$a_h=0.1$	$a_h=0.3$	$a_h=0.5$	$a_h=0.7$
Unit weight (γ , pcf)	Mean	160	160	160	160	160
	Stdev	8.0	8.0	8.0	8.0	8.0
	FS(γ) -	1.04	0.83	0.52	0.32	0.17
	FS(γ) +	1.07	0.85	0.55	0.34	0.19
	$d(FS)/d(\gamma)$	0.002	0.001	0.002	0.001	0.001
Tangent of Friction Angle	Mean	1.000	1.000	1.000	1.000	1.000
	Stdev	0.105	0.105	0.105	0.105	0.105
	FS(ϕ) -	0.86	0.68	0.43	0.27	0.15
	FS(ϕ) +	1.31	1.04	0.66	0.41	0.22
	$d(FS)/d(\tan\phi)$	2.141	1.713	1.094	0.666	0.333
Cohesion (psf)	Mean	0	0	0	0	0
	Stdev	0	0	0	0	0
	FS(C) -	1.06	0.84	0.54	0.33	0.18
	FS(C) +	1.06	0.84	0.54	0.33	0.18
	$d(FS)/d(c)$	0.000	0.000	0.000	0.000	0.000
Factor of Safety (FS)	Mean FS	1.06	0.84	0.54	0.33	0.18
	Stdev(FS)	0.225	0.180	0.116	0.071	0.036
	COV(FS)	0.213	0.215	0.215	0.214	0.202
Reliability Index	β	0.266	-0.888	-3.966	-9.475	-22.527
Probability of Failure ($P(FS < 1.0)$)	P(f)	0.39509	0.81260	0.99996	1.00000	1.00000

Note :

1. "FS (i) - and FS (i) +" are FS values from "mean - std and mean + std" of i parameter

2. cov (γ) = 3-7 %, 5 % (8 pcf) is assumed in this analysis.

3. cov (ϕ) = 2-13 %, But 13 % (6 degree) is assumed in this analysis.

4. cov (c) = 13-40 %, 24 % is assumed in this study.

Table 7.19A Probability of failure for wedge J3 & J4 in the ETF Slope

Parameters		$H_w/H_{slope}=0$				
		$a_h=0.0$	$a_h=0.1$	$a_h=0.3$	$a_h=0.5$	$a_h=0.7$
Unit weight (γ , pcf)	Mean	160	160	160	160	160
	Stdev	8.0	8.0	8.0	8.0	8.0
	FS(γ) -	1.71	1.40	0.93	0.59	0.34
	FS(γ) +	1.71	1.40	0.93	0.59	0.34
	d(FS)/d(γ)	0.000	0.000	0.000	0.000	0.000
Tangent of Friction Angle	Mean	1.000	1.000	1.000	1.000	1.000
	Stdev	0.105	0.105	0.105	0.105	0.105
	FS(ϕ) -	1.38	1.13	0.75	0.48	0.28
	FS(ϕ) +	2.11	1.73	1.15	0.73	0.42
	d(FS)/d($\tan\phi$)	3.473	2.854	1.903	1.189	0.666
Cohesion (psf)	Mean	0	0	0	0	0
	Stdev	0	0	0	0	0
	FS(C) -	1.71	1.40	0.93	0.59	0.34
	FS(C) +	1.71	1.40	0.93	0.59	0.34
	d(FS)/d(c)	0.000	0.000	0.000	0.000	0.000
Factor of Safety (FS)	Mean FS	1.71	1.40	0.93	0.59	0.34
	Stdev(FS)	0.365	0.300	0.200	0.125	0.070
	COV(FS)	0.213	0.214	0.215	0.212	0.206
Reliability Index	β	1.945	1.333	-0.350	-3.280	-9.429
Probability of Failure ($P(FS < 1.0)$)	P(f)	0.025875	0.091211	0.636831	0.999481	1.000000

Note :

1. "FS (i) - and FS (i) +" are FS values from "mean - std and mean + std" of i parameter
2. cov (γ) = 3-7 %, 5 % (8 pcf) is assumed in this analysis.
3. cov (ϕ) = 2-13 %, But 13 % (6 degree) is assumed in this analysis.
4. cov (c) = 13-40 %, 24 % is assumed in this study.

Table 7.19B Probability of failure for wedge J3 & J4 in the ETF Slope

$H_w/H_{slope}=0.7$

Parameters		$a_h=0.0$	$a_h=0.1$	$a_h=0.3$	$a_h=0.5$
Unit weight (γ , pcf)	Mean	160	160	160	160
	Stdev	8.0	8.0	8.0	8.0
	FS(γ) -	1.04	0.80	0.43	0.16
	FS(γ) +	1.10	0.85	0.47	0.20
	d(FS)/d(γ)	0.004	0.003	0.003	0.003
Tangent of Friction Angle	Mean	1.000	1.000	1.000	1.000
	Stdev	0.105	0.105	0.105	0.105
	FS(ϕ) -	0.87	0.67	0.37	0.15
	FS(ϕ) +	1.32	1.02	0.56	0.23
	d(FS)/d($\tan\phi$)	2.141	1.665	0.904	0.381
Cohesion (psf)	Mean	0	0	0	0
	Stdev	0	0	0	0
	FS(C) -	1.07	0.83	0.45	0.18
	FS(C) +	1.07	0.83	0.45	0.18
	d(FS)/d(c)	0.000	0.000	0.000	0.000
Factor of Safety (FS)	Mean FS	1.07	0.83	0.45	0.18
	Stdev(FS)	0.227	0.177	0.097	0.045
	COV(FS)	0.212	0.213	0.216	0.248
Reliability Index	β	0.308	-0.962	-5.665	-18.336
Probability of Failure (P(FS<1.0))	P(f)	0.37890	0.83189	1.00000	1.00000

Note :

1. "FS (i) - and FS (i) +" are FS values from "mean - std and mean + std" of i parameter
2. cov (γ) = 3-7 %, 5 % (8 pcf) is assumed in this analysis.
3. cov (ϕ) = 2-13 %, But 13 % (6 degree) is assumed in this analysis.
4. cov (c) = 13-40 %, 24 % is assumed in this study.

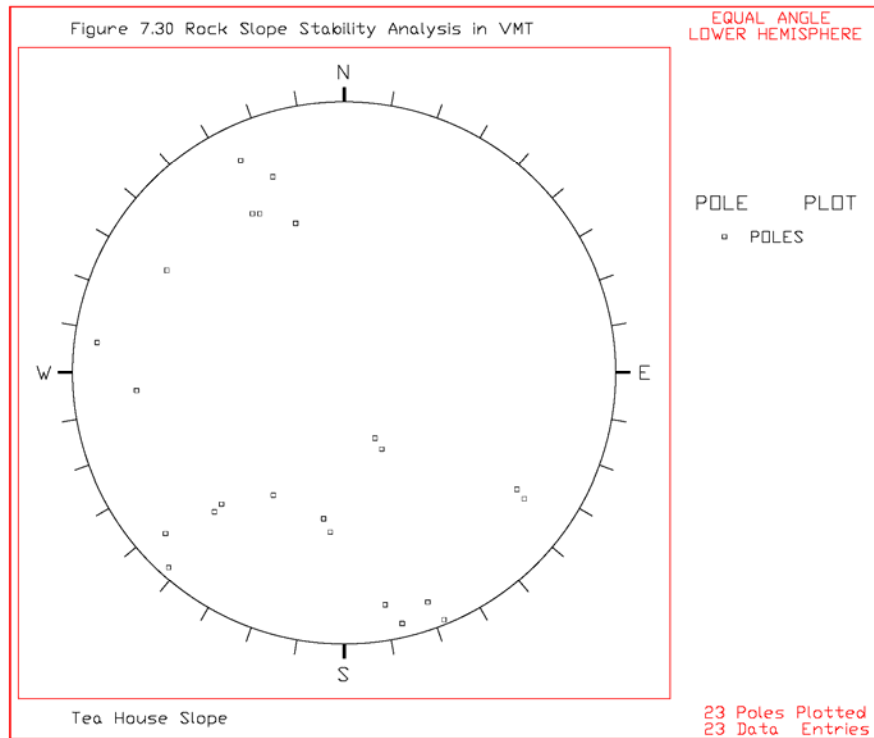
Table 7.20 Discontinuities in the T-Shelter Slope

Slope Face	Trend= Face Angle=	N85E 53NW	Dip Dir=	355
No.	Strike	Dip (+/-)	Dip	Dip Direction
1	N82W	57+	57NE	8
2	N35E	78-	78NW	305
3	N48W	88+	88NE	42
4	N72E	60+	60SE	162
5	N70E	84-	84NW	340
6	N70E	75+	75SE	160
7	N68E	89-	89NW	338
8	N47W	67+	67NE	43
9	N62E	67+	67SE	152
10	N80E	82-	82NW	350
11	N60E	68+	68SE	150
12	N65E	30-	30NW	335
13	N47W	70+	70NE	43
14	N64E	82+	82SE	154
15	N42W	83+	83NE	48
16	N34E	75-	75NW	304
17	N30E	74+	74SE	120
18	N5W	75+	75NE	85
19	N77E	87-	87NW	347
20	N60W	55+	55NE	30
21	N7E	85+	85SE	97
22	N85W	61+	61NE	5
23	N64E	35-	35NW	334

Table 7.21 Discontinuities in the Power House Road Slope

Slope Face	Trend= Face Angle=	EW 85S	Dip Dir= 180
No.	Strike	Dip (+/-)	Dip Dip Direction
1	EW	62+	62S 180
2	N80E	44+	44SE 170
3	N32E	83+	83SE 122
4	N32E	30-	30NW 352
5	N62W	65+	65NE 28

Slope Face	Trend= Face Angle=	EW 65N	Dip Dir= 0
6	N75W	77+	77NE 15
7	N20E	89-	89NW 290
8	N85E	65-	65NW 355
9	N10W	70+	70NE 80
10	N36E	76-	76NW 306
11	N13E	80-	80NW 283
12	N15W	87-	87SW 255



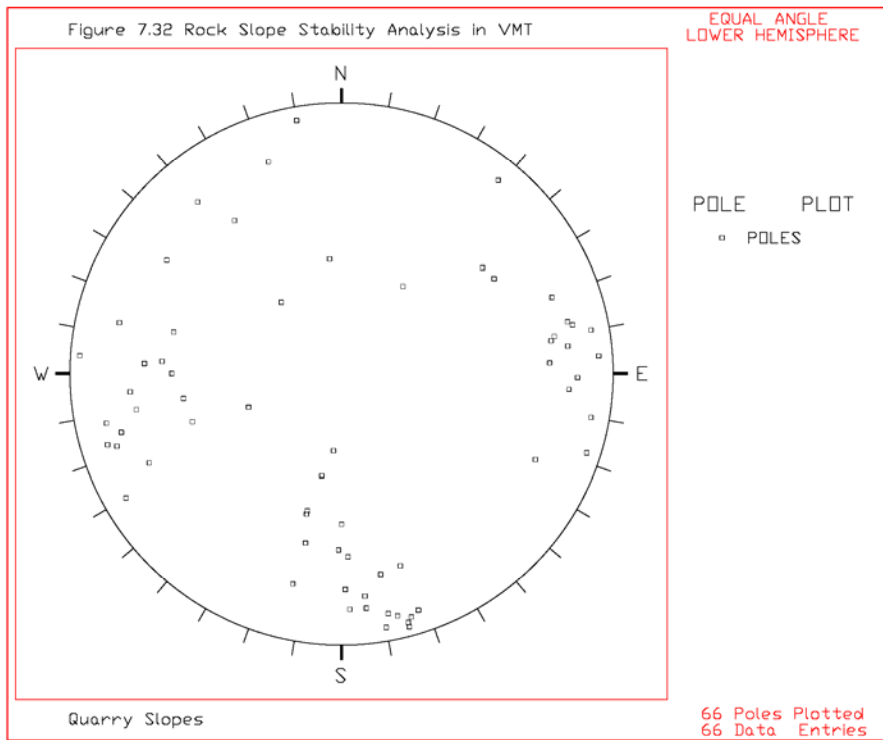
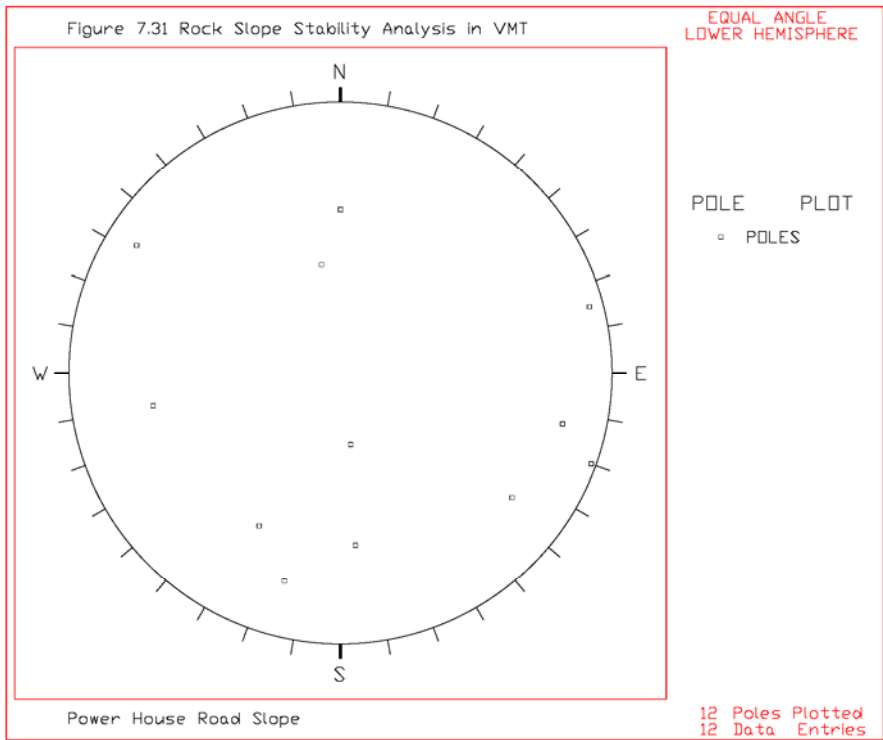


Table 7.22 Discontinuities in the Rock Quarry Slope

Slope Face	Trend= Face Angle=	N80W 65-69NE	Dip Dir=	10
No.	Strike	Dip (+/-)	Dip	Dip Direction
1	N25W	76+	76NE	65
2	N18W	82+	82NE	72
3	N10E	86-	86NW	280
4	N37W	66-	66SW	233
5	N1E	82-	82NW	271
6	N84E	82-	82NW	354
7	EW	58-	58N	360
8	N78W	65+	65NE	12
9	N18E	87-	87NW	288
10	N75E	87-	87NW	345
11	N75E	88-	88NW	345
12	N76W	55+	55NE	14
13	N24E	76-	76NW	294
14	N84E	79-	79NW	354
15	N18W	60+	60NE	72
16	N9W	61+	61NE	81
17	N20W	40+	40NE	70
18	N77W	77+	77NE	13
19	N4E	67+	67SE	94
20	N13W	81-	81SW	257
21	N79E	74-	74NW	349
22	N5W	76+	76NE	85
23	N13W	81-	81SW	257
24	N79E	74-	74NW	349
25	N4W	87-	87SW	266
26	N7W	80-	80SW	263
27	N84W	32+	32NE	6
28	N50E	38+	38SE	140
29	N14E	79+	79SE	104
30	NS	64+	64E	90
31	N10W	75+	75NE	80
32	N13E	80+	80SE	103
33	N72E	85-	85NW	342
34	N74E	86-	86NW	344
35	N9W	76-	76SW	261

Table 7.22 Discontinuities in the Rock Quarry Slope (Continued.)

36	N77E	85-	85NW	347
37	N10W	77-	77SW	260
38	N12W	82-	82SW	258
39	N20W	79-	79SW	250
40	N4E	88+	88SE	94
41	N71E	79+	79SE	161
42	N10W	86-	86SW	260
43	N17W	84+	84NE	73
44	N80E	87-	87NW	350
45	N79E	84-	84NW	349
46	N79W	42+	42NE	11
47	N15W	80+	80NE	75
48	N32W	67-	67SW	238
49	N55E	69+	69SE	145
50	N30W	85+	85NE	60
51	N3E	72+	72SE	93
52	N89E	77-	77NW	359
53	N4E	80-	80NW	274
54	N33E	75+	75SE	123
Quarry (North Slope)				
55	N89W	66+	66NE	1
56	N76W	56+	56NE	14
57	N88E	68-	68NW	358
58	N80E	87+	87SE	170
59	N55W	43-	43SW	215
60	N84E	46+	46SE	174
61	N73E	73-	73NW	343
62	N12W	83+	83NE	78
63	N3W	75-	75SW	267
64	N88E	82-	82NW	358
65	N51W	85-	85SW	219
66	N14E	65+	65SE	104

8. CONCLUSIONS

Based on the field investigations performed to evaluate stability of the existing rock slopes at the VMT and subsequent data analysis, the following conclusions are obtained. It should be noted that the stability analyses for this project were performed using limited information on the strength of the rock discontinuities and rock bolts, and limited access to rock slopes. It also should be noted that the kinetic analysis used in this project is considered to be conservative for the slope stability analysis because of rock mass strength considerations. Through-going discontinuities are assumed and this likely is not the case in all situations. Therefore, the FS may actually be greater than the values calculated.

A more precise evaluation of rock slope stability at VMT would require a detailed field evaluation of the site. This would require an accurate location of all rock bolts, drainage holes and piezometers, including the length and orientation of these units. This information was not available in the current study. Also, the condition of the rock bolts and drainage holes is needed.

Based on the kinematic analyses of the BWT Slope, the orientations of the discontinuities observed in this slope indicate that both planar and wedge type failures may occur. However, due to the in-place strength of the discontinuities, it appears that the slope is stable under current conditions. Based upon the kinetic analysis, considering various earthquake and pore pressure conditions imposed by the prolonged rainfall and snow melt, it is anticipated that the external loading conditions equal to $0.7H_w/H_{\text{slope}}$ when pore pressure only is applied and equal to pore pressure of $0.6H_w/H_{\text{slope}}$ with 0.1g of

horizontal acceleration when both earthquake and pore pressure are imposed, will cause the BWT Slope to become unstable.

The kinematic analyses of the PVR Slope indicated that both planar and wedge type failures may occur. However, due to the in-place strength of the discontinuities, it appears that the slope is stable under current conditions. However, for this wedge failure mode, the external loading conditions equal to $0.85H_w/H_{\text{slope}}$ when pore pressure only is applied and equal to pore pressure of $0.8H_w/H_{\text{slope}}$ with 0.1g of horizontal acceleration or $0.55H_w/H_{\text{slope}}$ with 0.2g of horizontal acceleration when both earthquake and pore pressure are imposed may cause the PVR Slope to become unstable.

Based on the kinematic analyses of the West Manifold Slope, the orientations of the discontinuities observed here indicate that wedge type failure may occur. However, due to the in-place strength of the discontinuities, it appears that the slope is stable under current conditions. However, based on a kinetic analysis considering various earthquake and pore pressure conditions, it is anticipated that the external loading conditions equal to $0.35H_w/H_{\text{slope}}$ when only pore pressure is applied, and the external loading conditions equal to pore pressure of $0.15H_w/H_{\text{slope}}$ with 0.1g of horizontal acceleration when both earthquake and pore pressure are imposed, may cause the West Manifold Slope to become unstable.

The kinematic analyses of the East Tank Farm Slope indicated that both planar and wedge type failures may occur. However, due to the in-place strength of the discontinuities, it appears that the slope is stable under current conditions. However, the external loading conditions equal to $0.7H_w/H_{\text{slope}}$ when pore pressure only is applied, and the external loading conditions equal to pore pressure of $0.45H_w/H_{\text{slope}}$ with 0.1g of

horizontal acceleration when both earthquake and pore pressure are imposed, may cause the East Tank Farm Slope to become unstable.

The kinematic analyses on the West Tank Farm Slope indicated that wedge type failure may occur. However, due to the in-place strength of the discontinuities, it appears that the slope is stable under current conditions. However, the external loading conditions equal to $0.65H_w/H_{\text{slope}}$ when pore pressure only is applied and the external loading conditions equal to pore pressure of $0.5H_w/H_{\text{slope}}$ with 0.1g of horizontal acceleration when both earthquake and pore pressure are imposed may cause the East Tank Farm Slope to become unstable.

Evaluation of the existing pore pressure values in piezometers was not included in this rock slope study of the project. Thus, various pore pressure conditions with earthquake loading conditions were selected to identify the minimum external loading conditions at which slopes of the VMT become unstable. The detailed results of the kinematic and kinetic analyses are included in this report as indicated in the previous sections.

Details on the conditions of the drainage holes in the various rock slopes at VMT were not provided for this study. It is not clear at this time whether or not this information is known in detail. This should be determined in order to perform a more precise evaluation of slope stability for the site.

Also it could not be determined whether or not a contingency plan has been developed at VMT to address an occurrence of rising piezometer levels (increased pore pressures) under increased precipitation conditions. Conclusions reached in this study, based on the

assumptions made, indicated that high pore pressures with moderate earthquake shaking can give rise to unstable slope conditions.

6. RECOMMENDATIONS

The purpose of this project was mainly to evaluate the stability of rock slopes of the VMT during potential earthquake conditions. This report has been prepared for the purpose of assisting RCAC and Alyeska in deciding a future agenda for maintaining the rock slopes to provide stable conditions. It should be noted that this report is not intended to be used as a part of any contract document or as a design document.

As indicated in the conclusion, it appears that the slopes are stable under current conditions except for the local and small sized planar and wedge failures occurring in the space between adjacent rock bolts. Therefore, we recommended the following remediation measures:

The ditches above the rock slopes should have steep enough grades to avoid water-ponding, thereby preventing infiltration of ponded water which can increase pore pressures. Also, it is recommended that any cracks at the top of the slope be sealed with grout or asphalt.

It was observed that some of the installed piezometers were clogged. Therefore, it is recommended that these piezometers in the VMT slopes be regularly cleaned and measured frequently to monitor pore pressures. A program of frequent measurements would show the annual fluctuation of piezometer level. It is anticipated that the rock slope may undergo unstable conditions when the slope is fully saturated ($H_w/H_{\text{slope}}=1.0$).

It is also recommended that more rock bolts be installed in the areas where the existing rock bolts are loosened and where rock bolts have not been installed. Methods of installation including rock bolt pattern, length and grouting should be determined by a consulting firm performing this specialty. Therefore, it is recommended that the existing rock bolts be examined before more rock bolts are added.

Rock slope stability calculations presented in this report are based on a number of assumptions concerning rock mass strength and slope stabilization. The latter includes rock bolt distribution and drainage hole location and extent. In order to conduct a more precise evaluation than is presented here, these additional data must be obtained.

REFERENCES CITED

- Bukovansky, Michael, 1990, Valdez Terminal Rock Cuts and Tank Foundations, CH2MHill, Consultants.
- Cho, K.H., 2002, Deterministic and Probabilistic Analysis of Rock Slope Stability under Earthquake Loading Conditions, Ph.D. thesis, Purdue University.
- Cohen, Stan, The Great Alaska Pipeline, Pictorial Histories Publishing Co., Missoula, Montana, 134 pages, with information contributed by Alyeska Pipeline Service Company.
- Connor, Cathy and O'Haire, Daniel, 1988, Roadside Geology of Alaska, Mountain Press Publishing Co., Missoula, Montana, 250 pages.
- Davies, John N., 1985, Overview of Alaskan Historical Seismicity, Public Data File Report 85-12, Alaska Division of Geological and Geophysical Surveys.
- Davies, John N. and House, Leigh, 1979, Aleutian Subduction Zone Seismicity, Volcano-Trench Separation and Their Relation to Great Thrust-Type Earthquakes, Journal of Geophysical Research, Vol. 84, No. B9.
- DIPS 2.2, Data Interpretating Package Using Stereographic Projection, Rocscience, Inc.
- Duncan, J. M., 2000, Factors of Safety and Reliability in Geotechnical Engineering, Journal of Geotechnical and Geoenvironmental Engineering, Vol. 126, No. 4, pp 307-316.
- Hoek, E. and Bray, J. W., 1981, Rock Slope Engineering, Revised 3rd Edition, 358 pages.
- Keefer, D. K., 1984, Landslide Caused by Earthquakes, Geological Society of America Bulletin, Vol. 95, pp 406-421.

- Kovari, K. and Fritz, P., 1975, Stability analysis of rock slopes for plane and wedge failure with the aid of a programmable pocket calculator, 16th US Rock Mechanics Symposium, Minneapolis, USA, pp 25-33.
- Norrish, N. I. and Wyllie, D.C., 1996, Rock slope stability analysis, Landslide—Investigation and Mitigation, TRB Special Report 247, Chapter 15, pp 391-425. Transportation Research Board, Washington D. C.
- Santi, P. M., Elifrits, C. D. and Liljegren, J. A., 2001, Design and Installation of Horizontal Wick Drains for Landslide Stabilization, Transportation Research Board 1757, pp 58-66.
- Singh, J.P. and Associates, 1999, Closure to Geotechnical and Slope Stability Review, Valdez Marine Terminal, Valdez, Alaska.
- TAPS, 1973, Revised 1974, Summary Report Geotechnical Aspects, Design Manual for Alaska Pipeline, Appendix Volume 3.
- Tart, Rupert G., 2002, Rock Slopes at the Valdez Marine Terminal, Seismic Status Report PowerPoint Presentation, 31 pages.
- Tart, Rupert G., Personal Communication, August, 2006.
- Verigin, William M. and Harder, Leslie F., Jr., 1989, Seismic Deformation Analysis of Solomon Gulch Dam, R.W. Beck and Associates, Inc., 65 pages.